ABERRANT V(D)J RECOMBINATION: MISREPAIR OF DNA BREAKS AND IMPLICATIONS FOR LYMPHOMAGENESIS

by

Tehmina Masud

A dissertation submitted in partial fulfillment
of the requirements for the degree of
Doctor of Philosophy
(Human Genetics)
in the University of Michigan
2013

Doctoral Committee:

Associate Professor JoAnn M. Sekiguchi, Chair
Assistant Professor Raymond Chan
Professor Thomas W. Glover
Associate Professor Mats Ljungman
Professor John V. Moran

Dedication

I dedicate this dissertation to my father who always valued education and scientific research and to my mother for her love and support while I was thousands of miles away from home.

Acknowledgements

I would like to thank my adviser, Dr. JoAnn Sekiguchi, for her splendid mentorship, for always being there to direct me in my scientific endeavors and for teaching me the skills of critical thinking. Under her leadership, I learned to be independent in my project which made this entire scientific process an utterly enjoyable experience. It would have been impossible to be where I am today without her constant encouragement. I also wish to thank my thesis committee members, Dr. Raymond Chan, Dr. Thomas Glover, Dr. Mats Ljungman and Dr. John Moran for their support and critical analysis of my experiments which was instrumental in the progress of this study and my own growth as a scientist. I am grateful to Dr. David Ferguson for his insightful scientific input and Dr. Tom Glaser for intellectually stimulating scientific and non-scientific discussions. I really appreciate that he allowed me to work on one of his projects in the lab while I was working on my dissertation. The past and current Sekiguchi lab members have been more than just colleagues. I would particularly like to acknowledge Ying Huang and William Lu for their wonderful friendship, Cheryl Jacobs, Ishita Das and Rudel Saunders for delightful conversations, Hilary Moale for being an amazing friend and neighbor in the lab and the extremely talented undergraduate students, Allen Washington Junior and James Kelly, for their assistance. I am grateful to the Ferguson lab members, Kishore Chiruvella, Human Genetics faculty, staff and everyone else at the University of Michigan who has helped me along this process. Drs. Barry Sleckman at the Washington University School of Medicine and Craig Bassing at the University of Pennsylvania School of Medicine most graciously provided us the pre-B cell lines and I am thankful to them.

I would also like to express my gratitude to all my friends. I have met some of the most amazing people during my stay in the US. I would particularly like to acknowledge Kate Shimshock and her parents, Rick Shimshock and Susan Kladstrup, for all their kindness and fun-filled trips to Minnesota, but most of all for letting me be a part of their family and lives. My sisters, Noshin and Asma, my niece and nephew, Dania and Ezhan, always make me look at things from another perspective and I appreciate them for this.

Most of all, I would like to thank my parents, Masud Ahmad and Rafia Masud, for all their love and support. My father has always been a continuous source of inspiration for me. I will forever be grateful to him for being very understanding and supportive when I decided to quit clinical practice to pursue a career in scientific research, and for everything else in my life. Finally, I am grateful to Joshua Regal for his patience and useful suggestions especially in the last few months when he was preparing for his own defense. I could not have made it through without him.

Table of Contents

List of Figures

List of Tables

List of Abbreviations

ATM	Ataxia telangiectasia mutated
A-NHEJ/A-EJ	Alternative non-homologous end joining
Art	Artemis
Art-P70	Truncated Artemis
β-CASP	Beta-Csp1, Artemis, Snm1, Pso2
BCR	B cell receptor
C-NHEJ	Canonical non-homologous end-joining
CtIP	CtBP-interacting protein
DNA-PKcs	DNA-dependent protein kinase, catalytic subunit
DSB	Double strand breaks
γH2AX	Phosphorylated histone variant 2AX
H3K4me3	Histone H3 trimethylated at lysine 4
HR	Homologous recombination
IgH	Immunoglobulin heavy chain
IgL	Immunoglobulin light chain
IR	Ionizing radiation
LigIV/III/I	DNA Ligases IV, III and I
MMEJ	Microhomology-mediated end joining
MRN	MRE11/NBS1/RAD50
N nucleotides	Non-templated nucleotides
NBS1	Nijmegen breakage syndrome 1
P nucleotides	P nucleotides
PC	Paired complex
PCC	Postcleavage complex
PIKK	Phosphoinositide 3-kinase-related
Polμ/λ	DNA polymerases meu and lambda
PolQ	DNA polymerase theta
RAG1, RAG2	Human Recombination activating genes 1 and 2
Rag1, Rag2	Murine Recombination activating gene 1 and 2
RAG1/2	Recombination activating proteins 1 and 2
RSS	Recombination signal sequences
SC	Synaptic complex
SCID	Severe combined immunodeficiency disorder
TCR	T cell receptor
TdT	Terminal deoxynucleotidyl transferase
WT	Wild-type
XLF	XRCC4-like factor
XRCC4	X-ray repair cross-complementing protein 4

Abstract

Canonical non-homologous end joining (C-NHEJ), a major DNA double-strand break (DSB) repair pathway, is required for the repair of general DSBs as well as programmed breaks generated during antigen receptor gene rearrangements by V(D)J recombination. During this process, the lymphocyte-specific RAG1/2 endonuclease generates DSBs at numerous V, D and J genomic segments. The DNA ends are maintained in a postcleavage complex to facilitate end joining by C-NHEJ proteins, including Artemis, a DNA nuclease. Proper end joining is essential for lymphocyte development, immune diversification and to suppress structural chromosomal aberrations. Patients with null and hypomorphic mutations in *RAG, Artemis* and other C-NHEJ genes develop immunodeficiency disorders. Hypomorphic *Artemis* mutations that result in loss of the C-terminus are also associated with lymphomas harboring chromosomal translocations at the antigen receptor loci. The mechanisms that promote genomic instability in these patients are not entirely clear. This dissertation is focused on elucidating the roles of RAG1 and Artemis in preventing genomic instability during V(D)J recombination. These studies provide the first *in vivo* evidence that hypomorphic *Rag1* and *Artemis* mutations result in unique molecular defects characterized by chromosomal translocations at the RAG-induced breaks in non-malignant cells. My findings suggest that RAG1 and Artemis play important roles in maintaining postcleavage complex stability. Disruption of these complexes in the hypomorphic mutant lymphocytes results in premature release of DNA ends that may engage in aberrant V(D)J recombination. Recurrent chromosomal translocations are also a hallmark of sporadic human hematological malignancies, and of progenitor-B cell lymphomas in mice with combined C-NHEJ and tumor suppressor p53 deficiencies. Distinct alternative end joining (A-EJ) mechanisms have been implicated in mediating these translocations. The mechanisms that activate A-EJ are poorly characterized. My studies have demonstrated that induction of DNA damage response triggers alternative end-joining (A-EJ) in lymphocytes in the absence of Artemis resulting in chromosomal translocations at RAG-induced breaks. In summary, I have identified novel functions for RAG and Artemis in maintaining chromosomal integrity during V(D)J

recombination. These studies have improved our understanding of the origin of potentially oncogenic chromosomal translocations and have important clinical implications for both inherited cancer predisposition and sporadic tumors.

Chapter 1

Mechanism and Regulation of V(D)J Recombination

1.1 Overview

The work presented in this thesis is focused on examining the functions of RAG1 and Artemis in maintaining genomic stability during V(D)J recombination. Chapter 1 offers an introduction to the process of V(D)J recombination and how it is regulated. I also discuss the mechanisms that lead to aberrant V(D)J recombination and genomic instability. Chapter 2 includes parts of two published studies that investigated the roles of RAG1 and Artemis in maintaining postcleavage complex stability during V(D)J recombination in mice. Chapter 3 is a manuscript in preparation. This study explores the role of ATM-dependent DNA damage response in inducing end joining in Artemis-deficient mouse lymphocytes. In the last chapter, I summarize my conclusions and discuss potential future directions and implications of these studies.

1.2 Abstract

V(D)J recombination is a series of lymphocyte-specific programmed genomic rearrangements essential for antigen receptor diversity and lymphocyte development. It is initiated by the generation of DNA double strand breaks by RAG1/2 endonuclease at the germline V, D and J segments generating hairpin sealed coding ends. The DNA ends are subsequently joined by canonical non-homologous end-joining (C-NHEJ), a major double strand break repair pathway. During end-joining, the hairpin intermediates are opened by DNA-PKcs-

dependent Artemis endonuclease activity, and then joined by DNA Ligase IV/XRCC4 with junctional modifications. Defective V(D)J recombination due to mutations in cleavage or end-joining factors results in impaired lymphocyte development and immunodeficiency. Proper end joining is also essential to maintain genomic integrity during this process. Hypomorphic *Artemis* and *DNA Ligase IV* mutations predispose to lymphomagenesis in patients, though the underlying mechanisms are not clear. Likewise, mutations in other DNA damage response factors result in lymphomas bearing chromosomal translocations at the antigen receptor loci in both patients and mice. Clonal oncogenic translocations involving the RAG-induced breaks are also a hallmark of sporadic human hematological malignancies. These rearrangements are mediated by distinct, but poorly understood, alternative end joining (A-EJ) mechanism(s). Error-prone A-EJ is also actively involved in *IgH* and *c-myc*/*N-myc* genes rearrangements observed in progenitor-B cell lymphomas in mice with combined C-NHEJ and p53 deficiencies. In this chapter, I discuss the functions of RAG1/2 and Artemis proteins in the regulation of V(D)J recombination, disorders associated with aberrant cleavage and end joining, the role of DNA damage response during this process, and how defects in these processes contribute to genomic instability and lymphomagenesis.

1.3 Introduction To V(D)J Recombination

The adaptive immune system in the jawed vertebrates (cartilaginous fishes to mammals) is characterized by a vastly diverse repertoire of antigen receptors known as the T cell receptors (TCR) and B cell receptors (BCR) or immunoglobulins (Ig) expressed on the T and B lymphocyte cell surfaces, respectively [1]. Each lymphocyte expresses several receptors of a single specificity. A TCR is a heterodimer consisting of either gamma/delta- ($\gamma\delta$), or alpha/beta- ($\alpha\beta$) chains. A BCR (or Ig) comprises of two identical heavy (IgH) and two identical light (IgL) chains (Figure 1.1, bottom panel). Each antigen receptor comprises of an N-terminus variable and a C-terminus constant region. The variable region is formed by about 100 to 120 amino acids and is important for antigen recognition and binding [1]. This highly polymorphic region is encoded by an exon that is assembled from an array of germline variable (V), diversity (D) and joining (J) segments in the developing lymphocytes through a series of DNA rearrangements collectively known as V(D)J recombination (Figure 1.1, top panel; Table 1.1) [2]. This complex

process is restricted to G1 phase of the cell cycle and can be broadly divided into two phases, the cleavage phase and the joining phase [3].

Figure 1.1: Genomic Rearrangements By V(D)J Recombination and Antigen Receptors

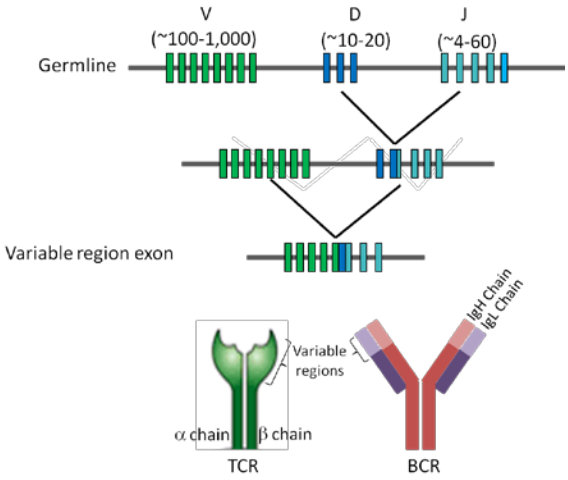

Table 1.1: Total Number of V, D and J Segments in Human and Mouse Genomes

Locus	Species	V		D		J	
		F	P	F	P	F	P
TCRγ	Human	6	5	-		5	-
	Mouse	7	-			4	-
TCRβ	Human	48	25	2	-	13	-
	Mouse	22	13	2	-	11	1
TCRα	Human	50	3	-		54	3
	Mouse	110	26			39	9
TCRδ	Human	3	-	3	-	4	-
	Mouse	5	1	2	-	2	-
IgH	Human	51	98	23	-	6	3
	Mouse	218	138	21	4	4	1
Igκ	Human	44	60	-		5	-
	Mouse	98	70			4	-
Igλ	Human	33	43	-		5	-
	Mouse	8	-			3	-

F = Functional P = Pseudogene
Based on information available in IMGT database

Cleavage phase.

V(D)J recombination is initiated by generation of site-specific DNA double strand breaks (DSBs) by a highly sophisticated, lymphocyte-restricted recombinase comprising of recombination activating gene products, RAG1 and RAG2, herein referred to as RAG1/2 (Figure 1.2) [4, 5]. Within accessible chromatin, RAG1/2 recombinase recognizes recombination signal sequences (RSSs) that flank individual V, D and J gene segments. Each RSS comprises of conserved heptamer and nonamer sequences (5'-CACAGTG-3' and 5'-ACAAAAACC-3', respectively) separated by a non-conserved spacer of either 12 or 23 nucleotides in length [6]. RSS-RAG1/2 interaction forms a signal complex which then captures a second appropriate RSS bringing two distant segments together in a stable synaptic or paired complex (capture model) (Figure 1.2) [7]. These two segments can be less than 20 kb to more than 100 kb apart. Recombination has a strong preference for 12/23 synapsis (based on spacer length) occurring only between two gene segments that are flanked by 12-RSS and 23-RSS to ensure ordered assembly of rearranging segments. Coupled cleavage within the two segments is initiated when RAG1/2 nicks at the 5' end of the heptamer (heptamer-coding sequence junction) resulting in 3'-OH which is used to catalyze a transesterification reaction on the opposite phosphodiester bond [8]. This generates four recombination intermediates, two covalently sealed hairpin coding ends and two 5' phosphorylated blunt signal ends [9, 10]. These DNA ends are held together by RAG proteins in a postcleavage complex (PCC) that protects the ends from degradation, prevents activation of p53-mediated apoptosis and also ensures proper joining [11].

Figure 1.2: RAG-Mediated Cleavage and DNA End Complex Assembly

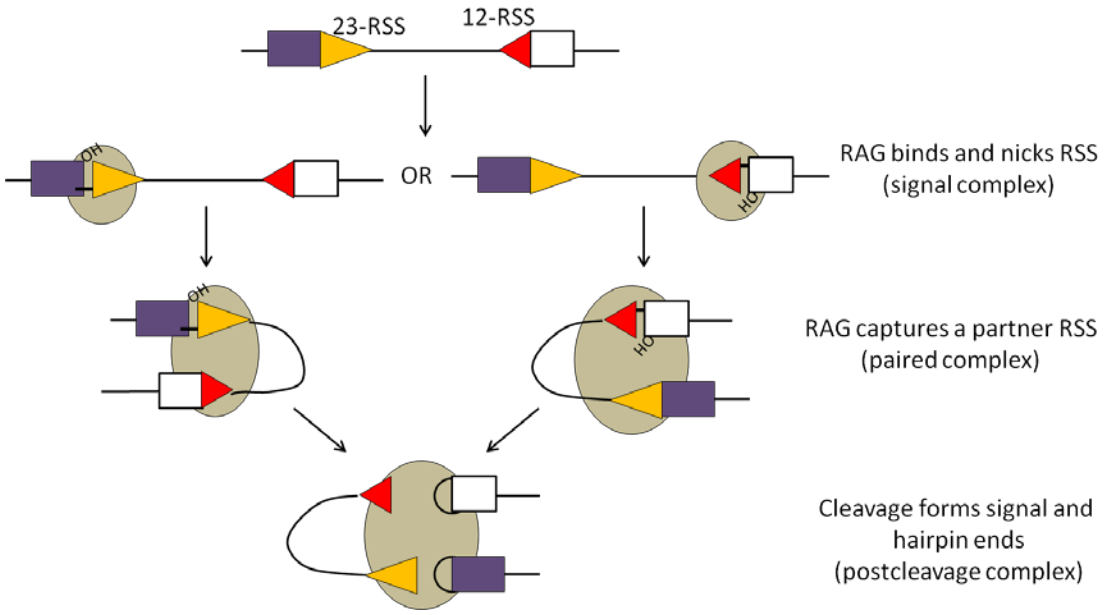

Joining phase- Role of Canonical Non-homologous End-Joining (C-NHEJ) Factors.

RAG-induced breaks are joined by the ubiquitously expressed canonical non-homologous end-joining (C-NHEJ) proteins including DNA-PK complex (comprising of Ku70/80 heterodimer and DNA-dependent protein kinase catalytic subunit, DNA-PKcs), Artemis, XRCC4, DNA ligase IV (LigIV) and XRCC4-like factor (XLF or Cernunnos) (Figure 1.3) [12-15]. The DNA ends are recognized and held together by Ku70/80 heterodimer which recruits DNA-PKcs [16]. Interaction with Ku and the DNA ends activates DNA-Pkcs kinase leading to autophosphorylation *in trans* as well as phosphorylation of Artemis [15, 17]. In complex with DNA-PKcs, Artemis acquires endonuclease activity which is required to open the hairpins at the coding ends [15]. An overhang at the coding end containing an inverted repeat, the palindromic (P) nucleotides, may result from asymmetrical hairpin opening 1 or 2 nucleotides away from the apex [18]. The coding junctions may be further diversified through exonuclease-mediated deletions. Nucleotides may also be added by template-dependent DNA polymerases (Pol μ/λ) or randomly (N nucleotides) by lymphocyte-specific template-independent Terminal deoxynucleotidyl Transferase (TdT) [19, 20]. The N nucleotides are usually GC-rich. The

modified ends are joined by DNA LigIV/XRCC4 to form a coding join or V(D)J exon [21]. Only one third of the exons formed by this process are in-frame and productive. The RSS ends are directly joined without any processing to form a precise signal joint. DNA-PKcs and Artemis are essential for only coding, and not signal, join formation [22, 23]. A detailed discussion of all the factors involved in V(D)J recombination is beyond the scope of this thesis. Since my thesis work is focused on RAG and Artemis, the structure and functions of these proteins will be discussed in detail in sections 1.3 and 1.4.

Figure 1.3: Cleavage and Joining Phases of V(D)J Recombination

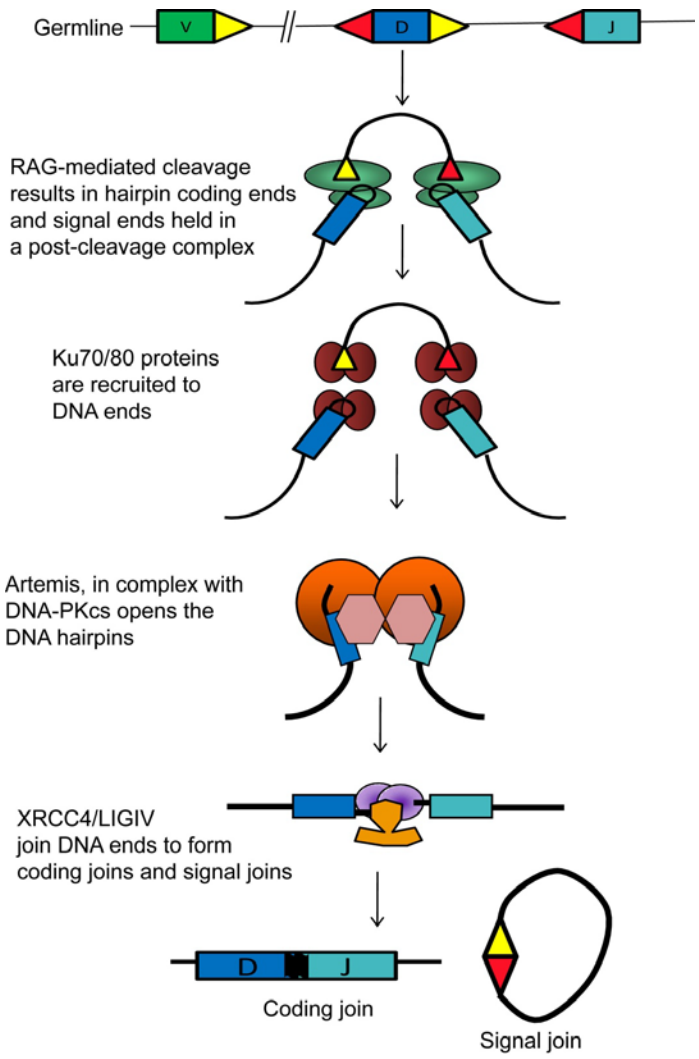

Coding end sequences are shown by boxes. Triangles represent signal end.

1.4 Structure and Functions of RAG1/2 Complex

The origin of *RAG* genes and Recombination Signal Sequences (RSS).

The functions of lymphocyte-specific TdT and RAG recombinase in V(D)J recombination were established about 500 million years ago between the divergence of the jawless and cartilaginous fishes, a span of almost 80 million years [24-26]. Several genetic and biochemical studies on the origin of V(D)J recombination suggest that sequences within the *RAG1* gene and RSSs were derived from transposons [27-29]. In 1979, Sakano *et al.* observed sequence similarities between RSSs and signal motifs at the termini of the integrated transposable elements [27]. *Transib* transposons in the genomes of nematodes, insects and sea urchin also contain RSS-like genetic elements [29]. Genomic sequences of unknown significance, similar to *RAG1* and *RAG2* genes have been discovered in sea urchin [30]. Additionally, RAG1 contains catalytic motif found in many integrases and transposases including the *Transib* transposases. Functional studies suggest that mechanism of DNA cleavage by direct transesterification is common between these enzymes [31, 32]. RAG complex has also been shown to be capable of functioning as a transposase *in vitro* and rarely *in vivo* [33-37]. These studies provide strong evidence that RAG1 and *Transib* transposases have a common progenitor.

RAG1 and RAG2 domain organization and functions.

The *RAG1* and *RAG2* genes are both located on human chromosome 11p13 and mouse chromosome 2p [5](*www.ncbi.nlm.nih.gov/)*. Murine RAG1 and RAG2 proteins contain 1040 and 527 amino acids, respectively. Only core RAG1 (384-1008aa) and core RAG2 (1-387aa) are required for recombination reaction in cell-free assays [8]. The non-core regions have been suggested to contain regulatory functions [38]. Mutagenesis and structural analyses have provided useful clues regarding their functions.

Core RAG1 contains (1) a nonamer binding domain (NBD) (aa 389-442), (2) a central domain (aa 528-760) and (3) a C-terminal domain (CTD) (aa761-979) (Figure 1.4, top panel) [39-41]. NBD, as the name indicates, binds the nonamer sequence within the RSS [42]. The central domain

interacts with RAG2, binds the heptamer sequence and single-stranded DNA. The CTD non-specifically binds double-stranded DNA. It also mediates interaction with the coding sequence adjacent to the RSS [43]. The central domain and CTD contain the catalytic DDE motif (asp-600, asp-708 and glu-962) [31, 44]. The distal non-core part of C-terminus (aa1009-1040) regulates RAG binding and cleavage activities by collaborating with RAG2 C-terminus. The non-core N terminal region plays roles in regulating protein levels, interaction with other proteins, coordination of zinc ions, and enhancing V(D)J recombination activity [43]. It also contains zinc-binding dimerization domain (aa 265-380).

RAG2 protein consists of (1) core RAG2 (aa 1-387) containing 6 kelch-like motifs (aa 1-350), (2) a flexible acidic hinge region (aa 360-408), and (3) C-terminal non-canonical plant homeodomain (PHD) (aa 414-487) (Figure 1.4, bottom panel) [40, 43]. Kelch like motifs are important for RAG1-RAG2 interaction and cleavage [45]. The PHD binds H3K4me3 (histone H3 trimethylated at lysine 4) and phosphoinositides. The C-terminus is also required to discriminate between the correct and off-target cleavage sites independent of its interaction with H3K4me3 [46]. A conserved threonine residue (T490) in the distal C-terminus mediates cell-cycle regulated degradation of RAG2 [43].

Figure 1.4: Domain Architecture of Murine RAG1 and RAG2 Proteins

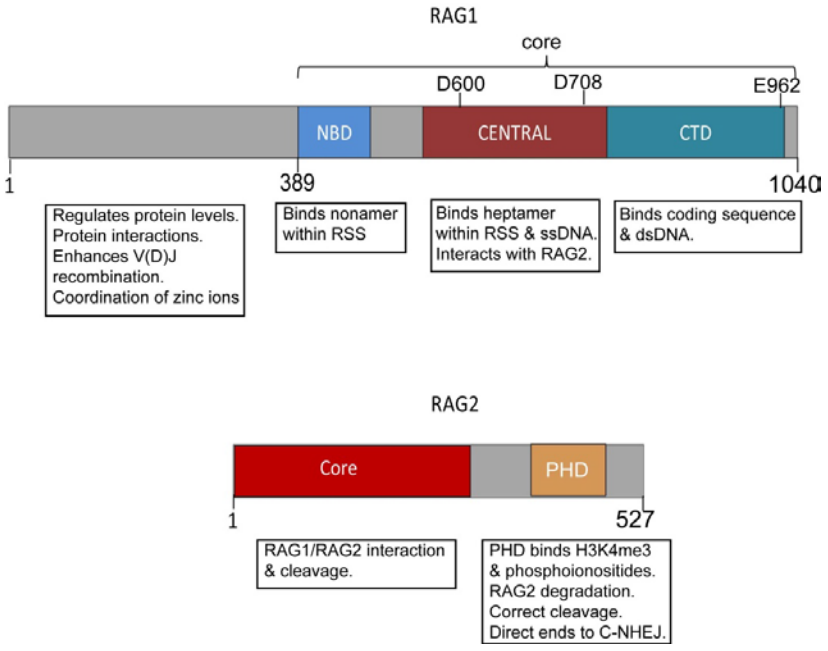

RAG1/2 interaction with accessible chromatin.

RAG1/2 plays important roles in regulating V(D)J recombination which exhibits remarkable tissue-, lineage-, development stage- and locus-specificity as well as allelic exclusion. This somatic recombination occurs only in lymphoid cells with Ig loci rearranging only in B-lineage cells and TCR loci in T-lineage cells. Moreover, recombination is restricted to certain development stages, as discussed in detail in section 1.6. The locus specificity is also temporally regulated with D-J rearrangements occurring prior to V-DJ. In addition, productive rearrangement of one allele prevents rearrangement at another allele via allelic exclusion at TCRβ, IgH and IgL loci [47]. It is very tempting to postulate that all these regulatory functions are mediated by accessibility to antigen receptor loci in a spatial and temporal manner. Indeed, over the last few years, several studies have offered insight into epigenetic modifications associated with V(D)J recombination linking regulatory RAG functions to specific alterations in chromatin architecture.

Studies using ChIP analysis have shown enrichment of H3K4me3 at genomic regions undergoing V(D)J recombination which also correlates with tissue, lineage and development stage-specificity [7]. For example, H3K4me3 deposition at antigen receptor loci was not observed in fibroblasts. Also, its enrichment at IgH locus was only observed in pro-B cells, and at TCRβ locus in pro-T cells. H3K4me3 marks the transcription start sites of protein-coding genes in the genomes of non-malignant cells [48]. RAG2 PHD domain has recently been shown to recognize H3K4me3 in a high-resolution crystal structure analysis. Reduced H3K4me3 retention impairs V(D)J recombination. Similarly, abrogation of PHD-H3K4me3 interaction severely reduce V(D)J recombination *in vivo*. However, additional factors must be involved to specifically target RAG proteins to antigen receptor loci since H3K4me3 is present at many other genomic regions. In this context, sequence-specific targeting to RSSs and additional chromatin modifications together might ensure RAG targeting to these loci [49]. High mobility group box proteins (HMGB1/2)- the DNA-binding and bending proteins- have also been shown to enhance affinity of RAG1 for 23RSS *in vitro* [50, 51]. The *in vivo* significance of HMGB1/2 proteins in V(D)J recombination is yet to be established [52]. In summary, several factors govern RAG binding to

DNA including sequence specificity, accessibility within the chromatin and proteins interacting with RAG [53].

Enhancers, promoters and transcription regulate RAG binding to DNA

Transcription occurs concomitantly with V(D)J recombination at an antigen receptor locus suggesting a coordination between the two processes [54]. Both *cis*- and *trans*-acting elements mediate chromatin modifications that are essential for locus accessibility during V(D)J recombination [55]. Loss of *cis* elements and certain transcription factors is associated with loss of both transcription and V(D)J recombination at these loci [56]. Additionally, transcription elongation itself regulates recombination [55]. It is not known if the transcription machinery interacts directly with RAG recombinase and mechanisms of transcription-recombination coupling need to be further investigated.

Overview of complex assembly and coupled cleavage by RAG

Quite a few biochemical studies have provided useful insight into the mechanisms of signal and paired complex assembly and coupled RSS cleavage by RAG1/2. Here, I give a brief overview of the mechanisms involved in complex assembly and cleavage.

RAG1/2 is necessary and sufficient for cleavage at RSS-coding end [41, 57]. Most of the residues responsible for DNA binding and cleavage are found in RAG1 [58]. RAG2 itself has no DNA-binding activity but enhances RAG1 interaction with the heptamer and specificity of this interaction [39, 40]. It is also an important co-factor for the cleavage activity [7]. Several studies report that synaptic and paired complexes (SC, PC) contain a RAG1 dimer with two RAG2 molecules within each complex [7, 59-61]. Other biochemical studies report contradictory findings regarding the stoichiometry of RAG1/RAG2 in the SC and PC and this needs to be further characterized [62, 63]. Some studies suggest that RAG1/2 interacts with 23-RSS first in a SC and then captures a 12-RSS. Others reports show that the order of interaction is independent of the spacer length [41]. The mechanisms underlying 12/23 synapsis are also not entirely clear. Not all 12/23 pairs exhibit the same recombination efficiency, indicating that factors beyond 12/23 pair also restrict cleavage [64]. The three residues within the DDE motif of

RAG1 together contribute to a single catalytic site which mediates nicking and hairpin formation *in trans* [41, 44]. After cleavage, the four newly generated ends are held together in a post-cleavage complex, the signal ends more stably so than the coding ends [35].

RAG1/2 channels DNA ends to C-NHEJ.

DNA DSBs generated during V(D)J recombination (referred to as RAG breaks in this thesis) are primarily repaired via C-NHEJ. It is still unclear how the ends are specifically directed to the C-NHEJ machinery. Deriano *et al.* recently showed that lack of RAG2 C-terminus in mice allows the ends to be repaired by error-prone alternative mechanisms of end-joining even in the presence of intact C-NHEJ [65]. This suggests a key role of RAG2 in maintaining post-cleavage complex stability or interaction with C-NHEJ factors and channeling the ends to the proper repair pathway.

Cell cycle-dependent RAG2 degradation

A conserved threonine residue (T490) in the distal C-terminus of RAG2 mediates cell-cycle regulated degradation of RAG2 via ubiquitination [66]. On G1 to S transition, this residue is phosphorylated by cyclinA/Cdk2 which allows RAG2 polyubiquitylation followed by proteasomal degradation. This is important to restrict V(D)J recombination to G1 phase and to prevent propagation of breaks to G2. Indeed, a RAG2 mutant, p.Thr490Ala, that interferes with its degradation allows for homologous recombination-mediated aberrant recombination.

1.5 Structure and Functions of Artemis

The *Artemis* gene is located on the short arm of chromosome 10 in humans and on chromosome 2 in mice (*www.ncbi.nlm.nih.gov/)*. Murine Artemis is 705 amino acids long. Mouse and human cDNAs share 73% sequence identity and 81% sequence similarity. It is a ubiquitously expressed nuclear protein that plays an essential role in V(D)J recombination. Artemis is also important for general DNA double strand break repair via C-NHEJ. It is a member of the metallo β–lactamase superfamily based on sequence similarities and the predicted secondary structure of its catalytic domain.

Domain organization

The highly conserved N-terminus contains β-lactamase and β-CASP domains (Figure 1.5) [18, 67, 68]. These two domains together constitute the catalytic core of Artemis specific for nucleic acids [68]. A histidine residue (his-254) within the β-CASP domain has been reported to be critical for full Artemis catalytic activity *in vitro* [69, 70]. The C-terminus regulatory domain, is encoded by a single exon 14 [68]. It occupies almost half the protein, is less conserved and its significance is not entirely clear. This region is dispensable for catalytic activity during V(D)J recombination on plasmid substrates [68]. It contains at least 14 phosphorylation sites for phosphatidylinositol 3-kinase like kinases (PIKKs) including DNA-PKcs and Ataxia-Telangiectasia Mutated (ATM) (Figure 1.5) [71, 72] as indicated by the presence of S/T-Q motifs (serine or threonine followed by glutamine) [73]. L401 and R402 residues are important for Artemis recruitment to the DNA ends by DNA-PKcs (Figure 1.5) [74, 75]. Recent biochemical and structural studies have shown that the Artemis C-terminus also directly binds the DNA-binding domain (DBD) of DNA LigIV at three critical regions, W489, F492, F493 (Figure 1.5) [76-78].

Figure 1.5: Domain Architecture of Artemis

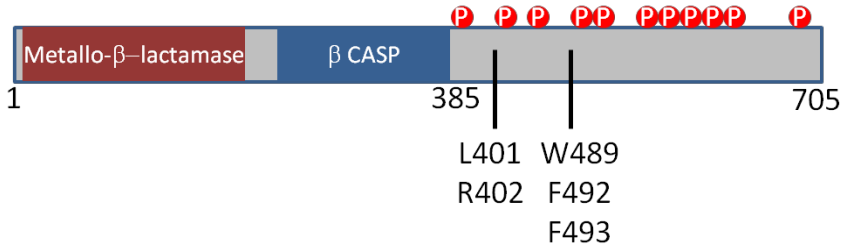

Artemis substrates

Artemis, in complex with DNA-PKcs, acquires structure-specific endonuclease activity for single-stranded to double-stranded DNA (ssDNA-dsDNA) transitions including 3' and 5' overhangs, and hairpin structures, generating blunt or 3' overhangs [15]. In addition, Artemis/DNA-PKcs complex also has endonucleolytic activities on flaps, stem-loops, heterologous loops and gaps [79]. This versatility is important in the removal of secondary structures during DNA repair by NEHJ.

Regulation of Artemis endonucleolytic activity

The endonuclease activity of Artemis-DNA-PKcs complex is required to open the hairpin intermediates generated during V(D)J recombination [80]. Artemis is also important in repair of a subset of complex DSBs induced by ionizing radiation [81]. Artemis C-terminus plays important roles in regulating its endonuclease activity. Expression of N terminus alone is not sufficient to rescue radiosensitivity in Artemis-null cells suggesting that C-terminus has important roles in DNA repair [73]. Interaction of Artemis with DNA-PKcs results in its recruitment to the DNA ends [74, 75]. Artemis phosphorylation by DNA-PKcs is not necessary for activation of its endonucleolytic activity [17, 71]. A mutant Artemis protein that lacks majority of phosphorylation sites but retains its interaction with DNA-PKcs exhibits significant endonucleolytic activity in a mouse model generated in our lab [82]. Instead, DNA-PKcs autophosphorylation at T2609-T2647 cluster enhances Artemis endonucleotlytic activity [17, 83]. It has been suggested that the conformational change induced in Artemis by the activated DNA-PKcs allows it to acquire endonucleolytic activity.

1.6 Antigen Receptor Loci Assembly

B and T lymphocytes contain seven antigen receptor loci; IgH, IgLκ, IgLλ and TCRα, β, γ, δ (Table 1.1). At IgH, TCRβ and TCRδ loci, DJ rearrangement is followed by V to DJ recombination. At IgL, TCRα and TCRγ loci, V to J rearrangements occur directly.

Recombination occurs by deletion or inversion depending on the relative orientation of the RSSs. Deletional rearrangement occurs when RSSs are in the opposite orientation and results in the retention of the coding join in the chromosome and deletion of the circular chromosome containing the signal join (Figure 1.2). When the RSSs are in the same orientation (within Igκ, TCRδ and TCRβV14 loci), the intervening genomic region is inverted to form a coding join with retention of both joins in the chromosome (Figure 1.6) [84]. Non-functional recombination can occur rarely when a coding end joins a signal end (1) in the original configuration (open-and-shut join) [41, 85, 86] or (2) from the other segment (hybrid join) (Figure 1.2) [41, 85, 86]. Since most of this thesis work is focused on examining TCRβ locus rearrangements, I will be discussing this in detail here. Recombination at other loci follows the same pattern.

Figure 1.6: Inversional Rearrangement

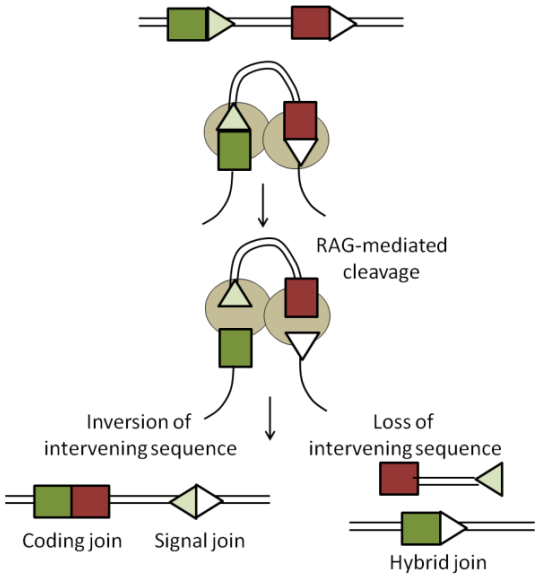

TCRβ locus comprises of 35 V segments; 22 functional and 13 pseudogenes. All but one functional segment are located in the 5' region followed by two clusters of D-J-C (C=constant) segments (Figure 1.7) [87]. Vβ14 is located 3' to D-J-C clusters in the opposite transcriptional direction with an enhancer lying between Vβ14 and Cβ2. Rearrangements between 5' V and DJ segments occur by deletion whereas rearrangements between Vβ14 and DJ clusters occur via inversion. After rearrangement, promoter region upstream of V region, now closer to enhancer, regulates rearranged gene transcription. During mRNA processing, V(D)J exon is spliced together with the C exon to be translated in to TCRβ chain.

Figure 1.7: Murine TCRβ Locus

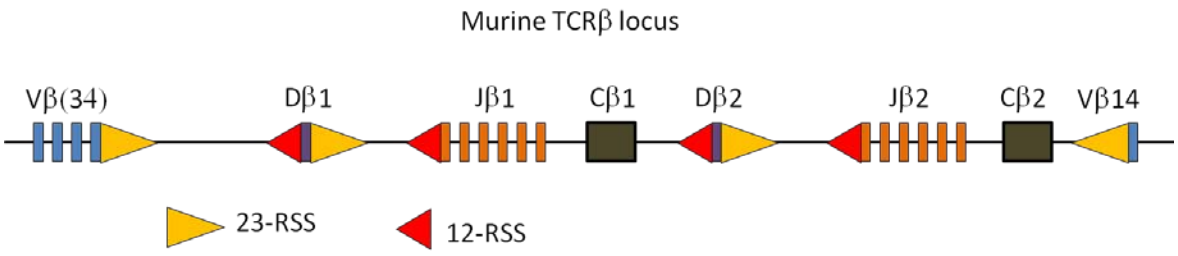

1.7 Coordination Between V(D)J Rearrangements and Lymphocyte Development

The regulation of V(D)J recombination in a cell lineage- and stage-specific manner is evident by its coordination with lymphocyte development [88].

T cell development.

After early precursor cells move to thymus from bone marrow, they go through several stages of development which can be broadly classified in to three stages based on the expression of CD4 and CD8 cell surface receptors: $CD4^-CD8^-$ (double negative, DN), $CD4^+CD8^+$ (double positive, DP) and $CD4^+$ or $CD8^+$ (single positive, SP) cell stages. DN cells are further divided in to four stages, DN1, DN2, DN3 and DN4, based on CD44 and CD25 expression (Figure 1.8) [89]. TCRβ, γ and δ rearrangements occur in DN cells. TCRγ and δ, which are expressed in $\gamma\delta$-T cells, have been suggested to rearrange in DN1/2 stage [90]. However, rearrangement of these two loci does not affect progression to the next stage. TCR Dβ-to-Jβ rearrangements occur in DN2 cells followed by Vβ-to-DJ rearrangements mostly in DN3 stage. The rearranged TCRβ chain, along with pre-Tα and CD3 forms pre-TCR. Pre-TCR signaling decreases CD25 and RAG expression resulting in DN4 cells committed to $\alpha\beta$ T cell lineage. Cells that have successfully rearranged TCRβ now go through β-selection with a proliferative burst, accompanied by up-regulation of CD4 and CD8 resulting in DP cells. TCRα rearrangements occur at this stage that leads to the formation of $\alpha\beta$ TCR heterodimer ($\alpha\beta$-T cells). DP cells undergo positive selection (cells that only react to foreign antigens and not to self antigens) and differentiate in to $CD4^+$ or $CD8^+$ SP cells which can eventually populate the peripheral lymphoid organs such as spleen and lymph nodes [89].

Figure 1.8: Coordination Between T Lymphocyte Development and V(D)J Recombination

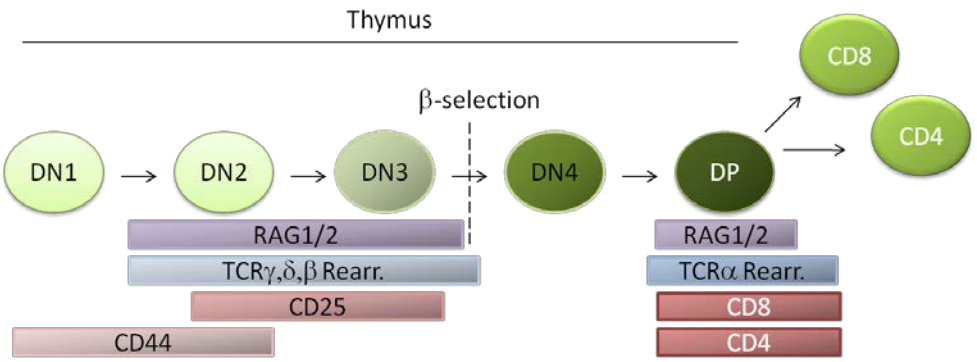

B cell development.

D_H to J_H rearrangements within the IgH locus start in early and common lymphoid progenitors (ELP/CLP) before B lineage specification. V_H to DJ_H rearrangement is completed during B lymphocyte development in $B220^+CD43^+$ pro B cells, [91, 92] followed by the generation of $B220^+CD43^-$ pre B cells. IgH, together with surrogate light chains λ5 and Vpre-B, is expressed as pre-BCR. This triggers signaling for cell proliferation, selecting cells with functional IgH [93]. Light chain locus rearrangement occurs subsequently in the pre-B cells. There are two light chain isotypes in mammals; kappa (Igκ) and lambda (Igλ) light chains. Igκ is rearranged before Igλ. In each cell, IgH and IgL proteins are expressed from only one rearranged corresponding allele (allelic exclusion) and IgL protein comprises of either Igκ or Igλ isotype (isotype exclusion). Successful light chain rearrangement results in transition to premature IgM^+ B cells.

Figure 1.9: Coordination Between B Lymphocyte Development and V(D)J Recombination

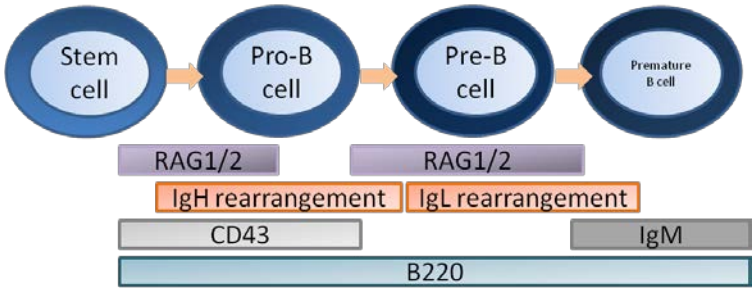

1.8 DNA Damage Response (DDR) and Mechanisms of End-joining

DNA DSBs arise as necessary intermediates during meiosis, V(D)J recombination and class switch recombination (CSR). CSR is a B lymphocyte-specific process important for immunoglobulin isotype switching. In addition, genotoxic DSBs result from ionizing radiation (IR), chemotherapeutic drugs, replication across a nick and oxidative free radicals. These breaks are detected by MRN complex comprising of MRE11/RAD50/NBS1. The MRN complex tethers DNA ends together keeping them in close proximity [94, 95] and activates PIK serine/threonine protein kinases which include Ataxia-Telangiectasia Mutated (ATM), DNA-PKcs and ATM- and Rad3-Related (ATR) [96]. These kinases, in turn, phosphorylate effector proteins. ATM and DNA-PKcs can be activated at any stage of cell cycle. However, ATR is primarily activated in post-replication phase and will not be discussed here.

Cell cycle checkpoints are important phosphorylation targets that arrest the cell cycle in response to DNA damage to allow for DNA repair. There are two major DSB repair pathways: homologous recombination (HR) and C-NHEJ. HR requires a homologous sequence on a sister chromatid and is active only after DNA replication [97]. C-NHEJ involves direct ligation of ends and is active throughout the cell cycle. My studies are focused on the NHEJ pathway for DSB repair. If DNA repair fails, cells undergo senescence or apoptosis. Rarely, DSBs are misrepaired leading to structural chromosomal aberrations like deletions, inversions and translocations which can be potentially oncogenic. Here, I will discuss aspects of DNA damage response

relevant to this thesis work. This includes the role of ATM kinase and end-joining mechanisms particularly during V(D)J recombination.

Ataxia Telangiectasia Mutated (ATM).

ATM kinase exists as an inactive homodimer [98]. In response to DSBs, it is recruited to the site of damage through direct interaction with NBS1, a member of the MRN complex [98]. At the site of damage, it undergoes autophosphorylation at serine 1981 forming active monomers and in turn regulates numerous processes that include cell cycle checkpoint activation, DNA repair, apoptosis and gene transcription [99, 100]. Some of its important phosphorylation targets are checkpoint kinase Chk2, H2 histone variant H2AX, tumor suppressor p53, MRE11 and NBS1 [101-103]. H2AX is phorphorylated at Serine 139 (γH2AX) by ATM, ATR and DNA-PKcs on DNA damage [104]. This helps in recruiting other DDR proteins or retaining them at the site of damage. p53-mediated apoptosis is important to remove cells with unrepaired breaks. *ATM* mutations are associated with genomic instability disorders discussed in detail in sections 1.9 and 1.10.

C-NHEJ during general DNA DSB repair:

During general DSB repair, NHEJ factors repair the ends with minimal end modifications to preserve genetic information. About 90% of the DSBs are repaired by NHEJ [105].The core C-NHEJ factors- Ku70, Ku80, Ligase IV and XRCC4- are conserved from yeast to mammals and sufficient to join compatible DNA DSBs [106]. Radiation-induced breaks, that often contain complex nucleotide damage, require processing by nucleases and/or gap-filling synthesis by polymerases to be joined [107]. Artemis and DNA polymerases μ/λ are required to repair this subset of DSBs. Another factor, XLF, enhances the ligation activity on the non-compatible ends *in vitro* [14] and gap-filling by polymerases [108]. The process of end-joining during DSB repair proceeds as described for V(D)J recombination in section 1.2.

Alternative non-homologous end-joining pathway(s) (A-NHEJ).

End-joining that occurs in the absence of C-NHEJ and is not reliant on long stretches of homology is broadly defined as alternative end-joining [106]. However, it may involve one or

more distinct pathways [64, 83, 109]. It appears to be kinetically slower than C-NHEJ [110-113]. Previously, microhomology-mediated end-joining (MMEJ) was considered to be responsible for all A-NHEJ. More recently, it has been suggested that this is not an absolute requirement although the use of terminal microhomology may be increased in A-NHEJ [64, 83, 109]. This pathway was first reported in mammalian cells in 1986 and to this date not much is known about its molecular components [114]. Several proteins that have key roles in other repair pathways including homologous recombination have been implicated such as Poly (ADP-Ribose) Polymerase I (PARP1), NBS1, MRE11, CtIP, DNA Ligase III (LigIII) and Ligase I (LigI), XRCC1 [113, 115-118]. CTIP interacts with MRE11 and both function in DNA end-resection during homologous recombination [113, 118-122]. MRE11 has 3' to 5' exonuclease activity but it can also open DNA hairpin loop [123]. MRE11 overexpression is associated with increase in A-NHEJ and its interaction with DNA LigIII/XRCC1 is increased after DNA damage induction in DNA LigIV-deficient cell lines [120, 124]. Yun and Hiom revealed that CtIP is required for microhomology-mediated en joining (MMEJ) in an avian B cell line in the G1 phase of the cell cycle [122]. DNA LigIII, XRCC1 and PARP1, are usually involved in ssDNA repair [118, 124]. Currently, the molecular components as well as activation and regulation of this pathway are poorly understood, and thus need to be investigated in detail.

DNA damage response factors in V(D)J recombination.

Although largely dispensable for V(D)J recombination, ATM is localized to the RAG-induced breaks indicating that it plays some role during V(D)J recombination [125]. Similarly, other DDR proteins including MRE11, NBS1 and γH2AX are not required for normal V(D)J recombination. However, loss of these proteins increases interchromosomal rearrangements and chromosomal deletions at the antigen receptor loci [126-128]. The mechanisms underlying these end-joining defects are discussed in detail in section 1.11. In brief, ATM kinase activity has been suggested to play important roles in maintaining post-cleavage complex stability during V(D)J recombination, most likely by modulating the DNA tethering activity of its downstream targets including MRN complex and/or by regulating chromatin modifications through γH2AX [127, 129]. Altogether, ATM, MRE11, H2AX and NBS1 are not essential for normal V(D)J

recombination but are more likely important to prevent misrepair of the RAG-breaks and genomic instability.

A-NHEJ is not utilized during normal V(D)J recombination [106]. [118] However, the contribution of this pathway to V(D)J recombination may be masked by intact C-NHEJ and needs to be further characterized. It has been shown to play a role in aberrant V(D)J recombination. MRE11 and CtIP have been implicated in error-prone alternative end-joining during the G1 phase of the cell cycle [121, 124, 126]. NBS1 is required for alternative end joining of hairpin coding ends [118]. CtIP also promotes end resection of RAG-generated breaks via MMEJ in the absence of H2AX and this resection is dependent on ATM kinase [126]. In summary, there is some evidence for the role of DDR during V(D)J recombination but the regulation of these process is still not entirely understood and needs to be defined in the context of both the normal and aberrant rearrangements.

1.9 Inherited Defects in V(D)J Recombination and Human Disease

Primary immunodeficiences.

This includes a broad spectrum of diseases ranging from Severe Combined Immunodeficeincy Disorder (SCID) to combined immunodeficiency [130, 131]. Defective V(D)J recombination is responsible for about 30% of cases. These patients present with recurrent respiratory and gastrointestinal infections with a failure to thrive at an early age. These infections are frequently caused by opportunistic organisms (*Pneumocystis carinii; Aspergillus)* and viruses (*Cytomegalovirus*). The life expectancy is usually less than a year unless the patient receives a successful bone marrow transplant [132].

Null and hypomorphic mutations in *RAG1*, *RAG2* or C-NHEJ genes lead to primary immunodeficiencies. *RAG* mutations are responsible for 10% of all SCID cases reported [133]. The autosomal recessive disorder due to RAG deficiency usually leads to classical T^-B^- SCID. The carrier individuals with heterozygous mutations have no immunological deficiencies (MIM #179615 and #179616).

Defects in C-NHEJ factors lead to immunodeficiency with general DNA repair defect and cellular sensitivity to ionizing radiation, a condition known as Radiosensitive (RS)-SCID (Table 1.2) [131, 134]. Molecular and genetic analyses of the patient cell lines and experimental animal models were instrumental in the discovery of many DNA repair factors, including Artemis [135]. At least 48 different immunodeficiency-associated mutant *Artemis* alleles have been identified and most of these mutations affect the N-terminus catalytic domain [136, 137]. Null mutations usually lead to $T^{-}B^{-}NK^{+}$ SCID. Patients with hypomorphic mutations present with varying degree of immunodeficiency ($B^{-/low}T^{-/low}$ SCID) due to residual V(D)J recombination activity.

Defects in other C-NHEJ factors have also been reported. A misense mutation in *PRKDC*, the gene that encodes DNA-PKcs, results in a mutant protein (p.Leu3062Arg) that reduces Artemis endonucleolytic activity [138]. *LIG4* mutations leads to SCID or Ligase IV syndrome characterized by immunodeficiency, chromosomal instability, growth retardation, microcephaly and unusal facies (distinct facial features associated with a medical condition) (Table 1.2) [139, 140]. *XLF* mutations also cause immunodeficiency, bird-like facies, growth retardation and microcephaly [141]. There are no known defects in Ku70/80.

Omenn syndrome.

This is an autoimmune-like disorder characterized by a range of immunocompromised states associated with activated T lymphocytes of highly restricted TCR heterogeneity in the peripheral tissues, elevated levels of eosinophils and IgE, hepatosplenomegaly and lymphadenopathy [142]. These patients usually present with skin rash and colitis due to infiltration with the activated T lymphocytes, and alopecia (hair loss). It ultimately requires allogenic bone marrow transplant.

It was first clinically described in 1965 by Gilbert Omenn [143]. Mutations in *RAG1*, *RAG2* and *Artemis* genes responsible for this syndrome have only recently been identified [144-146]. These mutations are considered hypomorphic because of residual (> 1%) V(D)J recombination as compared to the wild-type levels and leaky lymphocyte development.

Table 1.2: Human Genetic Disorders Associated with Defects in C-NHEJ Factors

C-NHEJ Factor	Mutations	Disease	Predisposition to lymphomas
Ku70/80	Not known	-	
DNA-PKcs	Hypomorphic	RS-SCID	Not known
Artemis	Null	RS-SCID	Not known
	Hypomorphic	Combined immunodeficiency , RS Omenn Syndrome	EBV-associated lymphomas
Ligase IV	Hypomorphic	Ligase IV syndrome/ Dubowitz syndrome	T Cell leukemia (2) B cell lymphoma (1) Myelodysplasia (1) EBV-associated lymphoma (1) Squamous cell carcinoma (1)
XRCC4	No human mutations identified		
XLF	Yes	Growth retardation, immunodeficiency, RS	Not known

Number within parantehsis indicate number of patients
RS=Radiosensitive

Predisposition to lymphomas.

Hypomorphic Artemis mutations. So far, no *RAG1*/2 mutations and no null *Artemis* mutations have been reported to be associated with tumors in humans. Two patients with hypomorphic *Artemis* mutations (D432fsX15, D451fsX10) developed aggressive EBV-associated lymphomas. These mutations result in premature truncation of C-terminus. Unlike other EBV-associated lymphomas, these patient tumors had clonal origins and features of genomic instability indicating distinct pathological mechanisms underlying tumorigenesis [147]. We generated a mouse model in our lab based on D451fsX10 mutation and elucidated the oncogenic mechanisms. The findings from that study will be discussed in detail in Chapter 2.

LIG4 mutations. Hematological malignancies have been reported in patients with *LIG4* mutations. These include T cell leukemia (two cases), B cell lymphoma, myelodysplasia and EBV-associated lymphoma (one case for each tumor type) [139, 148, 149]. Recently, a patient diagnosed with Dubowitz syndrome at 1-year of age who developed squamous cell carcinoma almost four decades later, was also found to have compound heterozygous mutations in *LIG4* [150].

ATM, NBS1 and MRE11 mutations. Germline *ATM* mutations result in Ataxia-Telangiectasia (AT) which is characterized by cerebellar ataxia, ocular telangiectasia, lymphopenia, sensitivity to ionizing radiation and lymphoid tumors with translocations involving antigen receptor loci [151-153]. *NBS1* mutations result in Nijmegan breakage syndrome with IR sensitivity, immunodeficiency, chromosomal abnormalities and lymphomas very similar to those seen in AT patients [154, 155]. *MRE11* mutations in patients (Ataxia-Telangiectasia like disorder) have been associated with translocations involving antigen receptor loci and solid tumors [100, 156]. No lymphomas resulting from germline *MRE11* mutations have been reported so far.

1.10 Mouse Models of Defective V(D)J Recombination

RAG1-, RAG2- or Artemis-deficiency in mice recapitulates the patient phonotypes with T^-B^-SCID (RAG1/2-null mice) or $T^{-/low}B^-$ SCID (Artemis-null mice) [157, 158]. Lymphocytes are arrested at DN2/DN3 (T cells) and pro-B cell stage. RAG1- and RAG2-null mice do not develop any other anomalies.

Mutant Ku70, Ku80, DNA-PKcs and Artemis mice exhibit cellular sensitivity to ionizing radiation along with defective lymphocyte development [157, 159-162]. Ku70 or Ku80-deficiency also leads to growth retardation and sterility whereas DNA-PKcs- and Artemis-defective mice are normal in size and fertile. This suggests that DNA-PKcs and Ku70/Ku80 function together as a complex but also have distinct functions. The lymphocytes in C-NHEJ-defective mice harbor unresolved hairpin coding ends. Low levels of joins that are formed in the absence of Artemis and DNA-PKcs are qualitatively distinct with extensive deletions and an increase in the number of P nucleotides. XRCC4 or LigIV deficiency leads to late embryonic lethality due to neuronal apoptosis [163].

Two mouse models with mutant RAG1 (R972G) and RAG2(R229Q) proteins have been reported to develop features of Omenn Syndrome [164, 165].

Lymphomagenesis in mice with defects in C-NHEJ & DNA damage response (DDR).

Mice with C-NHEJ deficiency rarely present with lymphoid tumors most likely due to the p53-mediated cellular apoptosis. Mice with combined C-NHEJ and p53 deficiencies develop pro-B

lymphomas with non reciprocal translocations involving *IgH* and *c-Myc* genes resulting in amplification of both genes [110]. Mice with only p53 deficiency develop lymphoid tumors most of which do not harbor chromosomal aberrations at the RAG breaks.

Mice with defects in DNA damage response factors harbor elevated levels of genomic instability and unrepaired coding ends in their lymphocytes [129, 166]. ATM-deficient mice succumb to early onset thymic lymphomas similar to those observed in AT-patients [167-169]. These tumors bear chromosomal translocations involving the TCRα/δ locus. Targeted disruption of *Nbs1* in mice also leads to development of lymphomas harboring similar rearrangements as seen in *Atm*$^{-/-}$ mice [170]. Combined H2AX and p53 deficiencies also lead to the development of B cell lymphomas harboring chromosomal translocations including *IgH* to *c-Myc* translocations [171, 172].

In our lab, two mouse models with hypomorphic *Rag1* and *Artemis* mutations also developed lymphomas on a p53-deficient background providing the first *in vivo* evidence for roles of these proteins in preventing genomic instability. These studies are discussed in chapter 2.

1.11 Misrepair of RAG Breaks and Tumorigenesis

In addition to lymhomagenesis observed with the above-mentioned germline mutations, sporadic lymphoid tumors also frequently harbor recurrent structural chromosomal aberrations that result from mis-repair of RAG-breaks. These include translocations, deletions and inversions, all of which require DNA DSBs. Some of the most recurrent translocations are (1) t(14;18)-*BCL-2/IgH* in follicular lymphomas, (2) t(8;14)-*c-MYC/IgH* translocations in Burkitt's lymphoma (3) t(11;14)-*BCL-1/IgH* in mantle cell lymphoma [109, 110]. These recurrent events may result from selective pressures conferred by the deregulated expression of protooncogenes and/or spatial proximity bias for their formation. Chromosomal deletions and inversions may result if two DSBs are located on the same chromosome. In this section, I will discuss the mechanisms associated with germline and somatic defects that lead to misrepair of DNA breaks and genomic instability during V(D)J recombination. A combination of these factors along with loss of checkpoints contributes to tumorigenesis.

Substrate recognition errors.

Millions of cryptic RSSs have been identified in human and mouse genomes. These sequences resemble RSSs and are found in non-antigen receptor regions [173]. Many gene partners of antigen receptor loci in oncogenic translocations have breakpoints at these cryptic RSSs [173, 174]. Deletions and inversions of chromosomal segments at RSS-like sequences have also been observed in tumors. Deletion of *MTS1*, a tumor suppressor, in T-ALL (Acute lymphoblastic leukemia) contains a heptamer sequence at the breakpoint [175]. The broken chromosome ends are also joined by mechanisms suggestive of end-joining. Joining of breaks at two cryptic RSS also leads to aberrant events such as interstitial deletion between *SCL* and *SIL* [176, 177]. Recent studies have suggested that RAG2 C-terminus is required to discriminate between the correct and cryptic RSSs [46]. Mice lacking non-core RAG2 C-terminus develop lymphomas [65]. Loss of this discrimination and H3K4me3 specificity might at least partially account for the features of genomic instability in this mouse model.

Unusual structures like non-B DNA, when present adjacent to nonamer sequences, also serve as cleavage substrates for RAG complex [178, 179]. A non-B DNA structure located in *BCL2* genomic region is a major RAG cleavage target and generates t(14;18)*BCL-2/IgH* translocation.

In biochemical assays, RAG1 can bind DNA in the absence of RAG2, [52]. The *in vivo* evidence for such binding is lacking and RAG1 would still require RAG2 for its catalytic activity. However, if RAG1 can non-specifically bind DNA independently of RAG2 in phases when RAG2 is not present (S/G2/M) *in vivo*, this may also contribute to aberrant cleavage through other uncharacterized mechanisms.

Post-cleavage complex (PCC) Stability.

The cleaved DNA ends are held in complex with RAG and other proteins within PCC which ensures that ends are directed specifically to C-NHEJ pathway. Insight into the functions of RAG1/2 in maintaining PCC structural integrity was offered by genetic studies that used separation-of-function RAG mutants, including RAG1 p.Ser723Cys and Ser723Ala mutants. These mutants retained cleavage activity but affected interaction with the coding ends after

cleavage [180]. Kumar and Swanson reported that full-length RAG1 enhances coding end retention in PCC in biochemical assays [181]. In the same study, the authors observed that a RAG1 p.Lys980Ala mutant forms coding joins characterized by long deletions, long P nucleotides and microhomologies. Lack of RAG2 C-terminus also predisposes to end-joining by the use of microhomologies and deletional hybrid joins in mice [65]. This suggests that ends released prematurely from PCC do not engage in proper end-joining and are available for joining by error-prone A-NHEJ. Over the last seven years, other proteins that were previously considered dispensable for V(D)J recombination, have been implicated in maintaining PCC stability and suppressing chromosomal translocations at RAG breaks. These include ATM, MRN complex, and H2AX [127, 129, 182]. These studies provide a potential explanation for the development of translocations involving RAG breaks in cells with mutations in *ATM, NBS1* and *MRE11* genes. ATM-, NBS1- and H2AX- deficient mice also exhibit translocations involving antigen receptor loci in non-tumor cells and develop thymic lymphomas with $\alpha\delta$-translocations [170]. Presence of hybrid joins associated with aberrant deletional recombination in ATM-, MRE11-, and NBS1-deficient pre-B lymphocytes further supports this hypothesis [127, 129]. ATM has been suggested to mediate this effect by regulating DNA end tethering by MRN complex and H2AX-dependent chromatin modification along the cleaved DNA ends [182]. H2AX also prevents CtIP-mediated end-resection in an ATM-dependent manner [126].

Our lab showed the first *in vivo* evidence for a role of RAG1 and Artemis proteins in PCC stability and lymphomagenesis by examining the effect of hypomorphic mutations in these genes on V(D)J recombination. The findings from these studies are discussed in detail in Chapter 2.

Repair pathway choice.

Many chromosomal translocation breakpoints in hematological malignancies, and some solid tumors, show microhomologies indicating an active role of A-NHEJ in catalyzing translocations [110, 183]. Tumors associated with combined C-NHEJ- and p53- deficiencies in mice also harbor translocations that are RAG-dependent and exhibit microhomologies at the breakpoint junctions [184].

Why do translocations show increased use of A-NHEJ mechanisms? The underlying mechanisms for this preference are not entirely clear. Genome-wide analysis to compare translocations involving I-SceI-generated breaks between C-NHEJ deficient and wild-type cells did not show any significant qualitative differences. Thus, translocations may favor use of A-NHEJ over C-NHEJ even in wild-type cells [110]. In addition, A-NHEJ is active in lymphocytes with *Rag2* mutations that have intact C-NHEJ indicating that the two pathways co-exist in cells [65, 185]. Breaks that persist may undergo resection making them vulnerable to microhomology-mediated end-joining which may be less biased towards intrachromosomal joining. CtIP-dependent resection of coding ends in H2AX-deficient lymphocytes has been shown to promote the use of microhomologies [126].

DNA damage response.

In addition to stabilizing RAG breaks, ATM also plays important roles in activating checkpoints in response to DSBs generated by ionizing radiation and other genotoxic agents to ensure proper repair. Defects in ATM-mediated checkpoint activation results in persistence of the DSBs in the mature cells where they can be joined aberrantly. The breaks that persist through cell cycle may also join with DSBs produced during class switch recombination in mature B lymphocytes. Tumor suppressor p53-mediated apoptosis also suppresses lymphomagenesis as indicated by development of pro-B lymphomas with *IgH*/*c-Myc* co-amplification in C-NHEJ- and p53-deficient mice.

1.12 Concluding Remarks

Generation of DNA DSBs during V(D)J recombination is integral to lymphocyte development. Thus, several spatiotemporal regulatory mechanisms are active in developing lymphocytes to maintain genomic stability. Defects at each step of this process can lead to misrepair of the RAG breaks. A combination of these defects will eventually result in malignant transformation. An understanding of mechanisms underlying tumorigenesis in the developing lymphocytes is essential to improve the prognosis and clinical outcome in patients. Mouse models based on these mutations thus provide an invaluable *in vivo* system to investigate these processes.

Chapter 2

Spontaneous Genomic Instability and Lymphomagenesis in Mice Harboring Hypomorphic *RAG*1 and *Artemis* Mutations

2.1 Abstract

As discussed in Chapter 1, RAG1/2 and Artemis endonucleases play essential roles during V(D)J recombination by generating DNA double-strand breaks at specific recombination signal sequences and opening hairpin coding ends, respectively. Inactivating *RAG* and *Artemis* mutations cause a human severe combined immunodeficiency syndrome (SCID) characterized by arrested lymphocyte development due to impaired V(D)J recombination. This is also associated with cellular radiosensitivity in case of *Artemis* mutations. Hypomorphic mutations in these genes result in combined immunodeficiency or Omenn syndrome. Hypomorphic *Artemis* mutations associated with deletion of C-terminus, such as Artemis-P70 (D451fsX10), also predispose to lymphomas with clonal translocations in patients. The molecular mechanisms underlying tumor development in these patients are not clear. To date, no *RAG* mutations associated with human malignancy have been reported. However, *in vitro* biochemical and cellular transfection studies suggest that RAG1/2 may play postcleavage roles by forming complexes with the recombining ends to facilitate DNA end processing and ligation. In this regard, RAG1-S723C mutant protein was shown to be proficient for DNA cleavage, but defective in postcleavage complex formation and end joining *in vitro*. DNA ends prematurely released from end-complexes may undergo aberrant rearrangements such as chromosomal

translocations and deletions. To examine the roles of these mutations in aberrant V(D)J recombination and tumor predisposition, our lab has developed two knock-in mouse models- one harboring Artemis-P70 mutation and the other with RAG1-S723C mutation. Both RAG1-S723C and Artemis-P70 mutant mice exhibit reduced V(D)J rearrangements, impaired lymphocyte development and accumulation of DNA ends in developing lymphocytes. In the current study, we examined the fate of unrepaired and/or unprotected DNA ends in the developing lymphocytes harboring these hypomorphic mutations in order to gain insights into the mechanisms involved in proper DNA end processing and joining. We demonstrate that these mutations spontaneously lead to increased aberrant V(D)J joining events and predispose to thymic lymphomas associated with chromosomal translocations in a p53 mutant background. Tumors associated with Artemis-P70 mutation are distinct from those observed with Artemis nullizygosity in molecular defects, tumor spectrum and oncogenic chromosomal rearrangements. Thus, our study provides *in vivo* evidence that implicates partial loss-of-function alleles of *Rag1* and *Artemis* in aberrant end-joining, genome instability and tumor development.

2.2 Introduction

The immense diversity of genes encoding the variable regions of antigen receptors is generated through rearrangement of component V, D, and J segments via a cut-and-paste mechanism known as V(D)J recombination [186]. These site-specific chromosomal rearrangements are initiated in progenitor lymphocytes by the recombination activating gene 1 (RAG1) and RAG2 proteins that comprise a lymphoid-specific endonuclease, RAG1/2 [4, 5]. DNA double-strand breaks (DSBs) are generated by RAG1/2 at specific recombination signal sequences (RSSs) adjacent to the numerous rearranging V, D, and J coding exons [21]. The broken ends are then processed and joined by ubiquitously expressed nonhomologous end-joining (NHEJ) DNA repair factors, including Ku70, Ku80, the DNA-dependent protein kinase catalytic subunit (DNA-PKcs), Artemis, DNA ligase IV, XRCC4 and Cernunnos/XLF [13, 14, 186].

The RAG1/2 endonuclease initially binds to RSSs that are composed of a conserved heptamer and nonamer separated by relatively nonconserved spacer sequences of either 12 or 23

nucleotides [21]. Efficient cleavage requires recombination between one 12 RSS and one 23 RSS in the context of a synaptic, paired complex mediated by RAG1/2. RAG1/2 nicks the duplex DNA at the junction between the RSS heptamer and coding sequences then uses the resulting 3' OH in a direct transesterification reaction with the phosphodiester backbone of the opposing strand. The products of RAG1/2 cleavage are blunt, 5' phosphorylated signal ends and covalently closed, hairpin coding ends. Sequence elements within the nonconserved 12 and 23 spacers [187] and coding flanks [188-191] contribute to RAG1/2 interaction with the recombining DNA and strongly influence coding segment utilization [187]. Hence, the efficiency of binding and cleavage of individual RSSs is significantly affected by interactions of the RAG1/2 endonuclease with the heptamer, nonamer, 12 or 23 spacer, and coding sequences.

In addition to an essential role in the cleavage phase, RAG1/2 has also been suggested to possess post-cleavage functions during V(D)J recombination. *In vitro* biochemical and cellular transfection assays suggest that the RAG proteins are associated with the DNA ends in post-cleavage complexes [3, 34, 61, 180, 192-197]. RAG1/2 and the four DNA ends (two coding and two signal) form a transient cleaved signal complex (CSC) [34, 61, 180]. This complex may protect the coding ends from degradation and specifically direct them to C-NHEJ pathway. The coding ends, on release from the CSC, are rapidly processed and joined with junctional modifications. The signal ends remain associated with RAG1/2 in a stable signal end complex (SEC) until they are precisely ligated by the C-NHEJ factors to form signal joins [34, 193, 194].

Further evidence for important RAG1/2 post-cleavage roles is provided by separation-of-function mutations in *RAG* genes [180, 195-197]. A RAG1 mutant protein of our interest contains alanine or cysteine instead of serine at 723 position [180]. Biochemical assays showed that this mutant protein was proficient in cleavage activity [180, 198] but was defective in CSC-stability manifested as premature release of coding ends [180]. In transient V(D)J recombination assays using RAG1-S723C mutant protein, formation of both signal and coding joins was significantly reduced despite no obvious abnormality in interaction with signal ends [180, 192, 199]. However, the *in vivo* consequences of these mutations and post-cleavage complex instability still remain to be characterized.

To examine the *in vivo* effect of RAG1-S723C mutant in our lab, a mouse model harboring this mutation was generated [200]. These mice exhibit a significant impairment in lymphocyte development at stages when V(D)J rearrangements occur. In contrast to RAG1- and RAG2-null mice, the phenotypes of RAG1-S723C mice more closely parallel those of human leaky $T^{+}B^{-}$SCID [130]. In addition, low levels of D to J rearrangements were observed in the developing lymphocytes. Hence, mice harboring the RAG1-S723C hypomorphic allele can be clearly distinguished from RAG nullizygosity by the ability to catalyze a low level of productive V(D)J recombination events *in vivo*. DNA DSBs were readily detected in the mutant lymphocytes indicating that the cleavage activity of RAG1-S723C/RAG2 complex is intact. Cleavage products not corresponding to the expected sizes were also observed in these lymphocytes. These aberrant products can result from either aberrant DNA cleavage and/or premature end release [23, 158, 160, 162, 201-204]. Other studies have also found Omenn syndrome-like features in RAG1-S723C homozygous mice autoreactive B cell repertoire [205].

The role of Artemis in V(D)J recombination is discussed in detail in sections 1.2 and 1.4. Prior to ligation, the hairpin coding ends are nicked open by the Artemis endonuclease which is activated upon interaction with the DNA-dependent protein kinase catalytic subunit (DNA-PKcs) [79]. In the absence of Artemis function, unopened hairpin coding ends accumulate in developing lymphocytes and remain unjoined resulting in defective V(D)J recombination [158].

To date, at least 48 different mutant Artemis alleles have been identified in association with inherited combined immunodeficiency syndromes [136, 137]. The majority of mutations are located within a region encoding a highly conserved metallo-β-lactamase/βCASP N-terminal domain (aa 1–385). A smaller subset of Artemis alleles resides within a non-conserved C-terminus (aa 386–692), and these mutations are small nucleotide deletions or insertions resulting in frameshifts followed by premature translation termination. Patients harboring null mutations suffer from an absence of B and T lymphocytes, whereas partial loss-of-function Artemis alleles are associated with immunodeficiency syndromes of varying severity, including $B^{-/low}T^{-/low}$ SCID, $B^{-/low}$ SCID, chronic inflammatory bowel disease and Omenn syndrome [69, 136, 137, 145, 147, 206-215]. The unjoined DNA ends that accumulate in lymphocytes due to

defects in the NHEJ pathway can be misrepaired via alternative repair pathways, thereby leading to genome instability and potentially detrimental chromosomal aberrations, including oncogenic translocations [216].

Patients harboring Artemis mutations that result in premature translation termination within exon 14 leading to truncation of C terminus (D451fsX10) have been identified. This mutation will be referred to as P70, herein [147]. These patients develop partial B and T immunodeficiency and aggressive Epstein-Barr virus (EBV)-associated lymphomas. However, these tumors are distinct from general EBV-associated tumors on molecular analysis. These tumors (1) were of clonal origin, as shown by the rearrangement status of IgH locus, and (2) harbored chromosomal anomalies with increased genomic instability [147]. This suggests a potential onocgenic role of hypomorphic Artemis mutations. However, it is not yet established whether hypomorphic Artemis mutations predispose to lymphomas. Null Artemis mutations have not been reported to predispose to lymphomas in humans. This further raises the possibility that partial loss of function mutations resulting in C-terminus truncation may have greater oncogenic potential than null alleles.

The C-terminal domain interacts with DNA-PKcs and contains phosphorylation sites for DNA-PKcs [17, 71, 74]. The Artemis:DNA-PKcs complex contains endonucleolytic activities to cleave DNA at single-to-double-strand transitions, including hairpins and 5’ or 3’ overhangs [15, 75, 79, 217], as well as single strands [218]. However, DNA-PKcs dependent phosphorylation is not essential for activation of endonucleolytic activity in biochemical assays using site-specific mutations in Artemis C-terminus [17]. Artemis mutations with C-terminus truncations that retain stable Artemis:DNA-PKcs interaction but lack majority of phosphorylation sites, including Art-P70, exhibit reduced DNA-PKcs dependent endonucleolytic activity [75, 82]. Our lab has previously shown that a mouse model harboring the Art-P70 mutation recapitulates partial immunodeficiency phenotypes observed in patients [82]. Our lab determined that impaired lymphocyte development resulted from a substantial reduction in Artemis-mediated hairpin opening. These findings indicate that Artemis C-terminal domain has important function in modulating Artemis activities and facilitating DNA-PKcs interaction.

In the following study, we examine the *in vivo* impact of the RAG1-S723C and Art-P70 mutations on aberrant V(D)J rearrangements and tumorigenesis in two different mouse models. We show that RAG-induced breaks spontaneously engage in aberrant interchromosomal trans-rearrangements in RAG1-S723C and Art-P70 non-malignant lymphocytes. We also observe chromosomal deletions at the antigen recptor loci in Art-P70 lymphocytes. Moreover, both mutations result in predisposition to thymic lymphomas associated with chromosomal translocations on a p53 mutant background, with Art-P70 associated tumors being molecularly distinct from those associated with Artemis-nullizygosity. These findings provide insight into the potential roles of these protein in maintaining DNA end complex stability during V(D)J recombination and have important implications for tumorigenesis.

2.3 Results

RAG1-S723C and Artemis-P70 mutants lead to interchromosomal trans-rearrangements in non-malignant primary thymocytes.

We previously observed accumulation of DNA ends in *Rag1*$^{S723C/S723C}$ and *Art*$^{P70/P70}$ lymphocytes [82, 200]. To determine if unjoined DNA ends can engage in aberrant rearrangements, I examined trans-rearrangements between two T-cell receptor loci, TCRγ and TCRβ which are located on mouse chromosomes 13 and 6, respectively. TCR Vγ to Jγ and TCR Dβ to Jβ segments are actively rearranged in the DN2/DN3 cells, [219] and may recombine aberrantly. Interchromosomal trans-rearrangements indicate global chromosomal translocations and are observed at higher frequencies in T lymphocytes harboring mutations in genes that predispose to lymphoid neoplasia, including *ATM, DNA-PKcs, NBS1* and *53BP1* [170, 220-223]. I used nested PCR and Southern blot analyses to detect PCR products corresponding to transrearrangements between two specific segments, TCRγV3S1 and TCRβJ2 in RAG1-S723C and Art-P70 homozygous mutant thymocytes (Figure 2.1A). As previously shown, we detected robust levels of transrearrangement between TCRγ and TCRβ in ATM-null thymocytes [167, 220, 221, 224, 225] (Figure 2.1B). PCR products corresponding to interchromosomal V(D)J rearrangements in wild-type or *p53*$^{-/-}$ thymocytes were not readily observed, as previously

reported [170, 200, 224] (Figure 2.1A). In contrast, PCR products were readily observed in *Rag1*$^{S723C/S723C}$ but not in *Rag2*$^{-/-}$ thymocytes (Figure 2.1A).

Figure 2.1: Aberrant Trans-rearrangements in Rag1-S723C Lymphocytes

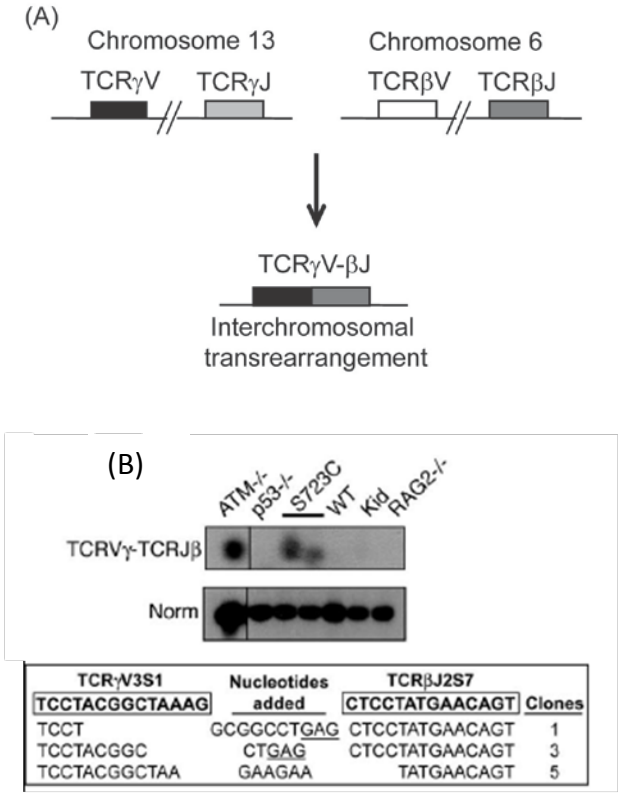

(A) Intrachromosomal TCRγ V-to-J (chr. 13) and TCRβ Dβ2-to-Jβ2 (chr 6) rearrangements and TCRγV–TCRβJ transrearrangements were PCR amplified from genomic thymocyte DNA isolated from mice of the indicated genotypes. PCR products were detected by Southern blot analysis. Levels of rearrangements were normalized to PCR-amplified non-rearranging locus. Representative results are shown. (B) TCRγV–TCRβJ transrearrangements (top panel) in wild-type (WT), *Atm*$^{-/-}$, *Rag1*$^{S723C/S723C}$ (S723C), *Rag2*$^{-/-}$ and *p53*$^{-/-}$ thymocytes. PCR products were subcloned and sequenced (bottom panel). Coding sequences are shown in boxes. Nucleotides added include P nucleotides (underlined) as well as N nucleotides. (B). Transrearrangement PCR products were sequenced and represented here, as described above.

In case of Art-P70 mice, we initially examined levels of normal TCRγ V-to-J and TCRβ D-to-J rearrangements by PCR amplification. As previously reported, we observed that TCRβ D-to-J rearrangements in *Art*$^{P70/P70}$ thymocytes were reduced and were not readily detected in *Art*$^{-/-}$

thymocytes [82, 158] (Figure 2.2A, top panel). In comparison, products corresponding to TCRγ intrachromosomal V-to-J rearrangements were not significantly decreased in *Art*$^{P70/P70}$ and *Art*$^{-/-}$ thymocytes compared with controls. These findings indicate that the Art-P70 and null mutations impair rearrangement at the TCRγ locus to a lesser extent compared with TCRβ rearrangements, as has been observed at the TCRδ locus in NHEJ-deficient backgrounds, including Artemis nullizygosity [22, 118, 161, 226].

Next, we determined whether transrearrangement occurs between TCRγV3S1 and TCRβJ2 (Figure 2.2A, bottom panel). Similar to *Atm*$^{-/-}$ lymphocytes, we detected substantially increased levels of interchromosomal events involving TCRγV3S1 and TCRβJ2 in *Art*$^{P70/P70}$ thymocytes (*n*= 5 mice) compared with controls (Figure 2.2A, data not shown). On the contrary, we observed a lower frequency of transrearrangement in *Art*$^{-/-}$ thymocytes. In this regard, two of seven Artemis-null mice harbored PCR products corresponding to TCRγ-to-TCRβ interchromosomal rearrangements (Fig. 2.2A, data not shown), and the events appeared to be clonal as only a single band was observed, compared with multiple bands observed in *Art*$^{P70/P70}$ and *Atm*$^{-/-}$ thymocytes. Thus, the Art-P70 mutation increases the propensity of unrepaired coding ends to engage in aberrant interchromosomal translocations involving rearranging V(D)J loci. Moreover, this phenotype is distinct from that observed in Artemis-null thymocytes which exhibit infrequent transrearrangements despite harboring a higher level of unjoined hairpin coding ends [82].

We next examined the frequency of interchromosomal rearrangements in Art-P70 heterozygous thymocytes to determine whether the hypomorphic mutation results in a dominant phenotype. TCRγV3S1 to TCRβJ2 transrearrangements were readily detected in *Art*$^{+/P70}$ thymocytes in more than half (six of ten) of the mice examined (Figure 2.1C). However, fewer PCR products corresponding to distinct rearrangements and lower levels of interchromosomal events were observed in *Art*$^{+/P70}$ compared with *Art*$^{P70/P70}$ and *Atm*$^{-/-}$ thymocytes. The levels of TCRβ D-to-J rearrangements in Art-P70 heterozygous thymocytes were similar to those observed in wild-type controls (Figure 2.3). These findings indicate that the C-terminally truncated Art-P70 protein does not substantially disrupt proper coding end

processing and joining, yet increases chromosomal anomalies, even when the wild-type enzyme is present.

Figure 2.2: Aberrant Trans-rearrangements In Art-P70 Lymphocytes

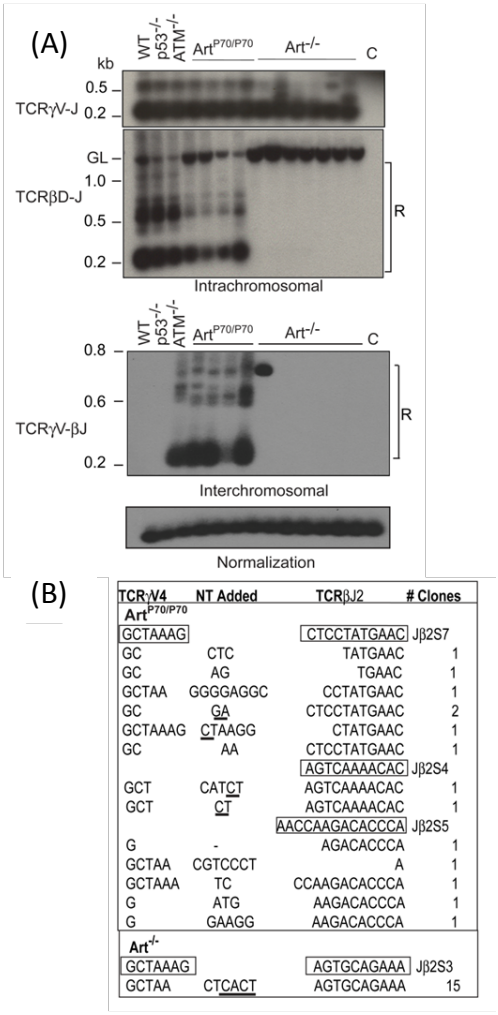

Intrachromosomal TCRγ V-to-J (chr. 13) and TCRβ Dβ2-to-Jβ2 (chr 6) rearrangements and TCRγV–TCRβJ transrearrangements were PCR amplified from genomic thymocyte DNA isolated from mice of the indicated genotypes. PCR products were detected by Southern blot analysis. Levels of rearrangements were normalized to PCR-amplified non-rearranging locus. Representative results are shown. (A) TCRγ V-to-J and TCRβ Dβ2-to-Jβ2 rearrangements (top) and TCRγV–TCRβJ transrearrangements (bottom) in WT, $Art^{P70/P70}$, $Art^{-/-}$, $Atm^{-/-}$ and $p53^{-/-}$ thymocytes. GL, germline, unrearranged band; R, bands corresponding to rearrangements; C or Kid, PCR amplification of kidney genomic DNA. (B). Transrearrangement PCR products were sequenced and represented here, as described above.

Figure 2.3: Aberrant Trans-rearrangements In *Art*$^{+/P70}$ Lymphocytes

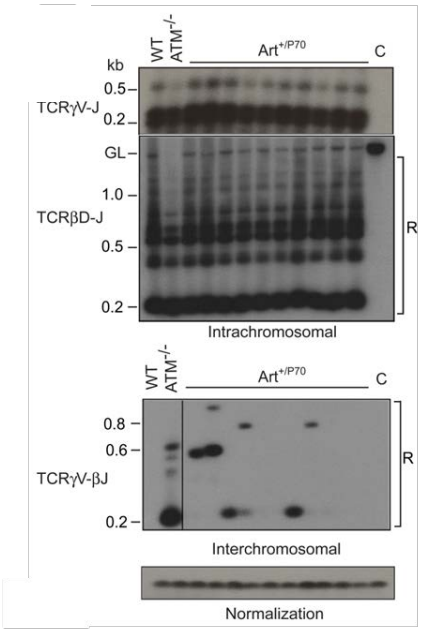

Intrachromosomal TCRγ V-to-J (chr. 13) and TCRβ Dβ2-to-Jβ2 (chr 6) rearrangements and TCRγV–TCRβJ transrearrangements were PCR amplified from genomic thymocyte DNA isolated from mice of the indicated genotypes. PCR products were detected by Southern blot analysis. Levels of rearrangements were normalized to PCR-amplified non-rearranging locus. Representative results are shown. (A) Examination of TCRγ V-to-J, TCRβ Dβ2-to-Jβ2 (top) and interchromosomal TCRγV–TCRβJ transrearrangements (bottom) in *Art*$^{+/P70}$ mice.

The nested PCR products from RAG1-S723C and Art-P70 mutant thymocytes were cloned and sequenced in order to verify that they represent the predicted interchromosomal events. We obtained several unique clones from RAG1-S723C and *Art*$^{P70/P70}$ mice (n=4) containing flanking sequence from TCRγV3S1 and TCRβJ2, thereby indicating that the PCR primers indeed amplified V(D)J transrearrangements (Figure 2.1B, bottom panel; Figure 2.2B). The junctions contained non-templated (N) and palindromic (P) nucleotides and small deletions, similar to the coding joints analyzed from intrachromosomal V(D)J recombination events in the wild-type mice [82]. We also cloned and sequenced the PCR products corresponding to the interchromosomal rearrangements obtained from *Art*$^{-/-}$ thymocytes.

Sequencing of multiple clones yielded one unique sequence, thereby indicating that the single PCR product likely represents a clonal event (Figure 2.2B).

These results support the notion that aberrant end processing due to RAG1-S723C and Art-P70 mutants generate V(D)J ends that engage in chromosomal translocations. In Art-P70 lymphocytes, these aberrant events occur at an elevated frequency compared with a complete absence of Artemis.

Increased deletional chromosomal hybrid joining in Artemis-P70 mice.

Hybrid joint formation occurs between a coding and a signal (RS) end and represents an unproductive V(D)J rearrangement. Inversional chromosomal rearrangements require that the two coding and two RS ends generated by the RAG endonuclease are maintained in proximity in order to facilitate coordinated processing and ligation. Increased levels of deletional chromosomal hybrid joining during inversional V(D)J rearrangement are hypothesized to result from inappropriate release of RAG-generated ends from DNA end complexes, thereby leading to the loss of the intervening genomic fragment, thus favoring the deletional event (refer to Figure 1.) [118, 128, 166]. Our observations of increased interchromosomal rearrangements in RAG1-S732C and Art-P70, but not *Art*$^{-/-}$ lymphocytes, led us to examine the frequency of deletional hybrid joining in these mutant backgrounds. To this end, we examined hybrid joint formation during immunoglobulin light chain kappa (Igκ) locus rearrangements in splenocytes. Productive rearrangement between Vκ6-23 and Jκ1 segments occurs via inversion; thus, hybrid joining results in deletion of the intervening DNA segment (Figure 2.2A).

Using a nested PCR approach, we readily detected Vκ to Jκ hybrid joints in *Art*$^{P70/P70}$ splenocytes in the majority (three of four) of mutant mice analyzed (Fig. 2.4A). The levels were lower than those observed in ATM deficiency, but markedly higher compared with wild-type and Art$^{-/-}$ splenocytes. We also observed decreased levels of Vκ to Jκ coding joining in Art-P70 mutant splenocytes compared with controls; therefore, the relative frequency of deletional hybrid joining compared with inversional coding joining within the IgLκ locus is substantially increased by the Art-P70 mutation.

Within the TCRβ locus, Vβ14-to-DJβ2 rearrangements also occur via inversion; thus, we examined deletional hybrid joining between Vβ14 and Dβ2 via nested PCR. We detected increased levels of Vβ14–Dβ2 hybrid joints in $Art^{P70/P70}$ thymocytes (two of four), albeit at lower levels compared with ATM deficiency (Fig. 2.4B). Hybrid joints were not detected in $Art^{-/-}$ thymocytes, as previously reported (47) (Figure 2.4B). Given our findings that interchromosomal rearrangements were detected in $Art^{+/P70}$ thymocytes, we assessed the impact of Art-P70 heterozygosity on Vβ14–Dβ2 hybrid joining (Figure 2.4B). We also detected hybrid joints in a subset of $Art^{+/P70}$ mice examined (two of five), thereby providing additional evidence that the Art-P70 allele may have a dominant effect in promoting aberrant rearrangements. However, deletional hybrid join products were not readily detected in RAG1-S723C lymphocytes from three homozygous mutant mice (data not shown).

Figure 2.4: Deletional Hybrid Join Formation in Art-P70 Mice

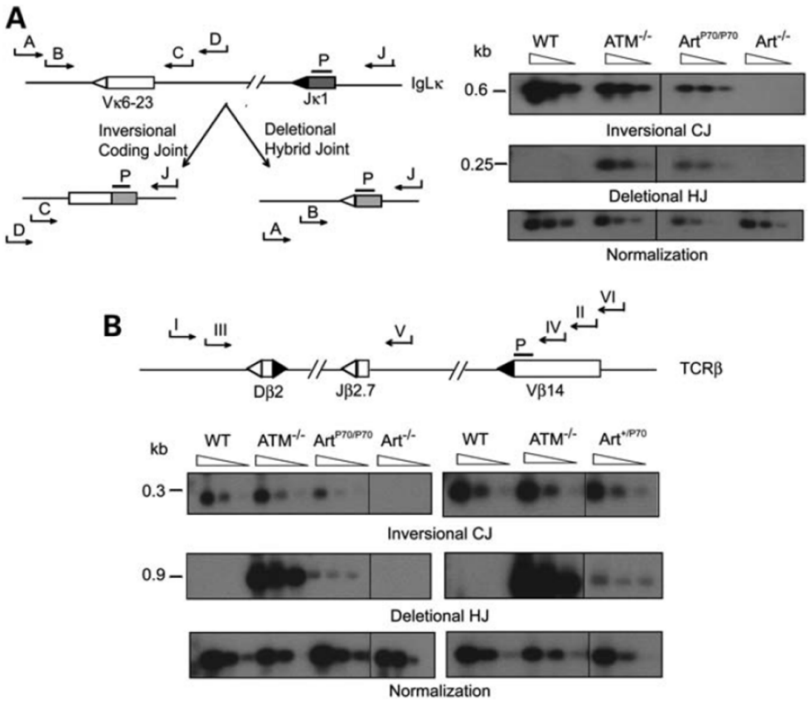

(A) Left panel: Schematic representation of nested PCR strategy for detecting coding and hybrid joints within the IgLκ locus. Relative orientation of Vκ6-23 and Jκ1 coding (rectangles) and RSSs (triangles) within the IgLk locus. Inversional (CJ) and deletional (HJ) products are depicted. Positions of primers (J = pκJa, A = pκ6a, B = pκ6b, C = pκ6c, D = pκ6d) and probe (P) are shown. Right panel: PCR analysis of Vκ6-23 to Jκ1 coding joins (CJs) and hybrid joins (HJs). Genomic splenocyte DNA was isolated from WT, $Atm^{-/-}$, $Art^{-/-}$ and $Art^{P70/P70}$ mice and amplified using primers (pκJa and pκ6d for CJ and pκJa and pκ6a for HJ). Serial 4-fold dilutions of the PCR reaction were amplified using nested primer pairs (pκJa and pκ6c for CJ, and pκJa and pκ6b for HJ). CJ and HJ bands are 0.6 and 0.25 kb, respectively. (B) Deletional hybrid joining and coding joining within the TCRβ locus. Upper panel: Schematic of nested PCR strategy. Relative orientation of Vβ14, Dβ2 and Jβ2.3 coding (rectangles) and RSSs (triangles) within the TCRβ locus. Positions of primers (I = pβa, II = pβb, III = pβc, IV = pβd, V = pβe, VI = pβf) and probe (P = pβg) are shown. Lower panel: PCR analysis of Vβ14 to Jβ2 coding and hybrid joints. Left panel shows CJ and HJ PCR analyses of genomic thymocyte DNA isolated from WT, $ATM^{-/-}$, $Art^{-/-}$ and $Art^{P70/P70}$ mice. Right panel shows CJ and HJ PCR analyses of $Art^{+/P70}$ and control thymocyte genomic DNA, as indicated. Primers for CJ were pβe and pβf. Primary primers for HJ were pβa and pβb. Serial 4-fold dilutions of this primary HJ reaction were amplified using primers pβc and pβd. CJ and HJ bands are 0.3 and 0.9 kb, respectively. PCR amplification of a non-rearranging locus was performed to normalize the input genomic DNA. Representative results are shown.

Tumor predisposition in RAG1-S723C and Art-P70 mice.

The occurrence of TCRγ-TCRβ trans-rearrangements in *Rag1*$^{S723C/S723C}$ and Art-P70 thymocytes suggested that DSBs generated by the mutant RAG1/2 and Artemis proteins could engage in aberrant chromosomal translocations; thus, we examined the mutant mice for tumor predisposition.

RAG1-S723C mice.

We observed that the RAG1-S723C homozygous mutation alone does not predispose to tumorigenesis, as the mutant mice survive tumor free beyond 12 months of age. To enhance the oncogenic potential of unrepaired DNA DSBs, we introduced p53 deficiency into the RAG1-S723C mutant background through mouse breedings. We observed that *Rag1*$^{S723C/S723C}$*p53*$^{-/-}$ mice exhibit a significant decrease in survival in comparison with the p53$^{-/-}$ cohort (*Rag1*$^{+/S723C}$*p53*$^{-/-}$ and *Rag1*$^{+/+}$*p53*$^{-/-}$ mice; $P = .017$, log-rank test) and controls ($P < .001$) (Figure 2.5A). All of the *Rag1*$^{S723C/S723C}$*p53*$^{-/-}$ mice succumbed to tumorigenesis, and the majority of tumors observed were immature TCRβ^{-} T-cell lymphomas (90%, Table 2.1). In comparison, although the control p53$^{-/-}$ cohort was also predominantly predisposed to T-cell lymphomas (66%, Table 2.1), [227, 228] the majority of these tumors (16 of 23 thymic lymphomas) were surface TCRβ^{+}, indicating they emanated from later stages of T-cell development compared with the RAG1-S723C/p53 mutant tumors ($P < .001$, 2-tailed Fisher exact test). Solid tumors and surface IgM^{+} B-cell lymphomas were frequently observed in the *p53*$^{-/-}$ cohort (12 of 35 tumors), whereas 3 of the 31 mice in the *Rag1*$^{S723C/S723C}$*p53*$^{-/-}$ cohort succumbed to solid tumors ($P = .02$, 2-tailed Fisher exact test), and no lymphoid tumors other than TCRβ^{-} T-cell lymphomas were observed (Table 2.1).

Artemis-P70 mice.

We examined cohorts of *Art*$^{P70/P70}$, *Art*$^{-/-}$ and wild-type mice over a period of 12 months to determine whether the Art-P70 mutation predisposes to lymphoid or other tumors. We observed that two of fourteen *Art*$^{P70/P70}$ mice became moribund at 7 and 9 months of age as a result of large thymic masses (Figure 2.5B). Flow cytometric analyses revealed that the thymic

lymphomas were primarily of a $CD4^+CD8^+TCR\beta^-$ origin (Table 2.2). In comparison, the wild-type and $Art^{-/-}$ control cohorts survived tumor-free within the 12-month period, which is consistent with previous reports (53,54).

To further assess the oncogenic potential of the Art-P70 hypomorphic allele, we examined the impact of p53 mutation on tumor predisposition through mouse breeding. The experimental cohorts were on a closely matched 129Sv/C57Bl6 background, thereby minimizing potential strain background effects. However, a subtle impact of genetic background cannot be entirely ruled out. Inactivation of the p53-dependent cell-cycle checkpoint in Artemis mutant lymphocytes allows cells harboring unrepaired DSBs or activated oncogenes to survive [229-233]. We observed that Art-P70/p53 double mutant mice exhibit significantly decreased survival compared with $p53^{-/-}$ controls (median survival of 11 and 18 weeks, respectively; P = 0.001; Figure 2.5B). As previously reported, we found that $Art^{-/-}p53^{-/-}$ mice also exhibited decreased survival compared with p53 null controls, and the median survival (13 weeks) was similar to that observed for Art-P70/p53 double-mutant cohort (Figure 2.5B). We found that the $Art^{-/-}p53^{-/-}$ and $Art^{P70/P70}p53^{-/-}$ mice succumbed to lymphoid tumors. Flow cytometric analysis of the tumors revealed that $Art^{-/-}p53^{-/-}$ mice were predominantly predisposed to disseminated $B220^+CD43^+IgM^-$ pro-B lymphomas, as has been previously reported [234] (Table 2.2). In contrast, the majority of tumors that arose in the Art-P70/p53 double-mutant background were $CD4^+CD8^+TCR\beta^-$ thymic lymphomas (Table 2.2). $B220^+CD43^+IgM^-$ pro-B lymphomas were also observed in $Art^{P70/P70}p53^{-/-}$ mice, similar to Art/p53 double null mice [234] (Table 2.2), albeit at a significantly lower frequency (P = 0.014; two-tailed Fisher's exact test). These findings indicate that the Art-P70 allele predisposes to lymphoid malignancies in a p53-deficient background, and the lymphoma spectrum observed in $Art^{P70/P70}p53^{-/-}$ mice is distinct from that observed in NHEJ/p53 double null backgrounds, including $Art^{-/-}p53^{-/-}$ mice [233, 234].

Figure 2.5: Decreased Survival of Rag1-S723C/p53 and Art-P70/p53 Mice

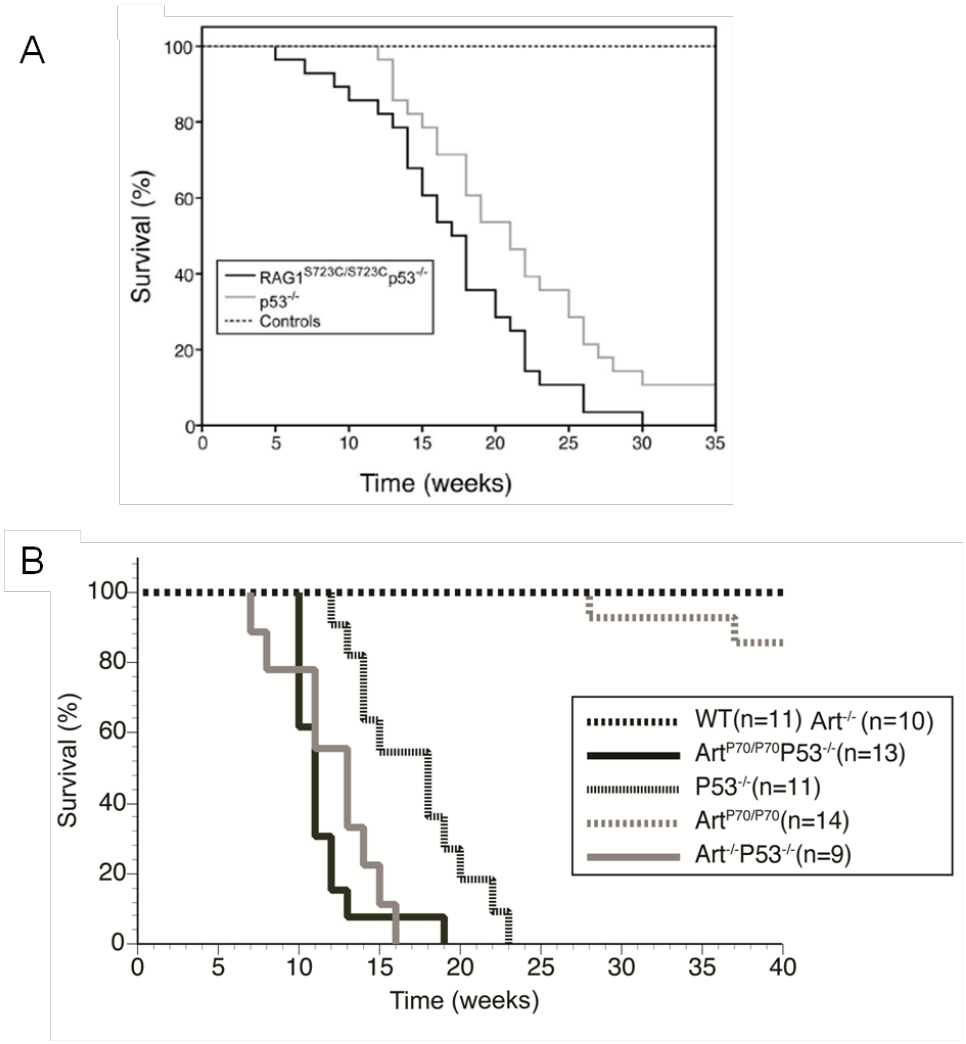

(A) Survival of a cohort of control (*Rag1*$^{+/+}$, *Rag1*$^{+/S723C}$, *Rag1*$^{S723C/S723C}$, n = 39), *p53*$^{-/-}$ (*Rag1*$^{+/+}$*p53*$^{-/-}$, *Rag1*$^{+/S723C}$*p53*$^{-/-}$, n = 35), and *Rag1*$^{S723C/S723C}$*p53*$^{-/-}$ (n = 31) mice was observed for a period of 35 weeks. Kaplan-Meier survival curves were compared using the 2-tailed log-rank test with a 95% confidence interval (*Rag1*$^{S723C/S723C}$*p53*$^{-/-}$ vs *p53*$^{-/-}$ cohorts, *P* = .017; *Rag1*$^{S723C/S723C}$*p53*$^{-/-}$ vs control cohorts, *P* < .001). (B) Decreased survival of Art-P70/p53 mice. Survival of a cohort of wild-type (*n*= 11), *Art*$^{-/-}$ (*n*= 10), *p53*$^{-/-}$ (*n*= 11), *Art*$^{P70/P70}$ (*n*= 14), *Art*$^{P70/P70}$*p53*$^{-/-}$ (*n*= 13) and *Art*$^{-/-}$*p53*$^{-/-}$ (*n*= 9) mice was observed for a period of 40 weeks. Shown are Kaplan–Meier survival curves representing the percentage of survival of cohort mice versus age in weeks.

Table 2.1: Tumor Spectrum in RAG1-S723C/p53 Mice

Tumor type	$RAG^{S723C/S723C}p53^{-/-}$	$*p53^{-/-}$	Controls**
	31	35	39
$TCR\beta^{-}$ T-cell lymphoma	28	7	0
$TCR\beta^{+}$ T-cell lymphoma	0	16	0
B-cell lymphoma	0	3	0
Sarcoma	3	9	0

$*RAG1^{S723C/+}p53^{-/-}$, $RAG1^{+/+}p53^{-/-}$
$**RAG1^{S723C/S723C}p53^{+/+}$; $RAG1^{+/S723C}p53^{+/+}$, $RAG1^{+/+}p53^{+/+}$

Table 2.2: Tumor Spectrum in Art-P70/p53 Mice

Tumor type	$Art^{P70/P70}$	$Art^{-/-}$	$Art^{P70/P70}p53^{-/-}$	$Art^{-/-}p53^{-/-}$	$p53^{-/-}$
Total number	2	0	13	8	11
ProB lymphoma	0	0	4	6	0
Mature B lymphoma	0	0	0	0	1
$TCR\beta^{-}$ T-cell lymphoma	2	0	9	2	0
TCRβ+ T-cell lymphoma	0	0	0	0	10
Sarcoma	0	0	0	0	0

Distinct chromosomal anomalies associated with RAG1-S723C/p53 and Art-P70/p53 lymphoid tumors.

We analyzed the rearrangement status of the TCRβ locus in the $Rag1^{S723C/S723C}p53^{-/-}$, $Art^{P70/P70}p53^{-/-}$ and $Art^{P70/P70}$ lymphomas to assess the molecular events that occurred in the tumors. We performed Southern blot analyses of *Eco*RI-digested genomic DNA isolated from the tumors using a probe located 5' of Dβ1 (Figure 2.6A). The majority of $Rag1^{S723C/S723C}p53^{-/-}$ tumors exhibited D-Jβ1 rearrangements on one of the 2 alleles. As Dβ to Jβ rearrangements are severely reduced in $Rag1^{S723C/S723C}$ thymocytes [200], the relative intensities of the germline and rearranged bands observed in DNA isolated from tumor cells suggest that the rearrangements are clonal. We also examined the Dβ1 to Jβ1, Dβ2, and Jβ2 and Vβ8 to DJβ1 rearrangements in $Rag1^{S723C/S723C}p53^{-/-}$ tumors via PCR amplification and observed several tumors harboring

specific D-Jβ or V-DJβ rearrangements (Figure 2.6B). Together, these results indicate that the mutant RAG1-S723C/RAG2 endonuclease was active in generating DSBs in progenitor lymphocytes from which the tumors emanated, and the lymphomas are of a clonal origin.

The *Art*$^{P70/P70}$*p53*$^{-/-}$ tumors were analyzed by another graduate student and the results are briefly summarized here. Thymic tumors and one pro-B tumor exhibited clonal rearrangements indicating the clonal origin of thymic, and some pro-B, lymphomas in Art-P70 mice. One pro-B lymphoma showed N-myc locus amplification which is commonly associated with *Art*$^{-/-}$*p53*$^{-/-}$ pro-B tumors. However, another *Art*$^{P70/P70}$*p53*$^{-/-}$ pro-B lymphoma with no genomic amplification of either c-myc or N-myc, showed elevated c-myc expression. These results indicate that the lymphomas arising in the Art-P70 arise via distinct mechanisms from null backgrounds.

Figure 2.6: Clonal Origin of Rag1-S723C/*p53*$^{-/-}$ Lymphomas

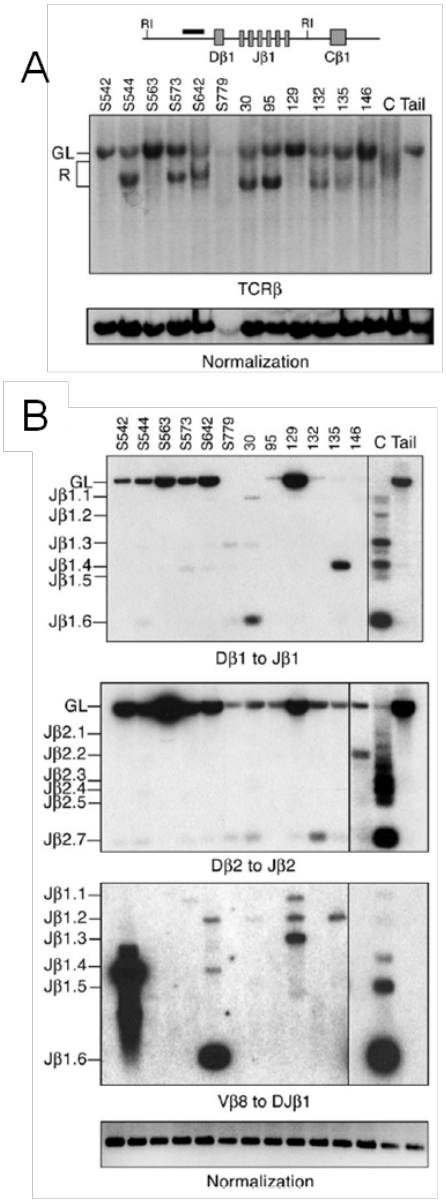

(A) Genomic DNA isolated from RAG1-S723C/p53 double-mutant lymphomas was digested with *Eco*RI then analyzed by Southern blot. Dβ1 to Jβ1 rearrangements were detected using a probe located 5′ of the Dβ1 segment (diagram). Individual tumors are indicated, top. C indicates wild-type thymus DNA; Kid, nonrearranging tissues; GL, unrearranged, germline band; and R, D-Jβ1 rearrangements. Amounts of input DNA were normalized to a nonrearranging locus (LR8). (B) PCR amplification of Dβ1 to Jβ1, Dβ2 to Jβ2, and Vβ8 to DJβ1 rearrangements were performed using genomic DNA (250 ng) isolated from RAG1-S723C/p53 double-mutant lymphomas (tumor numbers indicated, top), wild-type thymocytes (C), and a nonrearranging tissue (tail). Input DNA levels were normalized to a nonrearranging locus (*Atm*). Vertical lines have been inserted to indicate repositioned gel lanes.

Cytogenetic analyses of RAG1-S723C/p53 and Art-P70/p53 double-mutant lymphomas.

We next examined the cytogenetic events occurring in RAG1-S723C/p53 and Art-P70/p53 double-mutant lymphomas using spectral karyotyping (SKY) , a multicolor chromosome painting technique. We analyzed the karyotypes of metaphases from primary and early passage cultured tumor cells. Thymic lymphomas that arise in p53-deficient mice usually feature aneuploidy without clonal translocations, [171, 172, 234-238] although clonal chromosomal aberrations have been observed in a small subset of $p53^{-/-}$ lymphomas in a mixed C57BL/6;129/Sv genetic background (M. Gostissa and F.W.A., unpublished). RAG-null mice in a p53 mutant background are also predisposed to thymic lymphomas [236, 239]; however, similar to the p53-null tumors, they are characterized by aneuploidy and do not harbor clonal translocations involving rearranging loci [236]. Thus, in the absence of RAG-induced DSBs, clonal translocations are not a common feature of the lymphomas in p53 deficiency. Furthermore, inactivation of NHEJ genes, which are required for joining of V(D)J ends, does not increase the frequency of oncogenic translocations in the RAG/p53 double-null background. In this regard, thymic lymphomas that arise in $Ku80^{-/-}Rag2^{-/-}p53^{-/-}$ mutant mice lack clonal translocations [235], and $Xrcc4^{-/-}Rag2^{-/-}p53^{-/-}$ mice die without any sign of lymphoma [232]. Interestingly, DNA-PKcs mutation in a $Rag2^{-/-}p53^{-/-}$ background leads primarily to progenitor B-cell malignancies associated with translocations involving chromosomes without V(D)J loci, [240] thereby leading to the notion that DNA-PKcs deficiency leads to accumulation of unrepaired random DSBs that engage in oncogenic events.

We found that 6 of the 7 $Rag1^{S723C/S723C}p53^{-/-}$ lymphomas contained chromosomal translocations and/or short-arm fusions in a clonal population of tumor cells (Figure 2.7A; Table 2.3). We observed 2 tumors with translocations involving chromosomes that harbor rearranging TCR loci (chr 6 and 14), suggesting that the clonal events were initiated by the mutant RAG1-S723C/RAG2 endonuclease. Intriguingly, we also observed clonal translocations involving chromosomes lacking V(D)J loci. We also performed SKY analyses on several thymic lymphomas arising in $Rag1^{+/S723C}p53^{-/-}$ mice, as our analyses of lymphocyte development in older mice indicated that heterozygosity for the S723C mutation may confer additional phenotypes [200].

We found that *Rag1*$^{+/S723C}$*p53*$^{-/-}$ lymphomas also harbored clonal chromosomal translocations (Table 2.3). The thymic lymphomas arising in our p53-null cohort were largely characterized by aneuploidy with one harboring a clonal translocation, consistent with previous studies [171, 172, 234-238]. Thus, the RAG1-S723C/p53 thymic lymphomas featuring frequent clonal translocations and fusions are karyotypically distinct from the p53$^{-/-}$ lymphomas.

The results from SKY analysis on metaphase spreads from seven *Art*$^{P70/P70}$*p53*$^{-/-}$ thymic lymphomas will be summarized here. All of the Art-P70/p53 tumors analyzed contained clonal translocations involving chromosomes that harbor loci undergoing V(D)J rearrangements including chromosome 12 (IgH), chr. 13 (TCRγ), and chr. 6 (TCRβ) (data not shown).

Figure 2.7: Rag1-S723C/p53 and Art-P70/P53 Mice are Predisposed toTumors Harboring Chromosomal Translocations

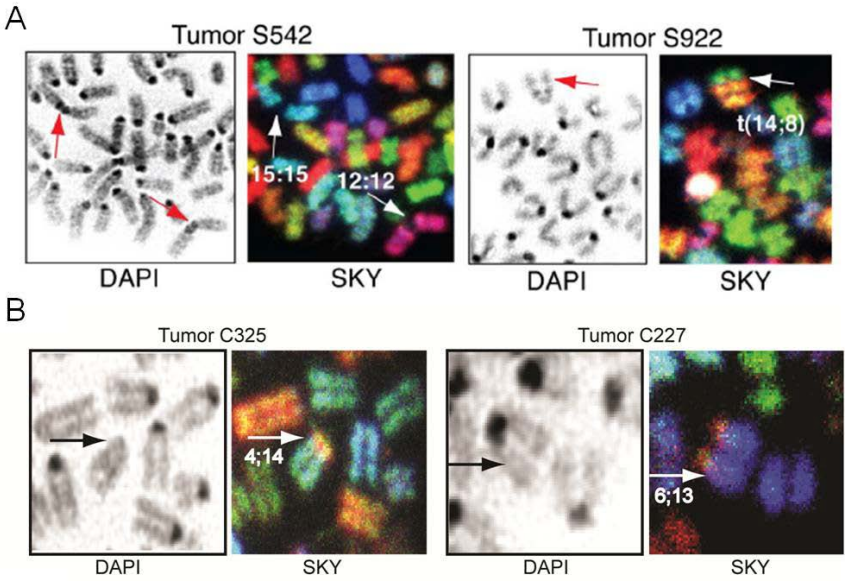

(A) *Rag1*$^{S723C/S723C}$*p53*$^{-/-}$ thymic lymphomas harbor chromosomal translocations and fusions. DAPI staining (left panels) and SKY analysis (right panels) of tumors S542 and S922 containing clonal chr 15;15 and 12;12 short-arm fusions and t(14;8) translocations, respectively. Arrows indicate translocated chromosomes. (**B**) SKY images of metaphase chromosomes from Art-P70/p53 tumors. DAPI staining (left panels) and SKY analysis (right panels) of tumor C325 and C227 containing clonal t(4;14) and t(6;13) translocations, respectively. Arrows indicate translocated chromosomes.

Table 2.3: Spectral Karyotyping of Thymic Lymphomas in Rag1-S723C/p53 Mice

Table 2. Spectral karyotyping of thymic lymphomas

Tumor	Genotype	Translocations	Frequency	Flow cytometry
83	RAG1$^{S723C/S723C}$p53$^{-/-}$	t(8;17)	20/20	CD4$^+$CD8$^+$TCRβ$^-$
		[2 translocated chromosomes per metaphase]		CD8SP
135	RAG1$^{S723C/S723C}$p53$^{-/-}$	t(15;12)	2/18	CD4$^+$CD8$^+$TCRβ$^-$
		t(10;5)	1/18	
S542	RAG1$^{S723C/S723C}$p53$^{-/-}$	Chr 15;15 SAFs	16/18	CD4$^+$CD8$^+$TCRβ$^-$
		Chr 12;12 SAFs	5/18	
		t(5;19)	1/18	
S642	RAG1$^{S723C/S723C}$p53$^{-/-}$	Chr 3;6 SAFs	5/24	CD4$^-$CD8$^-$
		t(14;1)	2/24	
S779	RAG1$^{S723C/S723C}$p53$^{-/-}$	t(15;12)	1/18	CD4$^+$CD8$^+$TCRβ$^-$
S878	RAG1$^{S723C/S723C}$p53$^{-/-}$	t(15;9)	17/18	CD4$^-$CD8$^+$TCRβ$^-$
S922	RAG1$^{S723C/S723C}$p53$^{-/-}$	t(14;8)	11/22	CD4$^+$CD8$^+$TCRβ$^-$
S786	RAG1$^{+/S723C}$p53$^{-/-}$	t(9;11)	2/9	CD4$^+$CD8$^+$TCRβ$^+$
S801	RAG1$^{+/S723C}$p53$^{-/-}$	Chr 15;15 SAFs	28/33	CD4$^+$CD8$^+$TCRβ$^-$
		Chr 11;11 SAFs	22/33	
		Chr X;X SAFs	5/33	
		Chr 16;16 SAFs	4/33	
		Chr 6;6 SAFs	4/33	
		Chr 3;3 SAFs	2/33	
		t(16;12)	1/33	
S900	RAG1$^{+/S723C}$p53$^{-/-}$	Chr 5;5 SAFs	15/24	CD4$^+$CD8$^+$TCRβ$^+$
		t(11;16)	13/24	
S771	RAG1$^{+/+}$p53$^{-/-}$	None	0/19	CD4$^-$CD8$^+$TCRβ$^+$
S839	RAG1$^{+/+}$p53$^{-/-}$	None	0/20	CD4$^-$CD8$^+$TCRβ$^+$
S908	RAG1$^{+/+}$p53$^{-/-}$	None	0/27	CD4$^+$CD8$^+$TCRβ$^+$
S919	RAG1$^{+/+}$p53$^{-/-}$	None	0/12	CD4$^-$CD8$^+$TCRβ$^+$
S926	RAG1$^{+/+}$p53$^{-/-}$	None	0/20	CD4$^-$CD8$^+$TCRβ$^+$
S1324	RAG1$^{+/+}$p53$^{-/-}$	t(15;14)	22/25	CD4$^+$CD8$^+$TCRβ$^-$

SAFs indicates short-arm fusions.

Table 2.4: Spectral Karyotyping of Art-P70/p53 Tumor Metaphases

Tumor	Translocations	Flow cytometry
C227	t(13;6) t(14;1)	CD4$^+$ CD8$^+$ TCRβ$^-$
C267	t(14;4)	CD4$^+$ CD8$^+$ TCRβ$^-$
C268	t(12;1)	CD4$^+$ CD8$^+$ TCRβ$^-$
C325	t(4;14)	CD4$^+$ CD8$^+$ TCRβ$^-$
C306	t(12;14) t(1;14)	CD4$^+$ CD8$^+$ TCRβ$^-$
C262	t(12;11) t(19;2)	CD4$^+$ CD8$^+$ TCRβ$^-$
C324	t(14;2)	CD4$^+$ CD8$^+$ TCRβ$^-$
C219	t(12;15)	IgM$^-$, B220$^+$, CD43$^+$

2.4 Discussion

In this study, we examined the impact of two hypomorphic mutations on aberrant V(D)J rearrangements and tumorigenesis in mice: RAG1-S723C mutant associated with unstable postcleavage complex *in vitro* and Artemis-P70 mutant that results in partial immunodeficiency and EBV-associated lymphomas in patients. We demonstrate that these mutations increase the frequency of aberrant chromosomal rearrangements in primary lymphocytes and predispose to lymphoid malignancy in mouse models. Thus, we reveal novel *in vivo* functions of RAG1 and Artemis proteins in maintaining genomic stability in the developing lymphocytes.

Distinct tumor spectra and molecular events in RAG1-S723C/p53 and Art-P70/p53 mice.

We demonstrate that RAG1-S723C/p53 double-mutant mice are predisposed to thymic lymphomas that harbor frequent chromosomal translocations. Two of the 7 $Rag1^{S723C/S723C}p53^{-/-}$ tumors harbored chromosome 6 or 14 translocations, consistent with the notion that RAG1-S723C/RAG2-induced DNA DSBs at the rearranging TCR loci may engage in aberrant repair events. Intriguingly, 4 of the 7 $Rag1^{S723C/S723C}p53^{-/-}$ lymphomas contained translocations and short-arm fusions that involve the chromosomes lacking rearranging TCR loci.

Similarly, the Art-P70 mutation in a p53 null background accelerates the timing of tumor onset compared with p53 mutation alone. Art-P70/p53 double mutant mice predominantly succumb to $CD4^{+}CD8^{+}TCR\beta^{-}$ thymic lymphomas that are associated with clonal chromosomal translocations involving the TCR or IgH loci; however, the majority of tumors do not harbor the hallmark gene amplification events observed in NHEJ/p53 double null lymphomas, including those arising in $Art^{-/-}p53^{-/-}$ mice [186, 233, 234]. We found that the $Art^{P70/P70}p53^{-/-}$ and $Art^{-/-}p53^{-/-}$ lymphomas arise with a similar latency, despite our observation of substantially higher levels of aberrant interchromosomal rearrangements in Art-P70 mutant lymphocytes. One potential explanation for these observations is that the timing of lymphoma incidence is influenced by the particular oncogenic events associated with tumorigenesis. In this regard, genomic amplification leading to elevated expression of c-myc or N-myc in $Art^{-/-}p53^{-/-}$

lymphomas may lead to a higher proliferative potential compared with oncogenic events in the *Art*$^{P70/P70}$*p53*$^{-/-}$ background, thereby accelerating tumorigenesis in Art/p53 double null mice.

The frequently arising *Art*$^{P70/P70}$*p53*$^{-/-}$ thymic lymphomas are associated with clonal translocations involving chr. 6, 12, 13 and 14 which harbor the murine TCRβ, IgH, TCRγ and TCRα/δ loci, respectively, with chr. 14 translocations observed in the majority of the tumors analyzed. Cytogenetic analyses of activated T cells isolated from human lymphoma patients harboring the hypomorphic allele modeled in the Art-P70 mouse and a similar C-terminal truncating mutation (T432SfsX16) revealed a translocation of chr. 7 and 14 and inversion of chr. 7, respectively [147]. In humans, the rearranging IgH and TCRα/δ loci reside on chr. 14, whereas TCRγ and TCRβ reside on chr. 7. Thus, Art-P70 hypomorphic allele results in translocations involving chromosomes that undergo V(D)J recombination in both human and murine lymphocytes.

Potential oncogenic mechanisms.

After our RAG1-S723C mouse study was published, Deriano *et al.* reported that mice expressing core RAG2 (cRAG2) that lacks C-terminal region also exhibit aberrant V(D)J rearrangements (translocations and hybrid joins at the antigen receptor loci) and, on a p53-mutant background, develop thymic lymphomas [65]. We propose the following explanations to account for the observed tumorigenesis.

1. RAG1-S723C mutant may predisopose to errors in substrate recognition.

Our observations that majority of the *Rag1*$^{S723C/S723C}$*p53*$^{-/-}$ lymphomas contained rearrangements that involve the chromosomes lacking rearranging TCR loci raise the intriguing possibility that the S723C mutant alters or loosens the cleavage specificity of the RAG1/2 endonuclease. The S723 residue resides within a central domain of RAG1 (amino acids 528-760 of 1040) that binds with sequence specificity to RSSs [241]. Biochemical studies of purified RAG1-S723C indicate that this amino acid is important for proper interactions with flanking coding region DNA during both precleavage and postcleavage events [199]. Thus, perturbations in specific contacts between RAG1/2 and the recombining DNA may alter cleavage activity.

What are the potential consequences of aberrant DNA cleavage by a dysfunctional RAG1/2 endonuclease? Cleavage of cryptic RSSs or non-B conformation DNA structures by RAG1/2 has been hypothesized as one mechanism by which oncogenic chromosomal translocations arise in some human lymphoid malignancies [178, 179]. In addition, unbiased scans of human and murine genomes revealed cryptic RSSs that can be efficiently cleaved by RAG1/2, [242, 243] indicating that abundant cleavage sites outside of the antigen receptor loci exist in mammalian genomes. A mutant RAG1/2 endonuclease with altered or loosened cleavage specificity could more frequently generate DNA breaks at the numerous cryptic RSS sequences or non-B form structures present in the genome. Thus, we speculate that the S723C mutation may permit more frequent endonucleolytic cleavage of cryptic RSSs or non-B form DNA structures within the genome, thereby generating substrates for aberrant DSB repair events, including chromosomal translocations.

2. End-joining errors- destabilization of post-cleavage complex.

RAG proteins may form a scaffold to hold the cleaved DNA ends. RAG1-S723C mutation results in premature release of DNA ends from post-cleavage complexes *in vitro*. Premature release of V(D)J ends in developing lymphocytes would result in accumulation of unprotected, unrepaired DSBs which can engage in chromosomal translocations. Failure to detect loss of DNA ends by inversional recombination analysis does not entirely preclude this hypothesis. Reduced hybrid join formation was also observed *in vitro* by Tsai et al. [180], and an underlying catalytic defect might account for the lack of hybrid join formation.

The Art-P70 mutation, which truncates the non-conserved C-terminus, results in elevated levels of V(D)J transrearrangements between loci located on different chromosomes and deletional hybrid joining in homozygous and heterozygous mutant lymphocytes. In comparison, undetectable or substantially lower levels of these chromosomal anomalies are present in Artemis null lymphocytes, thereby indicating that loss of functional regions within the C-terminal domain increases the potential for the DSB intermediates to engage in aberrant repair events.

Previously, our lab has demonstrated that a mutant Artemis protein modeled after the P70 allele, Art-D451X, interacted stably with DNA-PKcs and exhibited reduced DNA-PKcs-dependent endonucleolytic activity [82]. In addition, we found that loss of the C-terminal 241 amino acids markedly reduced DNA-PKcs-dependent phosphorylation due to deletion of the majority of phosphorylation sites. We hypothesized that these defects may impair the ability of Artemis to associate with and properly act upon DNA ends. Consistent with this notion, hairpin coding ends accumulate in $Art^{P70/P70}$ developing lymphocytes, whereas nicked hairpins with blunt or 5' or 3' overhanging ends are not detected [82]. In the current study, we observed increased levels of interchromosomal V(D)J rearrangements and deletional hybrid joints within the IgLκ and TCRβ loci in $Art^{P70/P70}$ primary lymphocytes.

The mechanism underlying these events presumably involves inappropriate release of RAG-generated DNA ends from post-cleavage complexes prior to joining [118, 128, 166]. In contrast, these aberrant rearrangements occur infrequently in Artemis null lymphocytes [244], despite harboring significantly higher levels of hairpin coding ends compared with Art-P70 mutant lymphocytes [82]. Although open hairpins are not detected in $Art^{P70/P70}$ lymphocytes, it is possible that a low level of nicked coding ends is present, and these end structures may be more likely to engage in aberrant events. However, interchromosomal rearrangements and deletional hybrid joining occur infrequently in wild-type lymphocytes in which hairpins are efficiently cleaved by Artemis. Likewise, coding ends in normal lymphocytes rarely serve as substrates for oncogenic translocations, even in a p53-deficient background which permits RAG-generated ends to persist throughout the cell cycle [171, 172, 200, 229, 234-238]. Thus, the Art-P70 allele likely causes molecular defects in coding end processing and joining beyond impaired hairpin nicking.

Mutations in *Atm*, *Mre11* or *Nbs1* significantly increase the frequency of aberrant chromosomal rearrangements in mutant lymphocytes, including interchromosomal transrearrangements and deletional hybrid joint formation [118, 128, 166, 167, 170, 220, 221, 224, 225]. These observations led to the hypothesis that the ATM kinase and MRN complex function during V(D)J recombination to enhance DNA end complex stability and promote proper joining of RAG-

generated breaks [118, 128, 166]. Our findings suggest that truncation of the C-terminus impairs functions of Artemis within post-cleavage DNA end complexes, thereby leading to inappropriate release and altered handling of V(D)J recombination intermediates. It is of interest to note that ATM phosphorylates Artemis at residues S503, S516 and S645 which are located within the C-terminal region that is deleted in the Art-P70 mutant protein [17]. ATM does not play a direct role in V(D)J recombination *per se* as ATM-deficient cells exhibit wild-type levels of V(D)J recombination on extra-chromosomal plasmid substrates [245]. However, ATM deficiency in mice leads to accumulation of V(D)J coding end intermediates, impaired lymphocyte development and aberrant, potentially oncogenic, chromosomal rearrangements [167, 169, 246-248]. Although ATM-dependent phosphorylation of Artemis is not required to activate intrinsic endonucleolytic activity *in vitro* nor is it required for V(D)J recombination on model plasmid substrates in cells [17], our findings raise the possibility that ATM phosphorylation may modulate Artemis functions during chromosomal V(D)J rearrangements to facilitate the stabilization of DNA end complexes *in vivo*.

We propose that the Art-P70 mutant protein is recruited to DNA ends via interaction with DNA-PKcs [82], and activation of DNA-PKcs upon autophosphorylation induces large conformational changes to allow the nuclease access to the hairpins [16, 17, 249]. Truncation of the Artemis C-terminal region that contains ATM and DNA-PKcs phosphorylation sites may prevent stable association within conformationally altered DNA end complexes that are poised for further end processing events. Inappropriate release of the RAG-generated ends from aborted post-cleavage complexes would render the ends more susceptible to misrepair, thereby increasing their potential to generate chromosomal aberrations, including oncogenic translocations [118].

The precise mechanisms underlying the distinct molecular events observed in Art-P70/p53 lymphomas have not yet been elucidated. Inactivation of the p53-dependent cell-cycle checkpoint has been hypothesized to allow unrepaired RAG-induced DNA ends generated during G1 to persist throughout the cell cycle and undergo mis-repair by alternative DSB repair pathways [186, 229, 233]. We speculate that unjoined coding ends in Art-P70 versus Artemis null lymphocytes may be repaired by distinct pathways that function during different cell-cycle

phases. Consistent with this notion, the junctional sequences of both intra- and interchromosomal V(D)J rearrangements in *Art*$^{P70/P70}$ lymphocytes are characteristic of joining mediated by the classical NHEJ pathway [82]. In comparison, an alternative pathway generates aberrant V(D)J junctions containing large deletions and long P nucleotide additions in *Art*$^{-/-}$ lymphocytes [158] and microhomology mediated translocations in *Art*$^{-/-}$*p53*$^{-/-}$ lymphomas [234]. An alternative, though not mutually exclusive, hypothesis is that defects in DNA end complex stability in Art-P70 mutant lymphocytes allow unrepaired breaks to be aberrantly localized in three-dimensional space and engage in translocations that do not require the chromosomal partner to be located in proximity. In this regard, recent studies have provided evidence that loci involved in recurrent oncogenic translocations are located in proximity in lymphocytes [110, 250-252]. This hypothesis does not preclude amplification from occurring in the Art-P70 background, and indeed we did observe N-myc amplification in one *Art*$^{P70/P70}$*p53*$^{-/-}$ pro-B lymphoma (C263). It will be of significant interest to further define the molecular mechanisms underlying the oncogenic translocations in Art-P70/p53 tumors.

In summary, these studies provide insight into the consequence of truncation of the Artemis C-terminal domain and dysfunctional RAG1 activity on the fate of chromosomal DNA ends during endogenous V(D)J rearrangements. Aberrant DNA ends generated by substrate selection error and/or destabilization of end bound complexes possess significant potential to engage spontaneously in oncogenic chromosomal translocations. Together, these findings have important implications for tumor predisposition associated with hypomorphic mutations in the *RAG* or *Artemis* genes in the human population.

2.5 Materials and Methods

Mice.

Gene-targeted ATM null, RAG1-S723C, RAG2 null, Artemis null and Art-P70 mice (mixed 129Svev/C57Bl6 genetic background) were previously generated [82, 158, 253, 254]. p53 mutant mice (Trp53^{tm1Tyj}) in a 129S2/Sv background were obtained from Jackson Laboratory and bred with *Rag1*$^{S723C/S723C}$, *Art*$^{-/-}$ and *Art*$^{P70/P70}$ animals. Double heterozygous *Art*$^{+/-}$*p53*$^{+/-}$ and *Art*$^{+/P70}$*p53*$^{+/-}$ mice were subsequently interbred to generate progeny of the desired genotypes

for the tumorigenesis studies (i.e. $Art^{+/+}p53^{+/+}$, $Art^{-/-}p53^{+/+}$, $Art^{-/-}p53^{-/-}$ $Art^{P70/P70}p53^{+/+}$, $Art^{P70/P70}p53^{-/-}$ and $Art^{+/+}p53^{-/-}$). The single- and double-mutant mice as well as wild-type controls used in the Art-P70 study were approximately 75% 129Sv and 25% C57Bl6; thus, the experimental cohorts are closely strain matched. Approval for use of animals in this study was granted by the University of Michigan UCUCA office (protocol number 08758). These mice were housed in a pathogen-free facility dedicated to immunocompromised animals.

Interchromosomal V(D)J rearrangements

Nested PCR amplification reactions used to detect TCRγ intrachromosomal and TCRγ-to-TCRβ interchromosomal transrearrangements were modified from methods as described previously [222]. Genomic DNA (100 ng) obtained from thymocytes isolated from 4- to 5-week-old mice [$Art^{+/+}$ (*n*= 3), $Art^{-/-}$ (*n*= 7), $Art^{P70/P70}$ (*n*= 5), $Art^{+/P70}$ (*n*= 10)] was amplified in 50 µl of reaction mixture containing set 'a' primers (10 pmol. The cycling conditions were: denaturation at 95°C, 30 cycles of amplification at 95°C for 15 s, 55°C for 15 s, 72°C for 30 s with a 6-s increment per cycle followed by 10 min elongation at 72°C. The products from the first reaction (5 µl) were used in a nested PCR reaction with the same conditions using primers set 'b'. The final PCR products (25 µl) were run on a 1.5% agarose gel followed by Southern blotting using probes (primers set 'c') internal to the primers used for PCR amplification. The second-round PCR products were subcloned into pCR 2.1-TOPO (Invitrogen; Carlsbad, CA, USA) and individual clones were sequenced. TCRβ Dβ2-to-Jβ2 intrachromosomal rearrangements were PCR amplified from thymic genomic DNA (100 ng) at an annealing temperature of 62°C (35 cycles). Each experiment was repeated at least thrice independently.

Hybrid join analysis

To analyze the levels of coding and hybrid joints between Vκ6–23 and Jκ1, PCR assays were used as described previously [128]. Genomic DNA (0.5 µg) isolated from mouse splenocytes for each genotype ($Art^{P70/P70}$; *n*= 4) was PCR amplified in 50 µl with 15 pmol of each primer. PCR conditions were as follows: 95°C for 5 min followed by 17 cycles of 94°C (30 s), 64°C (30 s), 72°C (30 s). A second PCR reaction was carried out under the same conditions for 25 amplification cycles using 4-fold dilutions of the first PCR reaction and nested primer pairs. The HJ and CJ PCR

products were transferred to Zetaprobe membrane and hybridized with pκg oligonucleotide. For normalization, 4-fold dilutions starting with 0.5 μg of genomic DNA were PCR amplified. For Vβ14 coding and hybrid joint analysis, genomic DNA (0.5 μg) was isolated from mouse thymocytes for each genotype [$Art^{P70/P70}$ (*n*= 2), $Art^{+/P70}$ (*n*= 5)], and PCR analysis was performed as described [128]. The PCR products were analyzed by Southern blotting using the pβg oligonucleotide as a probe.

Characterization of tumors

Lymphoid tumors were analyzed by flow cytometry with antibodies against surface B-cell (CD43, B220, IgM) and T-cell (CD4, CD8, CD3, TCRβ, CD44, CD25) markers. Solid tumors were fixed in Bouin solution, paraffin embedded, and analyzed histologically by hematoxylin and eosin staining of sections. Thymic and pro-B lymphomas were cultured in RPMI medium 1640 supplemented with 15% fetal calf serum, 25 U/ml IL-2 (BD Biosciences) and 25 ng/ml of IL-7 (PeproTech, Rocky Hill, NJ, USA). The proportion of pro-B and thymic lymphomas in the $Art^{P70/P70}p53^{-/-}$ cohort was calculated to be statistically significantly different from that observed for $Art^{-/-}p53^{-/-}$ lymphomas (P = 0.014, two-tailed Fisher's exact test). Data for $Art^{-/-}p53^{-/-}$ tumors also in a mixed 129Sv/C57Bl6 genetic background from a previous publication [234] were included in the calculation (total of 13 lymphomas: 10 pro-B and 3 thymic.)

Chromosomal analyses of tumor metaphases

Spectral karyotyping was performed either on metaphases from cells derived from the primary tumor (tumors 135, S542) or early passage tumor cells cultured as previously described [234] (all other tumors). SKY was performed using an interferometer (Applied Spectral Imaging; Vista, CA, USA) and SkyView software. Structural aberrations were considered clonal if present in 2 or more metaphases [172, 255]. For FISH analyses, early passage tumor cultures were exposed to 100 ng/ml Colcemid for 5.5 h. BAC probes for FISH analysis were obtained from the RPCI-23 library (Children's Hospital Oakland Research Institute; Oakland, CA, USA) and nick-translated using biotin-11-dUTP or digoxigenin-16-dUTP by standard procedures (Roche; Basel, Switzerland). BAC probes hybridizing to TCRα/δ are as follows: RPCI-23 204N18 (centromeric to

TCRα/δ region) and RPCI-23 269E2 (telomeric to TCRα/δ region). BAC probe hybridizing to TCRβ are as follows: RPCI-23 216J19 (spans TRBD1–TRBV31). BAC probe hybridizing to TCRγ are as follows: RPCI-23 212N5 (within TCRγ). BAC probes hybridizing to IgH are as follows: N-myc BAC A-10-1 [234], Bac199 (hybridizes to Cα), Bac 207 (hybridizes to V region). c-myc BAC probe was previously described [256]. At least 10 metaphases for each tumor were analyzed by SKY and at least 20 metaphases by FISH.

Southern blot and RT-PCR analyses

Genomic DNA (20 μg) isolated from control tissues (tail or kidney) or tumor masses was digested with *Eco*RI. Southern blotting was performed with previously characterized probes hybridizing within the TCRβ locus (Drd1), J_H region, HS3a, Cμ, N-myc and c-myc loci. Southern blots were visualized using a Phosphorimager. Band intensities were quantitated using Image Quant TL v2005 software, and relative levels were normalized to a non-lymphoid locus (LR8). Fold amplification was calculated compared with the intensities of bands in the kidney controls on the same membrane.

Reverse transcription of total RNA (1 μg) isolated from primary $Art^{P70/P70}p53^{-/-}$ (C219, C263) and $Art^{-/-}p53^{-/-}$ (C405) pro-B lymphomas and wild-type LN was performed using a poly-dT [208] primer and MLV-reverse transcriptase (Invitrogen). PCR amplification of cDNAs was performed using gene-specific primers to c-myc (exons 1 and 3) and N-myc (exons 2 and 3). cDNA levels were normalized to tubulin. Bands were quantitated using AlphaImager 2200 (AlphaInnotech; Santa Clara, CA, USA). RT-PCR reactions were repeated at least four times.

Acknowledgements

This work was previously published in two separate publications:

Giblin W, Chatterji M, Westfield G, **Masud T**, Theisen B, Cheng H, DeVido J, Alt F, Ferguson D, Schatz D, Sekiguchi J. *Leaky severe combined immunodeficiency and aberrant DNA rearrangements due to a hypomorphic RAG1 mutation.* Blood, 2009. **113**(13): p. 2965-75. PMID: 19126872

Jacobs C*, Huang Y*, **Masud T***, Lu W, Westfield G, Giblin W, Sekiguchi JM. (2010) A hypomorphic *Artemis human disease allele causes aberrant chromosomal rearrangements and tumorigenesis.* Hum Mol Genet. 2011 Feb 15. PMID: 21147755

In this chapter, I have reproduced parts of both manuscripts with some modifications. We thank all the authors for their contribution to the study and manuscript. For the RAG1-S723C study, W.G. and M.C. performed experiments and analyzed the results; G.W., B.T., H.-L.C. and I performed experiments; J.D. generated vital reagents in the laboratory of F.W.A.; D.G.S., D.O.F., and J.S. conceptualized and designed experiments and interpreted the results; J.S. wrote the paper; and all authors read and edited the paper. For Art-P70 study, we thank Drs. David Ferguson and John Moran for helpful discussions. C.J., Y.H. and I contributed equally to the authorship*. Y.H. analyzed the tumors. Southern blot and FISH analyses were done by C.J. W.L., G.W. and W.G. performed experiments not mentioned in this chapter.

Funding

RAG1-S723C mice study was supported in part by the National Institutes of Health (NIH, Bethesda, MD) through the University of Michigan's Cancer Center Support Grant (5 P30 CA46592); NIH grant AI063058 (NIAID), Pew Scholars Award (Pew Charitable Trusts, San Francisco, CA), Munn IDEA award (UM Cancer Center, Ann Arbor MI) to JoAnn Sekiguchi.; NIH grant A132524 (NIAID) to D.G.S.; and NIH grant A135714 (NIAID) to FWA. TM is a Fulbright Scholar. D.G.S. and F.W.A. are Investigators of the Howard Hughes Medical Institute. Art-P70 study was supported by NIH grant AI063058 (NIAID), Pew Scholar's Award (Pew Charitable Trusts), Munn IDEA award (UM Cancer Center) to J.M.S. and by the NIH UM Cancer Center Support Grant (5 P30 CA46592). C.J. received support from the NIH Genetics Training grant T32-GM07544 (NIGMS), T.M. is a Fulbright Scholar and W.L. received support from the Cellular and Molecular Biology Training Grant (T32-GM007315).

Chapter 3

Inhibition of ATM Kinase Activity Suppresses Ionizing Radiation-Induced Genomic Instability in Artemis-Deficient Lymphocytes

3.1 Abstract

The endonucleolytic activity of Artemis, an important canonical non-homologous end joining (C-NHEJ) factor, is required to process complex DNA double strand breaks post-irradiation. It is also essential to open the hairpin coding ends that are formed during V(D)J recombination, a process necessary for antigen receptor gene assembly and lymphocyte development. Artemis deficiency results in cellular radiosensitivity and immunodeficiency with accumulation of hairpin coding ends in lymphocytes. Low level end-joining occurs in these cells and is characterized by extensive deletions, microhomologies and long stretches of P nucleotides indicating the presence of error-prone alternative end-joining (A-EJ) factors. The mechanisms that regulate these factors and the contribution of the DNA damage response in activating this pathway are poorly defined. In this study, we report that low dose ionizing radiation (IR) induces limited lymphocyte development and robust V(D)J rearrangements including aberrant trans-rearrangements in the Artemis-deficient mice and v-abelson transformed pre-B cell lines. These rearrangements have complex breakpoint junctions. The IR-induced response is not observed in mice with both Artemis and ATM deficiency. Additionally, inhibition of ATM kinase activity in Artemis-null v-abl pre-B cells suppresses the formation of both coding joins and trans-rearrangements. Our data demonstrate that, in the developing lymphocytes, induction of ATM kinase activity can trigger an error-prone end-joining response

in the absence of Artemis leading to increased levels of genomic instability. This study offers useful insight into the mechanisms that regulate alternative end joining in lymphocytes and has important implications for cancer therapeutics.

3.2 Introduction

Genomic lesions such as chromosomal translocations, deletions and inversions are rare but serious outcomes of aberrant DNA double strand break (DSB) repair, and can lead to oncogenic transformation. DSBs result from exposure to cytotoxic agents (e.g., ionizing radiation and radiomimetic drugs) or arise as programmed intermediates during meiosis and lymphocyte-specific processes such as V(D)J recombination and class switch recombination [102].

V(D)J recombination is a series of DNA rearrangements that is responsible for generating the genes that encode the vastly diverse variable regions of the T cell receptors (TCR) and B cell immunoglobulins (Ig) for antigen binding. These variable region exons are assembled from an array of variable (V), diversity (D) and joining (J) genomic segments [2]. This process is initiated by a lymphocyte-specific, G1-restricted RAG1/2 endonuclease that binds the recombination signal sequences (RSSs) flanking individual V, D and J segments [5, 257]. Cleavage by RAG1/2 generates two covalently closed hairpin coding ends and two blunt signal ends which are held together by the RAG proteins in a postcleavage complex [33, 35, 258]. The coding ends are subsequently processed and joined by the canonical non-homologous end-joining (C-NHEJ) pathway.

C-NHEJ, a major DNA DSB repair pathway, does not need a homologous sister chromatid to restore genomic integrity. It is initiated by the recognition of the DNA ends by Ku70/80 heterodimer which then recruits DNA-dependent protein kinase catalytic subunit (DNA-PKcs), a serine/threonine protein kinase [111]. The RAG-induced breaks and a subset of general DSBs are subsequently processed by nucleases and polymerases [107]. *Artemis* (*DCLRE1C, DNA Crosslink Repair 1C*) gene encodes a nuclear protein which, in complex with DNA-PKcs, nucleolytically opens the hairpins at or near the apex with the addition of a few palindromic (P) nucleotides at the junctions [80]. Coding end processing is associated with loss of nucleotides as

well as de novo addition of non-templated N region nucleotides providing further junctional diversity [19, 20]. The processed DNA ends are then joined by DNA Ligase IV, XRCC4 and XLF to form a functional coding joint or V(D)J exon [13, 14, 259]. The RSS ends are directly joined without any processing to form a precise signal joint. DNA-PKcs and Artemis are largely dispensable for signal joint formation but are essential for coding end hairpin opening and processing. Since antigen receptor assembly is required for lymphocytes to develop, defects in V(D)J recombination due to mutations in RAG proteins or C-NHEJ factors lead to immunodeficiency disorders characterized by arrested B and T lymphocyte development. *Artemis* mutations are responsible for a subset of Severe Combined Immunodeficiency disorders with radiosensitivity (RS-SCID) which results from impaired repair of complex general DSBs. Some Artemis-deficient mice, however, have leaky T cell development [158].

Since DSBs are essential intermediates for V(D)J recombination, proper end joining is crucial to maintain chromosomal integrity in the developing and rapidly proliferating lymphocytes. Joining of the RAG-induced breaks by C-NHEJ pathway is regulated at many levels to avoid mis-joining particularly translocations [185, 198]. Rarely, due to an error in the V(D)J process, a proto-oncogene can be placed under the control of an Ig or TCR promoter region (e.g., immunoglobulin heavy chain *IgH* and *c-myc* translocations) leading to dysregulated cell growth, cell survial and malignant transformation. A majority of human progenitor and mature B-cell lymphomas and leukemias harbor recurrent clonal translocations involving RAG-induced breaks suggesting a role of aberrant end-joining in tumor initiation [109, 184, 260]. These tumor-associated translocations contain regions of microhomology at the junctions; thus, it has been hypothesized that alternative mechanisms of end-joining (A-EJ), which are frequently mediated by microhomologies may catalyze these events. Further evidence for the oncogenic role of A-EJ is provided by mice doubly deficient in C-NHEJ proteins (DNA-PKcs, Ku70, Ku80, Artemis, Ligase 4, XRCC4) and tumor suppressor, p53. These mice develop progenitor-B cell lymphomas harboring aberrant rearrangements involving the RAG-induced breaks [der(12)t(12;15) translocations and *IgH/c-myc* or IgH/*N-myc* coamplifications] [238, 240, 261]. The pro-B lymphomas that arise in Artemis/p53-null mice lack der(12)t(12;15) translocations and *IgH*/*c-myc* amplification [261]. Instead, they contain *IgH*/*N-myc* coamplifications. These

studies reveal the tumor suppressor functions of C-NHEJ factors and potential contribution of translocation-prone A-EJ mechanisms in lymphomageneis. However, the details of end-joining factors and mechanisms responsible for these events are still largely unknown.

Several studies over the last two decades have indirectly provided evidence for the existence of an A-EJ mechanism in the lymphocytes. C-NHEJ deficient mice are unable to join RAG-induced breaks and accumulate unresolved coding ends in their developing lymphocytes. Exposure of SCID mice with mutant DNA-PKcs to agents that induce DNA DSBS such as whole body gamma(γ) irradiation promotes the repair of preexisting unrepaired hairpins and induces rearrangements at TCR loci (TCR-β, δ, γ) in progenitor T lymphocytes [262, 263]. These V(D)J rearrangements are associated with a limited maturation of double negative (DN) progenitor T lymphocytes- characterized by the lack of expression of CD4 and CD8 cell surface receptors- to $CD4^+CD8^+$ double positive (DP) cells. RAG-null thymocytes that do not contain cleaved coding ends also progress to DP stage on exposure to γ-irradiation; they bypass β-selection indicating that development can occur through TCRβ chain-independent processes [264, 265]. Studies using extrachromosomal substrates in pre-B cells led to the hypothesis that γ-irradiation impacts V(D)J recombination directly, independent of the thymic stromal influences [266] leading to interesting speculations about the role of ionizing radiation (IR) in inducing end-joining in lymphocytes. However, the factors that regulate this response are still mostly unexplored. In addition, the contribution of Artemis and/or other nucleases in this response is also undefined. Thus, these mice are a valuable *in vivo* model system to further elucidate the role of various factors involved in IR-induced lymphocyte development and V(D)J rearrangements.

In addition to the C-NHEJ factors, other proteins of central importance in DSB repair play roles in facilitating efficient joining of RAG-induced breaks. DNA DSBs, including those induced by IR, are sensed by the MRE11/RAD50/NBS1 (MRN) complex which then activates ATM-dependent DNA damage response [267]. Ataxia telangiectasia mutated (ATM), a member of phosphatidylinositol 3-kinase-like kinase (PIKK) family, phosphorylates several substrates for cell cycle arrest and efficient DNA repair, and *ATM* mutations result in marked radiosensitivity

[268]. Although it is dispensable for the repair of RAG-induced breaks, ATM deficiency is also associated with mild to moderate immunodeficiency and predisposition to lymphomas associated with antigen receptor translocations [167, 269]. More recently, the immune phenotype was attributed to its role in regulating the stability of RAG-induced DNA ends in post-cleavage complexes [128]. ATM can be activated by RAG-induced DSBs and modulates transcriptional program important for normal lymphocyte development in the absence of Artemis [244, 270, 271]. IR-induced V(D)J rearrangements in C-NHEJ deficient mice suggest that DNA damage response (DDR) might also contribute to the activation of error-prone end-joining mechanisms. However, the exact role of ATM-dependent DNA damage response (DDR) in promoting aberrant V(D)J recombination still needs to be investigated.

In the current study, we examined the effect of low-dose IR on lymphocyte development and V(D)J rearrangements in Artemis-deficient mice T lymphocytes and Abelson transformed murine pre-B cell lines. We demonstrate that IR induces robust intra- and inter-locus end joining in these cells. Further, inhibition of ATM kinase activity suppresses the formation of these coding joins and translocations. Our study provides insight into the role of ATM-dependent DNA damage response in mediating chromosomal translocations in the lymphocytes. It also has implications for therapy-induced translocations and therapeutic interventions.

3.3 Results

T lymphocyte differentiation is induced in Artemis deficient mice by low-dose γ-irradiation.

Productive TCRβ gene rearrangement and subsequent surface expression of pre-TCR (comprising of TCRβ and pre-Tα chains, and CD3) allows $CD4^-CD8^-$ (DN) T lymphocytes to proliferate and advance to the $CD4^+CD8^+$ (DP) stage of development [89]. In the absence of Artemis endonuclease activity, hairpin coding ends fail to undergo rearrangements and the majority of T lymphocytes are arrested at the DN stage. To determine if low dose γ-irradiation leads to an induction of T lymphocyte differentiation in Artemis deficiency, 2.5 Gy of whole-body γ-irradiation was administered to 3 to 5-week-old Artemis null ($Art^{-/-}$) mice in a single dose. Three weeks later, thymocytes were examined for CD4, CD8 and TCRβ expression by flow

cytometry. Representative profiles of un-irradiated and irradiated wild-type (WT) and $Art^{-/-}$ thymocytes are shown in figure 3.1A and supplementary figure S3.1. As anticipated, a significantly lower percentage of DP and surface TCRβ positive ($sTCR\beta^{+}$) thymocytes were detectable in the thymi of the unirradiated *Art*$^{-/-}$ mice as compared to the WT mice (Figure 3.1B, 3.1C, Table 3.1). Upon irradiation, the WT mice did not exhibit significant changes in the mean percentages of thymocyte population from the control WT mice (Figure 3.1B, 3.1C; Figure S3.1). In contrast, we observed an over 870-fold increase in the percentage of DP thymocytes in *Art*$^{-/-}$ mice after irradiation (Figure 3.1C, Table 3.1). The percentage of $sTCR\beta^{+}$ thymocytes was also significantly increased by 3.5-fold after irradiation. Next, the intracellular expression of TCRβ (icTCRβ) was examined. The increase in $icTCR\beta^{+}$ cells was striking with a 28-fold increase in the irradiated *Art*$^{-/-}$ mice as compared to the unirradiated mice of the same genotype (Figure 3.1D, Table 3.1). This indicates that productive in-frame TCRβ rearrangements were induced by low-dose IR even in the absence of Artemis. The progression in development stage in these mice was not accompanied by a large increase in thymic cellularity (Table 3.1). We also failed to see an increase in distinct $CD4^{+}$ or $CD8^{+}$ single positive T-cell population in thymus or in the peripheral lymphoid tissues (spleen and lymph nodes) of the irradiated *Art*$^{-/-}$ mice (data not shown). A functional TCR comprised of TCRβ and TCRα chains is required for the transition of DP cells to mature single positive cells. Lack of peripheral $CD4^{+}$ or $CD8^{+}$ single positive cells in the irradiated *Art*$^{-/-}$ mice suggests that despite a significant increase in intracellular TCRβ, a functional TCR is not be formed in these cells.

Table 3.1: Impact of Ionizing Radiation on T Lymphocytes in *Art*$^{-/-}$ mice

Genotype	IR Dose (Gy)	N	Thymocyte count (x 10^6)	$CD4^{+}CD8^{+}$ cells (% of total)	$sTCR\beta^{+}$ cells (% of total)	$icTCR\beta^{+}$ cells (% of total)
WT	0	4	124.6 ± 24.9	83.4 ± 1.03	19.4 ± 1.3	28.8 ± 2.8
	2.5	4	100.3 ± 25	74.3 ± 2.02	18.2 ± 1.7	22.5 ± 1.2
$Art^{-/-}$	0	5	6 ± 2.6	0.06 ± 0.02	1.5 ± 0.2	0.4 ± 0.1
	2.5	6	8.4 ± 2.7	52.7 ± 5.2	5.3 ± 0.7	12.3 ± 4.2

To determine if IR induces *Art*$^{-/-}$ B lymphocyte differentiation, we examined the surface IgM expression in bone marrow cells and splenocytes by flow cytometry. In contrast to the induced development of thymocytes, γ-irradiation failed to simultaneously rescue B lymphocyte development in the *Art*$^{-/-}$ mice and cells were arrested at the immature B220^{+}IgM^{-} pro-B stage (Figure 3.1E, data not shown), as has been shown previously for the DNA-PKcs mutant SCID mice [262, 272]. Thus, our data demonstrate that sublethal irradiation of *Art*$^{-/-}$ mice induces a T lymphocyte-specific developmental progression with readily detectable DP cells expressing surface and intracellular TCRβ. However, this is not associated with an increase in CD4^{+} or CD8^{+} SP cells. Likewise, we do not observe IR-induced developmental progression in B lymphocytes.

Figure 3.1: Low-dose IR induces T lymphocyte development in *Art*$^{-/-}$ mice.

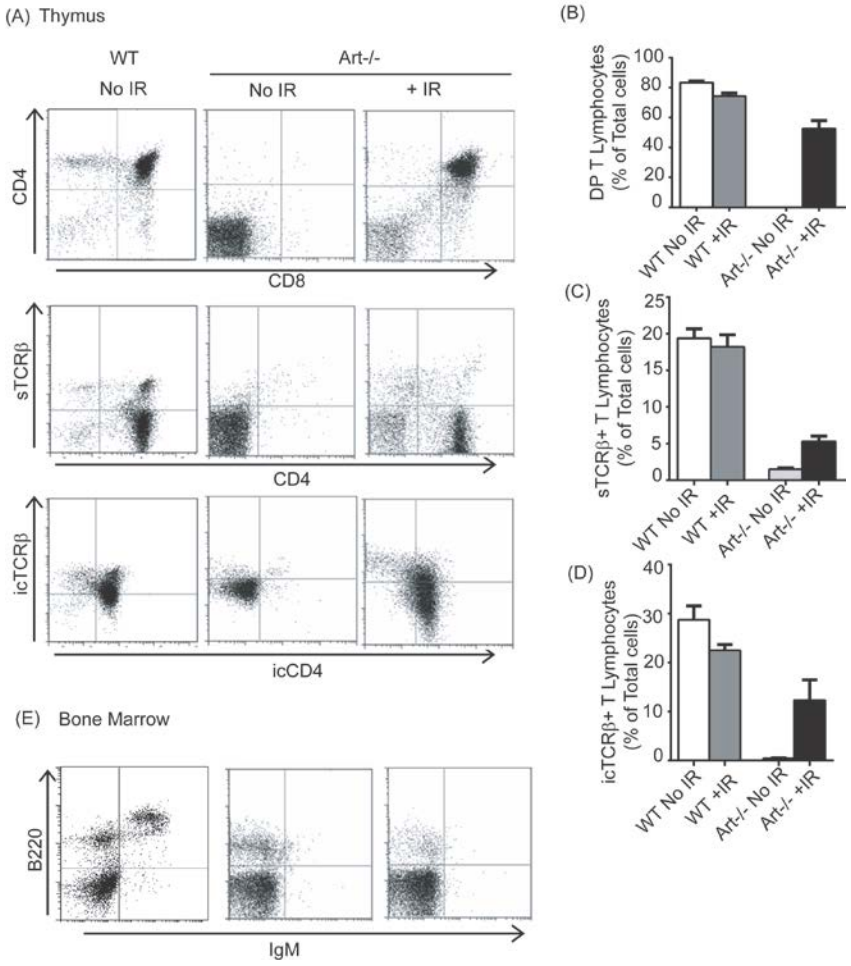

Figure 3.1. 3 to 5-weeks-old WT and *Art*$^{-/-}$ mice were exposed to 2.5 Gy and analyzed 3 weeks later for lymphocyte development. **(A)** Flow cytometric analysis was done on thymocytes from

the unirradiated and the irradiated mice for cell surface CD4, CD8, TCRβ and intracellular CD4 and TCRβ expression. **(B, C, D)** Graphs representing percentages of thymocytes expressing **(B)** cell surface CD4 and CD8, **(C)** surface TCRβ and **(D)** intracellular TCRβ. The bars represent means for each group with SEM. **(E)** Flow cytometric analysis was done on bone marrow cells from the unirradiated and the irradiated mice for $B220^{+}IgM^{+}$ B lymphocytes.

Irradiated *Art*$^{-/-}$ mice exhibit rearrangements at the TCRβ locus.

In the developing T lymphocytes, TCR Dβ-to-Jβ rearrangements occur at DN2 stage, followed by Vβ-to-DJβ rearrangements in DN3 cells. Detection of extra- and intracellular TCRβ in the irradiated *Art*$^{-/-}$ thymocytes led us to examine the status of V(D)J rearrangements at the TCRβ locus in response to γ-irradiation. The TCRβ locus consists of a cluster of V segments and two clusters of Dβ and Jβ segments, Dβ1 to Jβ1(1-6) and Dβ2 to Jβ2(1-7) (Figure 1.). Genomic DNA from individual thymi was analyzed by PCR and Southern blot analysis, using primers specific for Dβ1 to Jβ1 and Dβ2 to Jβ2. Figure 3.2A shows that there is no obvious difference in the levels of rearrangements between the unirradiated and the irradiated WT mice. Bands corresponding to rearranged Dβ1Jβ1 products were not detected in unirradiated *Art*$^{-/-}$ mice. In contrast, bands were readily detected in irradiated *Art*$^{-/-}$ mice to levels that are comparable to those seen within the WT thymus. Detection of multiple bands indicates polyclonal origin of TCRβ rearrangements. The same was observed for Dβ2Jβ2 rearrangements (data not shown). These results indicate that IR exposure of *Art*$^{-/-}$ mice not only promotes immature thymocyte differentiation, but also induces substantial TCR Dβ-to-Jβ rearrangements. Next, we examined Vβ10 to Jβ2 and Vβ12 to Jβ1 rearrangements by PCR analyses. Vβ-to-DJβ rearrangements were also detectable, albeit at lower levels, in the irradiated *Art*$^{-/-}$ mice as compared to the WT mice (Figure 3.2A, data not shown). This suggests that most of the rearranged D and J segments might not be able to undergo successful V to DJ rearrangements in the *Art*$^{-/-}$ mice upon irradiation.

Figure 3.2: Low-dose IR induces V(D)J rearrangements at TCRβ locus in *Art*$^{-/-}$ T lymphocytes.

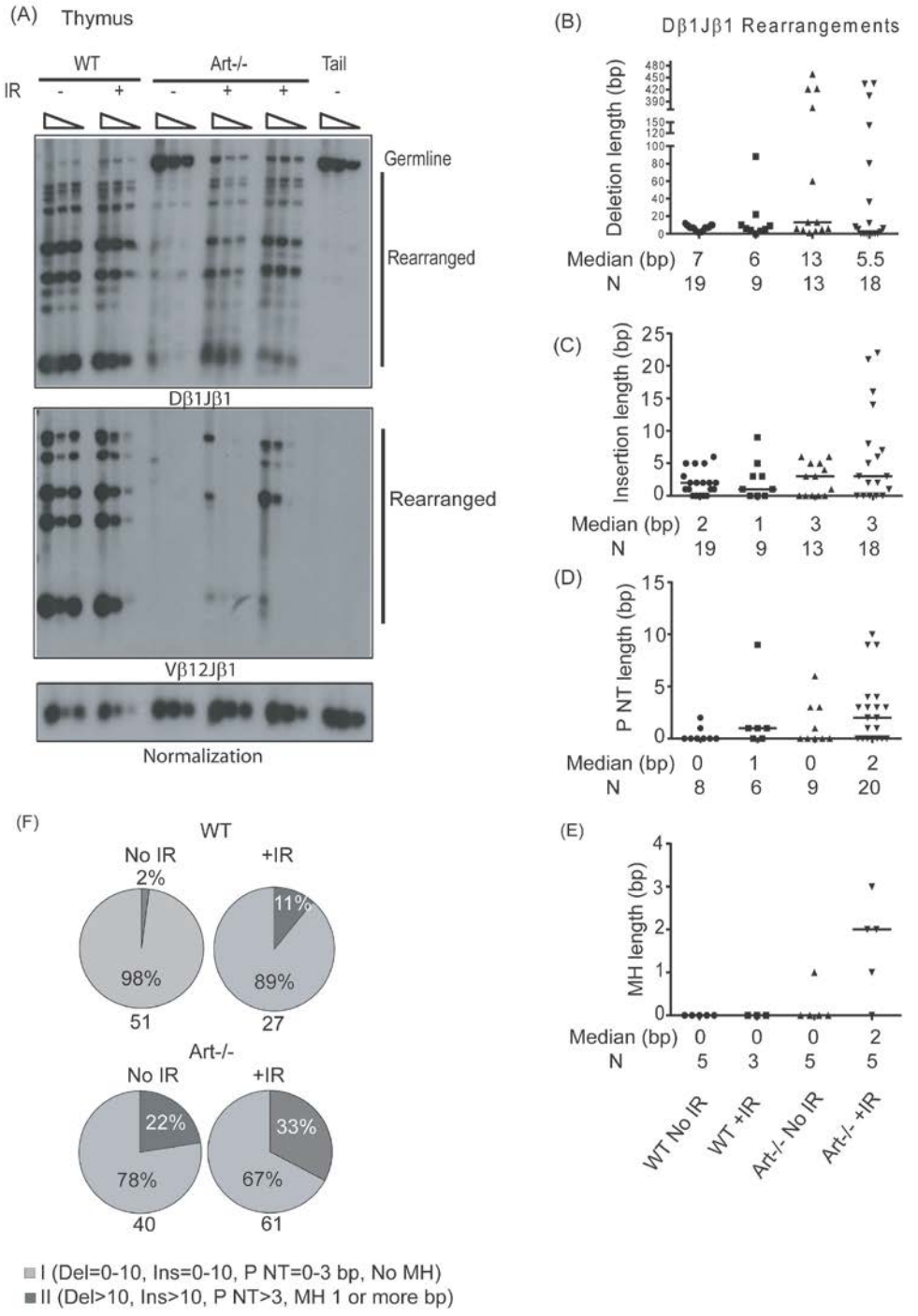

Figure 3.2. (A) Thymic DNA was prepared from the unirradiated and irradiated WT and *Art*$^{-/-}$ mice and PCR analyses done to determine Dβ1 to Jβ1 and Vβ12 to Jβ1 rearrangements. A non-lymphoid tissue (tail) was included as a negative control. DNA input was normalized using PCR for a non-rearranging gene. **(B, C, D, E)** PCR products for Dβ1 to Jβ1 rearrangements from two irradiated Art$^{-/-}$ mice were subcloned into the TOPO2.1 vector and sequenced. Plots representing the distributions of **(C)** deletion, **(D)** insertion, **(E)** P-nucleotide (P NT) and **(F)** microhomology (MH) lengths at the Dβ1 to Jβ1 breakpoint junctions are shown. The number of sequences (N) and median value for each experimental group is indicated below the graph. The horizontal bar represents the median value for each group. **(B)** Each value indicates combined deletion at both coding ends within a single junction. **(C)** Each value includes all the nucleotides inserted at the junction. **(D)** Each value represents P NT length at an individual coding end. **(E)** Each value indicates microhomology (MH) length at breakpoint junctions with no insertions. **(F)** All the sequence analyses were combined and segregated in to two groups. Pie charts representing the percentages for each group in the un-irradiated and irradiated WT and Art$^{-/-}$ mice are shown.

Intrachromosomal Dβ1 to Jβ1 joins from irradiated *Art*$^{-/-}$ mice are processed in a different manner from those in unirradiated mice.

Next, we sequenced the PCR products corresponding to Dβ1-to-Jβ1 rearrangements to get insight into the IR-induced mechanisms that facilitate the coding end joining. In the absence of Artemis, the defect in recombination is not absolute and rearrangements, albeit at lower levels, still occur. These coding joins are mostly structurally abnormal containing extensive deletions, microhomologies and long stretches of palindromic nucleotides (P NT) [214]. In contrast, when Artemis endonuclease activity and C-NHEJ are intact, the junctions are characterized by small deletions at the ends, short P and N nucleotide insertions, with rare use of microhomologies (Figure S3.7).

Figures 3.2B-3.2G and S3.2 show distributions and structural comparisons of the joins isolated from the WT and *Art*$^{-/-}$ mice. The junctional sequences are shown in Figure S3.4A. We analyzed these sequences for end-modifications including deletions, P and N nucleotide insertions and use of microhomologies. For all our sequence analyses, each deletion value represents combined deletions at both ends for each individual join. As expected, most of the

WT joins, with or without IR, contained deletions of <10 bp (Figure S3.2). The median deletion lengths were also less than 10bp (Figure 3.2B). Over half of the junctions in the *Art*$^{-/-}$ cells exhibited deletions of >10 bp and a higher median deletion length of 13 bp (Figure 3.2B, Figure S3.2). In the irradiated *Art*$^{-/-}$ mice, the frequency of joins containing deletions longer than 10bp (39%; median deletion length, 5.5bp) was lower as compared to the un-irradiated cohort. Surprisingly, we observed a striking increase (39%) in joins with no deletions in the *Art*$^{-/-}$ lymphocytes upon irradiation (0% in WT and in un-irradiated *Art*$^{-/-}$ cells).

The junctions were also different with regard to the length of nucleotide insertions (Figure 3.2C, Figure S3.2). We analyzed the total number of nucleotides added, including P NT (underlined sequences), in an individual join. In the WT and un-irradiated *Art*$^{-/-}$ mice, all the joins contained insertions of <10 bp with median insertion lengths of <4 bp. Upon irradiation of *Art*$^{-/-}$ mice, joins had more complex insertions. Approximately 22% of junctions had 11 to 22 bp long insertions with long stretches of non-P NT, although the median insertion length was only 3 bp. To determine if the non-P NT were randomly added or derived from a distant flanking sequence, we used Blast anlaysis to align them with the mouse TCRβ locus. Figure S3.2B shows some of these sequence alignments. “ATATTTCCC” or “GATATTTC”, parts of an inserted sequence, could have been derived 10 kb or 0.6 kb upstream of Dβ1 segment, respectively and inserted within the junction. However, because of the short length of these sequences, it is hard to make a conclusive statement about the origin of these nucleotides.

As for the P nucleotide length specifically, coding ends with no deletions were analyzed (Figure 3.2D, Figure S3.2A). All such coding ends within junctions from the unirradiated WT mice and over 85% from the un-irradiated *Art*$^{-/-}$ mice were <4 bp long with median P NT lengths of 0 bp each. One out of nine coding ends in the irradiated WT mice had 9 bp long P NT with extensive resection at the J segment and a 5 bp long MH residing within that end and the P NT sequence derived from the other end (Figure S3.7). On the other hand, 25% of the coding ends in the irradiated *Art*$^{-/-}$ mice had 4-10 bp long P NT with median length of 2 bp. These data show that the lengths of nucleotide insertions and P NT are increased at the V(D)J joins recovered

from the irradiated *Art*$^{-/-}$ thymocytes and rarely in the irradiated WT cells. Moreover, some of these joins exhibit complex nucleotide insertions.

For microhomologies (MH), joins with no insertions were analyzed. WT joins showed no MH whereas 20% of *Art*$^{-/-}$ junctions showed MH of 1-4 bp, the median MH length being 0 bp in each case (Figure 3.2E, Figure S3.2A). In contrast, after irradiation, 80% of the respective *Art*$^{-/-}$ junctions showed 1-4 bp long MH with a median length of 2 bp. Our results may not accurately reflect the actual proportion of junctions with MHs as the sample size for this analysis was very small (<6 joins for each genotype). Nonetheless, our results indicate that MH are used for end-joining in irradiated *Art*$^{-/-}$ mice.

Finally, to get an overall estimate of the proportion of abnormalities, we pooled our results in to two categories (Figure 3.2F). Group I includes all the WT-like analyses with (1) Deletions ≤10 bp, (2) Insertions ≤10 bp, (3) P NT ≤3 bp and (4) no MH. Group II includes all the abnormal analyses with (1) Deletions ≤10 bp, (2) insertions >10 bp (3) P NT >3 bp and (4) MH ≥1 bp. About 98% of the WT sequences are represented in Group I with only 2% in Group II. 22% of un-irradiated *Art*$^{-/-}$ and 33% of irradiated *Art*$^{-/-}$ sequences are, however, represented in Group II indicating an overall increase in aberrant joins in *Art*$^{-/-}$ mice which is further enhanced after IR. Altogether, our sequence analyses suggest that in the absence of Artemis, at least some chromosomal breaks are processed differently after IR.

Aberrant interchromosomal trans-rearrangements at the antigen receptor loci in irradiated *Art*$^{-/-}$ thymocytes.

To investigate if IR induces chromosomal translocations between RAG-induced breaks in Art$^{-/-}$ thymocytes, we examined aberrant interchromosomal trans-rearrangements between the TCRγ and TCRβ loci located on mouse chromosomes 13 and 6, respectively. TCR Vγ-to-Jγ and TCR Dβ-to-Jβ rearrangements are completed in DN2/DN3 cells [219]. We used a nested PCR method using primers flanking TCRγV and TCRβJ segments as shown in Figure 3.3A. The results were confirmed by Southern blot analysis. PCR products corresponding to translocations were not detected in the WT thymocytes (Figure 3.3B). In comparison, we detected elevated levels of

trans-rearrangements in *Atm*$^{-/-}$ thymocytes, as has been shown previously [220]. Surprisingly, low-dose IR (2.5 Gy) induced a substantial increase in interchromosomal rearrangements in the *Art*$^{-/-}$ mice. Detection of bands of different sizes indicated polyclonal origin of translocations. These data demonstrate that chromosomal breaks accumulating in *Art*$^{-/-}$ thymocytes can transition into chromosomal translocations after exposure to low dose γ-irradiation.

Next, the PCR products corresponding to trans-rearrangements in the irradiated *Art*$^{-/-}$ mice were subcloned and sequenced to gain a better understanding of the underlying end-joining mechanisms (Figure 3.3C, Figure S3.4B). The junctions were analyzed as described earlier. About 38% of the joins had deletions spanning more than 10 bp, 25% had insertions >10 bp and 27% coding ends contained unusually long P NT (6-8 bp). This was similar to what we observed in Dβ1Jβ1 junctions from these mice (Figures 3.3C and S3.2). We identified only one junction out of five with MH of 5 bp in length. Pooling these analyses in group I or II (as described earlier) revealed that 29% of the total analyses were structurally abnormal. Thus, our results demonstrate that translocations are catalyzed, for the most part, in a manner similar to the intrachromosomal joins in the irradiated *Art*$^{-/-}$ thymocytes.

Figure 3.3: Low-dose IR induces aberrant interchromosmal trans-rearrangements at the RAG-induced breaks in *Art*$^{-/-}$ T lymphocytes.

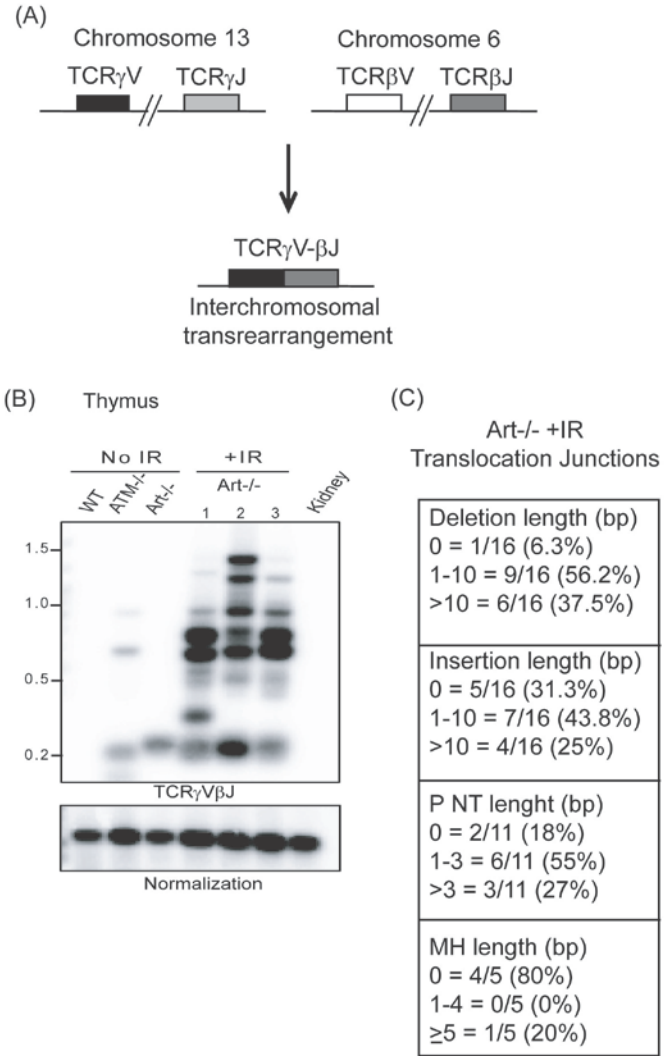

(A) Schematic of the interchromosomal trans-rearrangements between TCRγV and TCRβJ loci. **(B)** Nested PCR analyses were performed on thymic DNA isolated from the unirradiated and irradiated mice to determine TCRγV-βJ transrearrangements. DNA input was normalized using PCR for a non-rearranging gene. **(C)** PCR products corresponding to transrearrangements were subcloned in TOPO2.1 vector and sequence analysis was done. Table showing frequencies of the translocation junctions with deletions (0, 1-10, >10 bp), insertion (0, 1-10, >10 bp) and MH (0, 1-4 and ≥5 bp). Sequences were analyzed as described in Figure 3.2.

Coding joins are induced by IR in immortalized *Art*$^{-/-}$ pre-B cell lines.

Since the process of V(D)J rearrangement is essentially similar in T and B lymphocytes, we reasoned that IR might trigger apoptosis in *Art*$^{-/-}$ progenitor B cells *in vivo* which may account for the lack of IR-induced development. To examine the effect of IR on V(D)J recombination in immortalized *Art*$^{-/-}$ B lineage cells in chromosomal context, we used (v)-Abl kinase-transformed mouse pre-B cell lines with *Bcl2* transgene. The immunoglobulin light chain (*IgL*) locus has not undergone rearrangement in these cells. Treatment with Abelson kinase inhibitor, STI571 (gleevec), arrests the cells in G1 which is associated with RAG1/2 expression. This leads to rearrangements at the Igκ locus as well as a single copy retroviral recombination substrate (pMX-GFP-IRES-hCD4) or pMX-INV, which has been described previously [128]. Normal recombination in this substrate leads to the formation of coding join within the chromosome resulting in GFP expression which can be detected by flow cytometry (Figure 3.4A).

Upon RAG induction, Artemis deficiency is associated with accumulation of unrepaired coding ends in these cells [244]. We observed that arresting *Art*$^{-/-}$ cells (two clonal cell lines were used, c.30 and c. 4) in G1 induced an increase in the percentage of GFP^{+} cells; 8-13% GFP^{+} cells were detectable after G1-arrest for five days (Figure 3.4C). To rescue the end-joining defect, we expressed full-length (FL) Artemis in the *Art*$^{-/-}$ c.30 cell line. In these cells, approximately 85% GFP^{+} cells were detectable five days after G1 arrest, which was comparable to what we observe in a control WT pre-B cell line, WT INV5. Next, to examine the effect of IR on V(D)J recombination, cells were irradiated at 5 Gy and analyzed 72 hours post-irradiation (Figure 3.4B). There was no significant difference in the number of GFP^{+} cells between the untreated (no STI571/no IR) and only IR-treated cells of either genotype. Similarly, upon irradiation, there was no increase in the percentage of GFP^{+} cells beyond what we observe in unirradiated G1-arrested WT cells (WT INV5 and *Art*$^{-/-}$c.30+FL-Artemis) (Figure 3.4C; data not shown). However, in both G1-arrested *Art*$^{-/-}$ cell lines, there was a slight but significant increase of 3-5% in GFP^{+} cells after IR. (Figure 3.4C). The cell survival was not affected by IR treatment of the G1-arrested cells (Figure S3.3).

Figure 3.4: V(D)J rearrangements are induced upon irradiation in murine Abelson-transformed *Art*$^{-/-}$ pre-B lymphocytes.

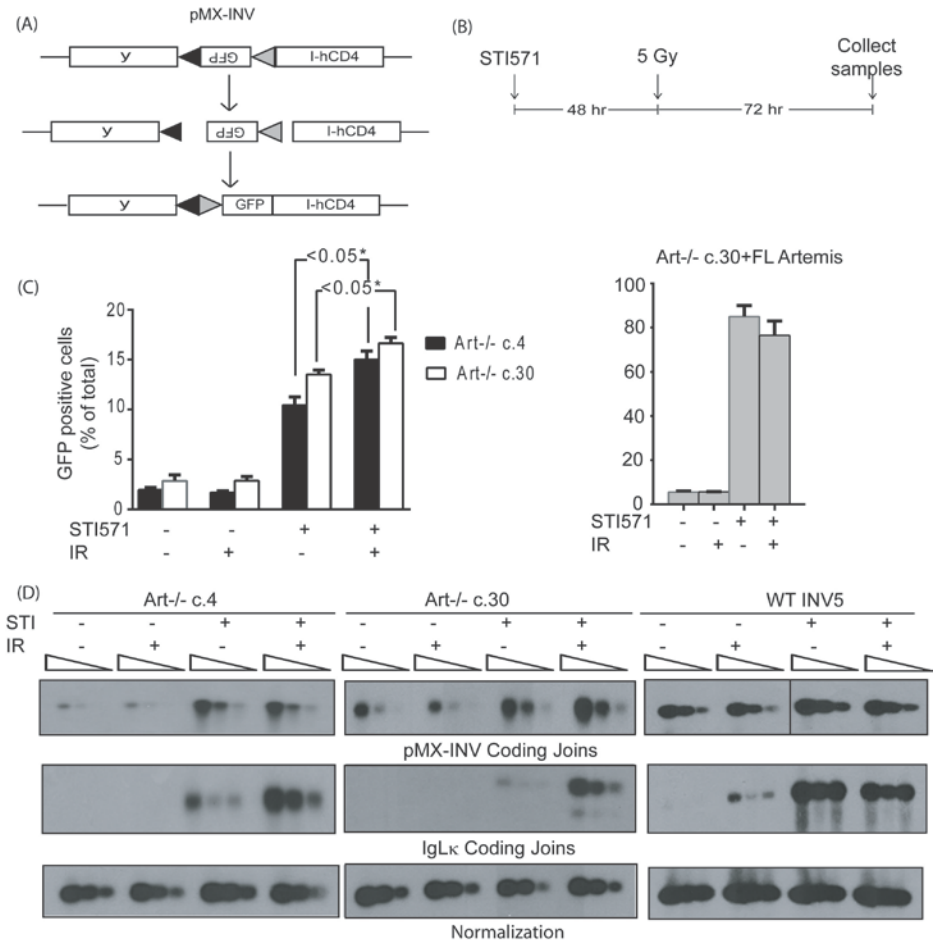

Figure 3.4. (A) Schematic diagram of pMX-INV V(D)J recombination substrate in non-rearranged, cleaved and rearranged forms. The RSS are shown in triangles. **(B)** v-abl pre-B lymphocytes are irradiated with 5 Gy 48 hours after being arrested in G1 by STI571. The cells are analyzed 72 hours after IR. **(C)** Graphs representing percentages of pre-B lymphocytes that are GFP positive 72 hours after IR. Percentages were determined by flow cytometry in the following cell lines: *Art*$^{-/-}$ c.30, *Art*$^{-/-}$ c.4 and *Art*$^{-/-}$c.30 with full-length Artemis. The bars and error bars indicate means and SEM, respectively. P values were calculated using unpaired Student's T test. The data are representative of at least three independent experiments. **(D)** Southern blot analyses for coding joins at the pMX-INV and Igκ loci. DNAs from pre-B lymphocytes were PCR amplified. The bands corresponding to coding joins are indicated. DNA input was normalized using PCR for a non-rearranging gene. The data are representative of at least three independent experiments.

We next examined the formation of coding joins (CJ) at Igκ (Vκ6-23 to Jκ1) and pMX-INV loci 72-hours after irradiation by PCR and Southern blot analysis. CJ were robustly induced in G1-arrested WT cells, however there was no obvious difference in the levels of joins at these loci with or without IR (Figure 3.4D). In the G1-arrested *Art*$^{-/-}$ cells, CJ were detectable at both loci. However, upon irradiation of the G1-arrested cells, the levels were markedly higher at the Igκ locus in both *Art*$^{-/-}$ cell lines (Figure 3.4D). At the pMX-INV locus, CJ were also induced after STI571 treatment, but we did not observe a difference in the CJ levels (Figure 3.4D). This might result from excessive cycling driving the PCR to saturation. Nonetheless, altogether these results demonstrate that low level of V(D)J recombination occurs in *Art*$^{-/-}$ pre-B cells after G1-arrest and this response is further enhanced by IR only in Artemis deficiency and not in the WT pre-B cells.

Sequence analysis of coding joins at Igκ and pMX-INV loci.

Next, we examined the junctional sequences of the CJ recovered from the G1-arrested WT INV5 and Art$^{-/-}$ cells, as described earlier for TCR rearrangements and in Figures 3.5, S3.5-S3.9. The subsequent analysis represents combined sequences from Vκ6-23 to Jκ1 and pMX-INV CJ recovered from each cohort. Altogether, in the WT cells less than 10% junctions analyzed were structurally abnormal (Group II) with or without IR (Figure 3.5A). In comparison, the percentage of abnormal joins that were included in Group II increased from 23% to 37% in *Art*$^{-/-}$ c.4 cells. In the *Art*$^{-/-}$ c.30 cells, the percentage of abnormal joins increased only by 3%.

As for the specific modifications, the joins were prominently different in total nucleotides and P NT inserted at the junctions (Figure 3.5B). The percentage of joins containing >10 bp long insertions increased from 0% to 11% and 16% in *Art*$^{-/-}$ c.4 and c.30, respectively. Similarly, the frequency of coding ends containing >3 P NT within a junction increased by 29% and 15% in the two lines. In comparison, only one WT junction contained >3 PNT. No insertions longer than 10 bp were observed in the WT junctions. Extensive deletions spanning more than 15 bp within a junction and microhomologies were utilized more frequently in the *Art*$^{-/-}$ cell lines as compared to the WT cells. However, no remarkable differences were observed

between the unirradiated and the irradiated groups. We also did not observe any remarkable difference in the median

Figure 3.5: Sequence analysis of breakpoint junctions from Igκ and pMX-Inv coding joins

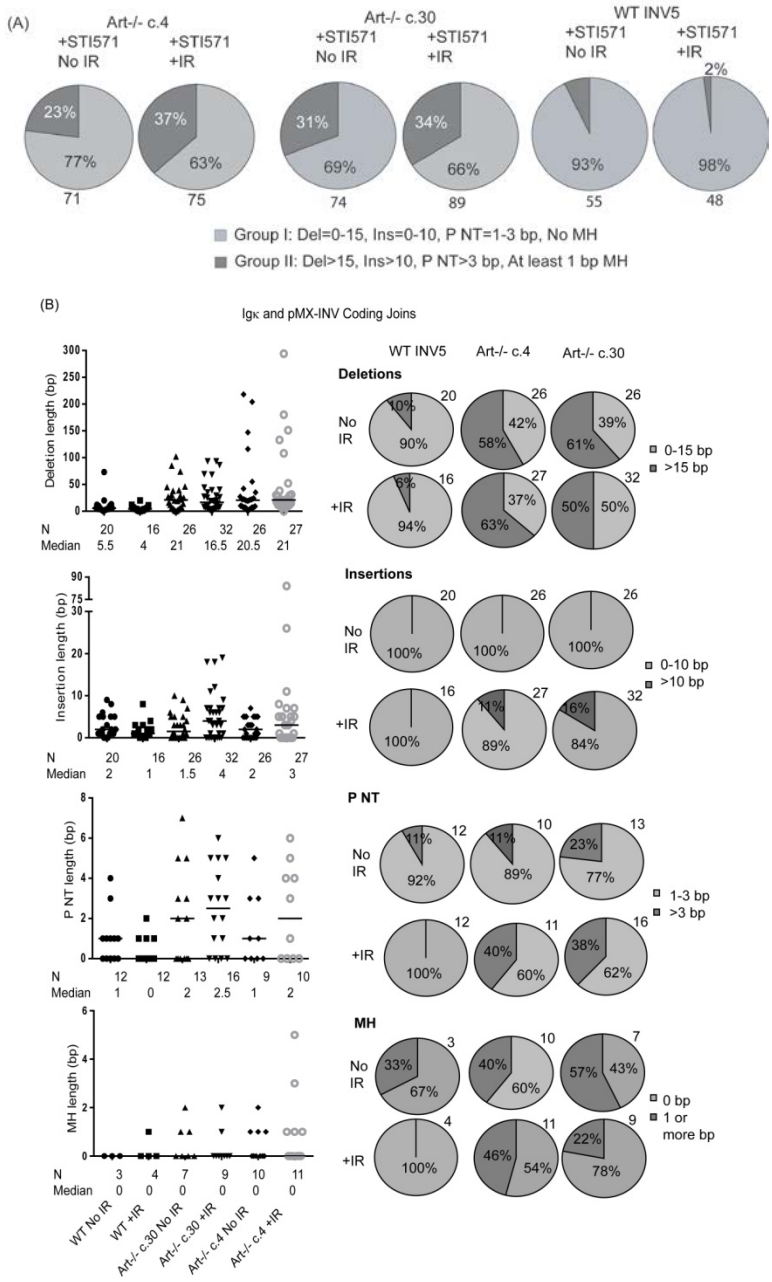

Figure 3.5. PCR products corresponding to coding joins at the Igκ and pMX-INV loci were subcloned into pCR TOPO2.1 and sequenced. **(A)** The sequence analyses for both loci were combined for each cohort and then pooled into two groups. Pie charts showing the percentages for the two groups are depicted here for *Art*$^{-/-}$ c.4, *Art*$^{-/-}$ c.30 and WT-INV5 cells. **(B, left panel)** Plots representing the combined distributions of deletion, insertion, P NT and MH lengths at

breakpoint junctions of coding joins from both loci are shown. The number of sequences (N) and median value for each experimental group is indicated below the graph. The horizontal bar represents the median value for each group. The sequences were analyzed as described in Figure 3.2. **(B, right panel)** Pie charts representing the percentages of joins with normal and longer deletions, insertions, P NT and MH lengths at the coding joins from both loci are shown for the indicated genotype.

lengths of deletions, insertions, P NT and MH. In sum, our analysis shows that IR not only induces V(D)J rearrangements in the G1-arrested pre-B cells but the joins are mostly catalyzed in the same manner as *in vivo* with long nucleotide insertion including palindromic nucleotides.

IR induces translocations between V(D)J loci in *Art*$^{-/-}$ pre-B cells.

To determine if mis-joining between V(D)J loci can occur in G1-arrested *Art*$^{-/-}$ pre-B cells after IR, we devised a PCR strategy to amplify trans-rearrangements between the Igκ and pMX-INV loci (Figure 3.6A). The results were confirmed by Southern blot analysis. PCR products corresponding to trans-rearrangements were rarely detectable in G1-arrested WT INV5 cells after IR (Figure 3.6B). The rearrangement products were observed in the *Art*$^{-/-}$ c.4 cells only after combined STI571 and IR treatment in all the samples from four independent experiments. The trans-rearrangement products were detectable in 50% of the samples from the STI571-treated *Art*$^{-/-}$ c.30 cells. We did not observe an increase in frequency in this cell line upon irradiation. These results suggest that trans-rearrangements can be observed infrequently in the WT pre-B cells after IR. These aberrant events can arise in *Art*$^{-/-}$ cells upon G1 arrest. However, the frequency of trans-rearrangements is increased after IR treatment of the G1-arrested *Art*$^{-/-}$ cells.

Next, we analyzed the junctional sequences of the trans-rearrangement products, as described earlier (Figure 3.6C). All junctions were structurally abnormal containing either >15 bp long deletions or complex insertions. Some sequences appeared to have been templated (in red) from the Vκ6-23 flanking sequence. In addition multiple single nucleotide misalignments

Figure 3.6: IR induces aberrant Vκ6-23-to-IRES transrearrangements in *Art*$^{-/-}$ pre-B cells.

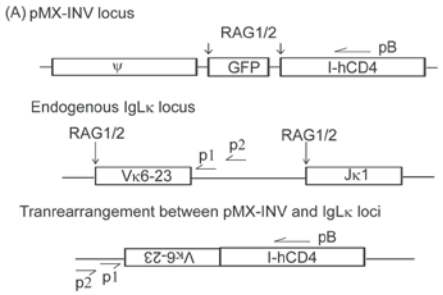

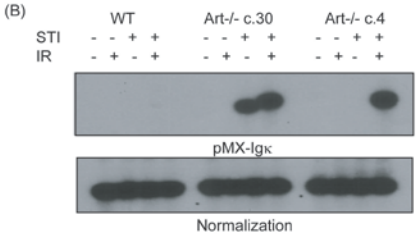

Frequency of Translocations	WT INV5	Art-/- c.30	Art-/- c.4
No STI	0/3	0/8	0/4
+STI	0/3	4/8	0/4
+STI +IR	1/3	4/8	4/4

(C)

Translocation Junctions	Art-/- c.30 No IR	Art-/- c.30 + IR	Art-/- c.4 + IR
Deletion length (bp)			
0	0/1	0/1	0/4
1-15	0/1	0/1	1/4
>10	1/1	1/1	3/4
Insertion length (bp)			
0	0/1	0/1	1/4
1-10	1/1	0/1	2/4
>10	0/1	1/1	1/4 (116bp)
P NT lenght (bp)			
0	0/0	0/0	0/0
1-3	0/0	0/0	0/0
>3	0/0	0/0	0/0
MH length (bp)			
0	0/0	0/0	1/1
1-4	0/0	0/0	1/1
>5	0/0	0/0	1/1

Vk6-23 to pMX-INV Translocations
Art-/- c.30
No IR

Vk6-23		IRES	#
TAGCAGCTATCCTCT		CAGCCTACAATTCCG	
-41 *	CGGC	-15	3

+IR

-17 **	CATTATAGCACTCCC	CCTACAATTCCG	5

Vk6-23 to pMX-INV Translocations
Art-/- c.4
+IR

Vk6-23		IRES	#
TAGCAGCTATCCTCT		CAGCCTACAATTCCG	
-17	CATTATAGTT	CAATTCCG	8
TAGCAGCTATCC	-	AATTCCG	5
-17	CATTAT	-127	5
-24	116 nt ***	-36	2

* CAGCAGTGTGCAGGCTGAAGAC
Vk-6-23 TAGCAATGTGCAGTCTGAAGAC

** Multiple single nucleotide mismatches at 5' end

*** 1-59 nt match with sequence on Ch. 3

Figure 3.6. (A) Schematic of PCR to analyze trans-rearrangement between pMX-INV and Igκ loci. **(B)** DNA was collected from pre-B lymphocytes 72 hours after IR and PCR analyses done to amplify the trans-rearrangement products. The PCR products were confirmed by Southern blot. DNA input was normalized using PCR for a non-rearranging gene (Top panel). The frequencies of trans-rearrangements are shown in the bottom panel **(C)** PCR products corresponding to transrearrangements were subcloned in TOPO2.1 vector and sequenced. The table in the top panel shows the frequencies of deletions, insertions, P NT insertions and MH length at the breakpoint junction. The bottom panel shows sfequences from two $Art^{-/-}$ lines. Coding end sequences are boxed above the rearrangements. P NT are underlined. N nucleotides are indicated between the coding segments. MH are represented in bold. Samples from at least three independent experiments for each cell line were used for this analysis.

were present within the coding end sequence adjacent to the breakpoint. One junction contained 116 bp long insertion, part of which (59 nt) was dervied from chromosome 3. In summary, our data demonstrate that translocations can arise in transformed $Art^{-/-}$ pre B cells and are further induced by IR. Moreover, these trans-rearrangements contain extensive deletions and complex junctional insertions.

ATM deficiency abrogates partial rescue in T lymphocyte development and V(D)J rearrangements in irradiated $Art^{-/-}$ mice.

Since ATM plays a key role in activating cellular responses to DNA damage, we hypothesized that IR-induced end joining in Artemis deficiency is triggered by ATM-dependent DNA damage response. To determine this, mice deficient in both Artemis and ATM were irradiated at 3 to 5 weeks of age with 2.5 Gy and analyzed 3 weeks later. Thymic cellularity was reduced in $Art^{-/-}Atm^{-/-}$ mice as compared to the $Art^{-/-}$ mice by about 50% (Table 3.2). Next, thymocytes were examined for CD4, CD8 and TCRβ expression by flow cytometry. Representative plots of un-irradiated and irradiated $Art^{-/-}Atm^{-/-}$ and $Atm^{-/-}$ thymocytes are shown in Figure 3.7A. As expected, the percentages of DP, sTCRβ+ and icTCRβ+ cells were markedly lower in $Art^{-/-}Atm^{-/-}$ mice as compared to the WT and $Atm^{-/-}$ mice, and similar to those in the $Art^{-/-}$ mice (Figure 3.7B, Table 1). The $Art^{-/-}Atm^{-/-}$ mice did not show a significant change in the number of DP and $sTCR\beta^{+}$ cells upon irradiation (Figure 3.7A, 3.7B). On comparison with the irradiated $Art^{-/-}$ mice, the $Art^{-/-}Atm^{-/-}$ mice showed a significant reduction in the response to IR

as determined by DP and sTCRβ+ cells. However, we observed a small increase in the percentage of icTCRβ+ cells (2.6% ± 0.3) in the *Art*$^{-/-}$*Atm*$^{-/-}$mice.

Table 3.2: Impact of IR on T lymphocyte development in *Art*$^{-/-}$*Atm*$^{-/-}$ mice

Genotype	IR Dose (Gy)	N	Thymocyte count (x 10^6)	$CD4^+CD8^+$ cells (% of total)	$sTCR\beta^+$ cells (% of total)	$icTCR\beta^+$ cells (% of total)
WT	0	4	124.6 ± 24.9	83.4 ± 1.03	19.4 ± 1.3	28.8 ± 2.8
	2.5	4	100.3 ± 25	74.3 ± 2.02	18.2 ± 1.7	22.5 ± 1.2
$Art^{-/-}$	0	5	6 ± 2.6	0.06 ± 0.02	1.5 ± 0.2	0.4 ± 0.1
	2.5	6	8.4 ± 2.7	52.7 ± 5.2	5.3 ± 0.7	12.3 ± 4.2
$Art^{-/-}ATM^{-/-}$	0	6	0.8 ± 0.1	0.4 ± 0.1	0.7 ± 0.3	0.4 ± 0.1
	2.5	8	0.8 ± 0.1	0.7 ± 0.6	1.5 ± 0.6	2.6 ± 0.3
$ATM^{-/-}$	0	6	100.1 ± 21.8	86.6 ± 1	2.2 ± 0.4	14.5 ± 0.01
	2.5	4	90.1 ± 50.6	70.7 ± 5.2	4.1 ± 0.6	31.5 ± 5.1

Figure 3.7: ATM deficiency abrogates IR-induced T lymphocytes differentiation in *Art*$^{-/-}$ mice.

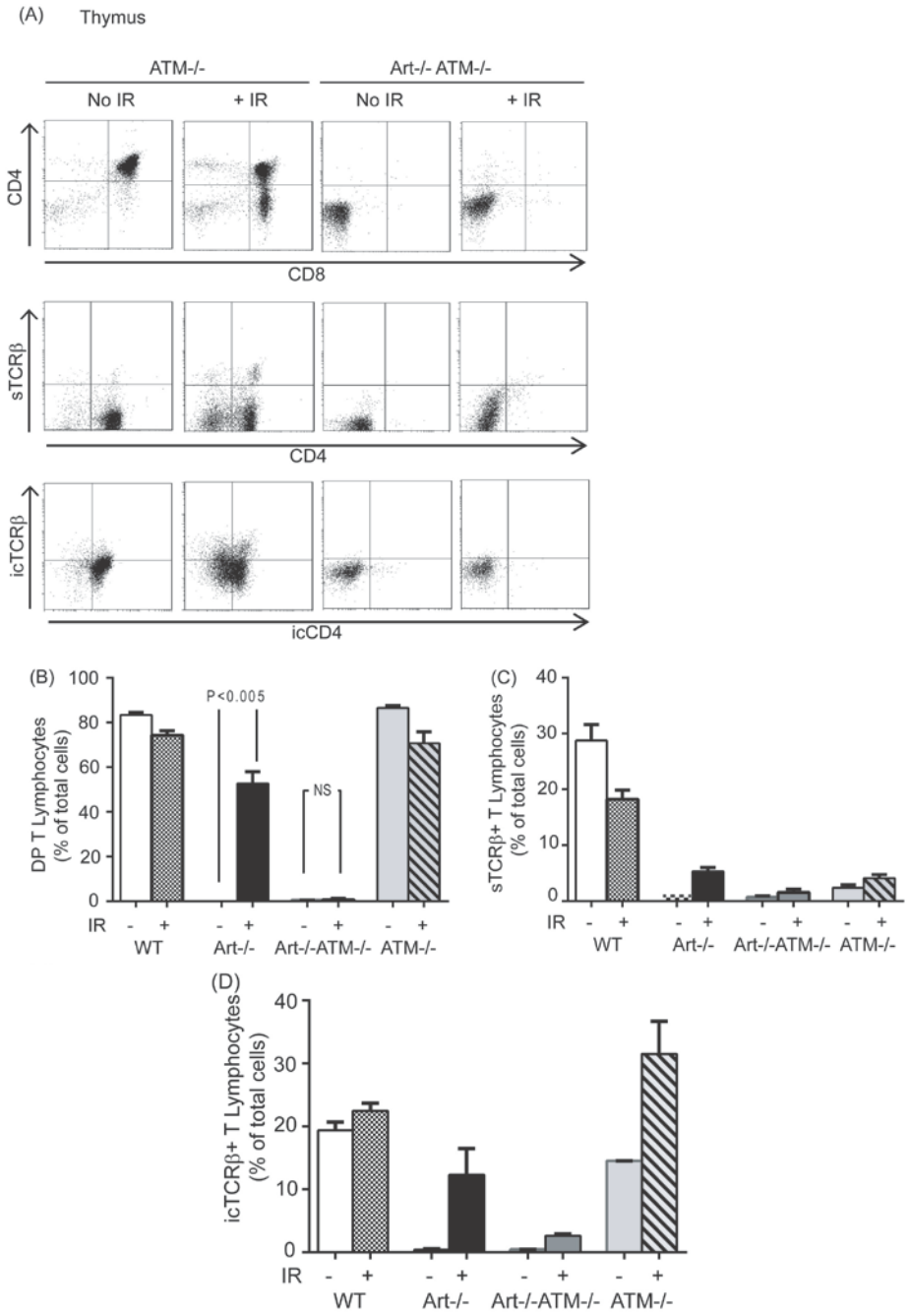

(A) 3-5 weeks old *Atm*$^{-/-}$ and *Art*$^{-/-}$*Atm*$^{-/-}$ mice were exposed to 2.5 Gy and analyzed 3 weeks later for lymphocyte development. **(A)** Flow cytometric analysis was done on thymocytes from the unirradiated and the irradiated mice for cell surface CD4, CD8, TCRβ and intracellular CD4 and TCRβ expression. **(B, C, D)** Graphs representing percentage of thymocytes expressing **(B)** surface CD4 and CD8, **(C)** surface TCRβ and **(D)** intracellular TCRβ. The bars represent means for each group with SEM.

Next, to investigate the potential role of ATM in IR-induced V(D)J recombination, we examined Dβ1 to Jβ1rearrangements in the DNA isolated from the individual thymus by using PCR and Southern blot analysis (Figure 3.8, Top panel). We observed fewer PCR bands corresponding to rearrangements and increased intensity of the germline band in all the *Art*$^{-/-}$ *Atm*$^{-/-}$ mice after IR as compared to the WT, *Atm*$^{-/-}$ and irradiated *Art*$^{-/-}$ mice (Figure 3.2). We sequenced these PCR products to analyze the breakpoint junctions and were able to isolate only 4 unique sequences from two mice. The only abnormality we observed was the presence of long P NT (7 and 8 bp long) in the two sequences from #1679 (Figure 3.8, Bottom panel).

To determine if trans-rearrangements form in *Art*$^{-/-}$*Atm*$^{-/-}$ thymocytes after irradiation PCR and Southern blot analysis was done for TCRγV to βJ trans-rearrangements. No trans-rearrangement products were detectable in unirradiated (n=2) and irradiated *Art*$^{-/-}$*Atm*$^{-/-}$ mice analyzed (n=5) (Figure 3.8A). These findings are in contrast to what we observed in *Art*$^{-/-}$ mice in which IR induced robust levels of transrearrangements (Figure 3.4). These results demonstrate that ATM deficiency substantially decreases IR-induced T lymphocyte development and Dβ1-to-Jβ1 rearrangements in the *Art*$^{-/-}$ mice. Interestingly, low levels of rearrangements can be detected after IR in some *Art*$^{-/-}$*Atm*$^{-/-}$ mice. In contrast, no aberrant trans-rearrangements were observed in these mice. Since thymic cellularity in *Art*$^{-/-}$*Atm*$^{-/-}$ mice was reduced than in *Art*$^{-/-}$ mice, these cells might be particularly radiosensitive with reduced cell viability. Therefore, it is possible that low levels of rearrangements and lack of translocations may result from reduced number of precursors in the thymus.

Figure 3.8: IR-induced V(D)J rearrangements in *Art*$^{-/-}$ T lymphocytes are suppressed by ATM deficiency.

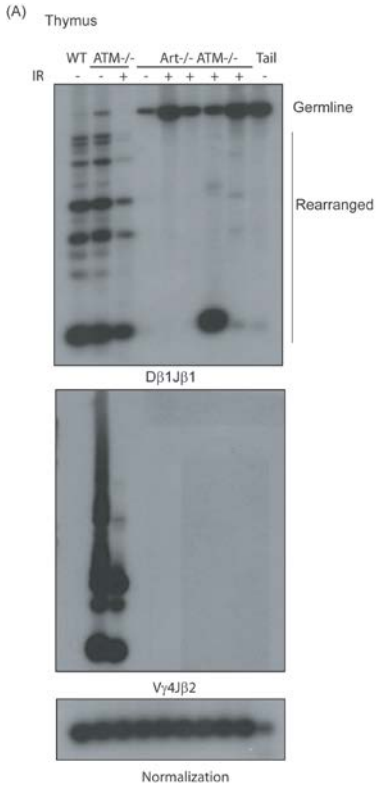

Dβ1		Jβ1.6
GACAGGGGGC		TTCCTATAAT
	#1679	
GACAGGG	CTCAATAGGAA	TTCCTATAAT
GACAGGGGGC	GCCCCCTGGATAGGAA	TTCCTATAAT
	#1682	
GACAGG	-	ATAAT
GACAGGGGGC	GC	TTCCTATAAT

Figure 3.8. (A) Thymic DNA was prepared from thymocytes isolated from the unirradiated and irradiated mice and PCR analyses done to determine Dβ1 to Jβ1 and aberrant TCRγV to TCRβJ rearrangements. A non-lymphoid tissue (tail) was included as a negative control. DNA input was normalized using PCR for a non-rearranging gene. **(B)** PCR products corresponding to Dβ1 to Jβ1 rearrangements were subcloned into the TOPO2.1 vector and sequenced. Sequences from two irradiated Art$^{-/-}$ATM$^{-/-}$ mice are shown. Dβ1 and Jβ1 coding end sequences are shown in boxes above the rearrangements. P NT are underlined. N NT are indicated between the coding segments. MH are represented in bold.

V(D)J rearrangements and translocations induced in irradiated *Art*$^{-/-}$ pre-B cells are suppressed by ATM kinase inhibition.

To confirm our above-mentioned findings in an immortalized system, the *Art*$^{-/-}$ pre-B cells were arrested in G1 and treated with a potent selective ATM kinase inhibitor, KU55933 (Figure 3.9A) [273]. KU55933 did not reduce cell survival in the G1-arrested cells (Figure S3.3). The inhibition of ATM kinase activity significantly decreased the percentages of GFP^{+} cells in unirradiated and irradiated *Art*$^{-/-}$ cells in G1 (Figure 3.9B). Further, levels of coding joins at the pMX-INV and Igκ loci, analyzed by PCR and Southern blot analyses, were markedly reduced in cells that were treated with STI571, KU55933 and IR (Figure 3.9C).

Next, we examined trans-rearrangements between the Igk and pMX-INV loci by PCR and Southern blot analysis (Figure 3.9D, left panel). We observed a decrease in frequency as well as levels of translocations after ATM kinase inhibition in the irradiated as well as unirradiated G1-arrested cells (Figure 3.9D, right panel). Altogether, these findings demonstrate that inhibition of ATM kinase activity suppresses IR-induced rearrangements including translocations during V(D)J recombination in G1-arrested *Art*$^{-/-}$ pre B cells.

Figure 3.9: ATM kinase inhibition in G1-arrested *Art*$^{-/-}$ pre-B lymphocytes suppresses normal and aberrant V(D)J rearrangements.

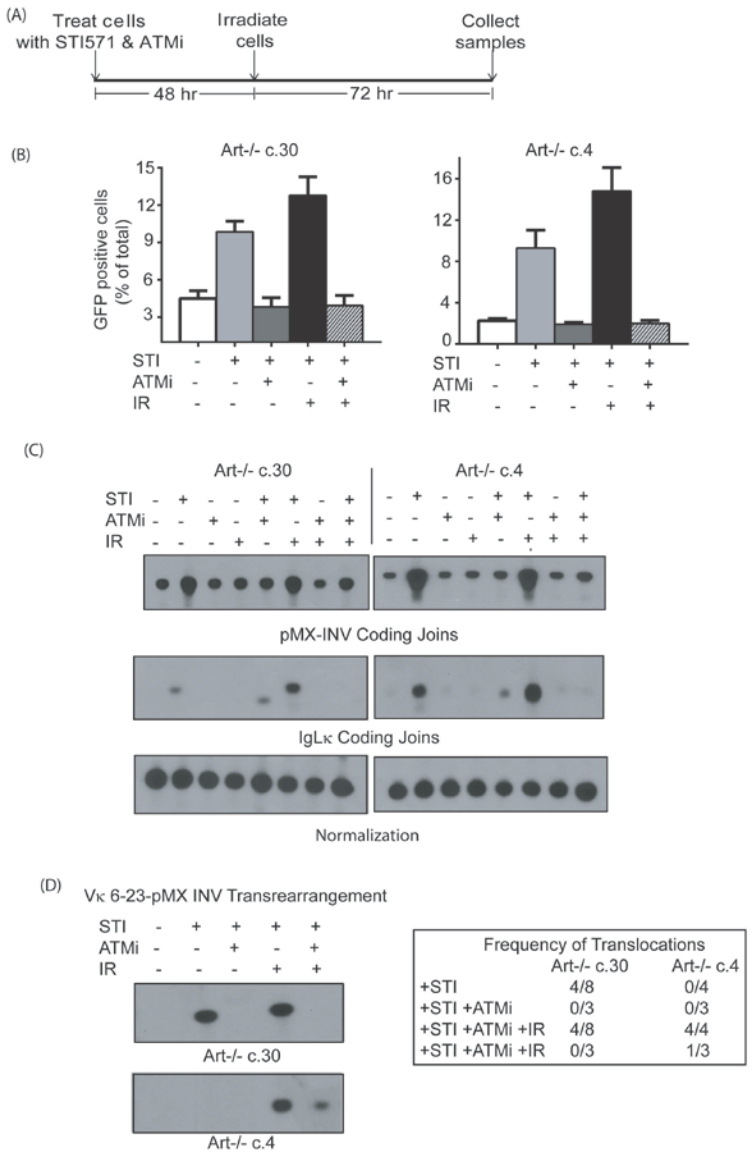

(A) v-abl Art$^{-/-}$ pre-B lymphocytes were treated with STI571 and KU55933 simultaneously. 48 hours later cells were irradiated with 5 Gy and analyzed 72 hours after IR. **(B)** Flow cytometry was done to determine the percentage of GFP^{+} cells 72 hours after IR. The bars represent means for each group with SEM. **(C)** DNA was collected and PCR analyses done to amplify the pMX-INV and IgLk coding joins. PCR products were confirmed by Southern blot analysis. DNA input was normalized using PCR for a non-rearranging locus. **(D)** Transrearrangements between pMX-INV and IgLk loci were amplified using PCR and confirmed by Southern blot analysis. DNA input was normalized using PCR for a non-rearranging gene. The table in the right panel shows the frequencies of trans-rearrangements.

3.4 Discussion

The role of the ATM-dependent DNA damage response in inducing alternative end-joining in the developing lymphocytes had not been fully characterized. Our studies reveal that upon irradiation in the absence of Artemis, RAG-induced breaks undergo robust V(D)J rearrangements, including chromosomal translocations. Using an inducible pre-B cell system, we show that this response is largely dependent on ATM-kinase activity. This study also demonstrates that chromosomal translocations can arise during the G1-phase of the cell cycle, independent of post-replication repair mechanisms and cell cycle checkpoints.

IR-induced lymphocyte development and V(D)J recombination in *Art*$^{-/-}$ lymphocytes

Low-dose IR partially rescued T lymphocyte development arrest in *Art*$^{-/-}$ mice. This rescue was associated with Dβ to Jβ rearrangements in nullizygous cells at levels comparable to those seen in the wild-type (WT) cells. Although TCRβ expression was also increased after IR in *Art*$^{-/-}$ mice, the levels were lower than those in the WT cells indicating that many of these rearrangements are not in-frame and are non-functional. Lack of peripheral single-positive T cells in irradiated *Art*$^{-/-}$ mice suggests that despite significantly increased intracellular TCRβ, the lymphocytes of these mice were not producing functional TCRs. This might indicate a requirement for a wave of IR-induced activity for subsequent rearrangements, as indicated by lower level of induction in Vβ to DJβ as compared to Dβ to Jβ rearrangements in *Art*$^{-/-}$ lymphocytes.

IR failed to rescue B lymphocyte development in *Art*$^{-/-}$ mice, as was previously reported for DNA-PKcs mutant SCID mice (SCID$^{DNA\text{-}PKcs}$) [262]. p53 nullizygosity rescues only T cell, and not B cell, development in SCID$^{DNA\text{-}PKcs}$ mice [274]. In contrast, Bcl2 overexpression, that inhibits cell death, promotes B cell development but has no effect on T cell development and differentiation in SCID$^{DNA\text{-}PKcs}$ mice [275]. This suggests that differences in the regulation of checkpoints are responsible for selective B or T lymphocyte development. In our study, end joining was increased in irradiated v-abelson transformed *Art*$^{-/-}$ pre-B cells indicating that this is not a T cell-specific response and that IR is inducing similar DNA repair mechanisms in both cell lineages. Increased availability of RAG-generated DNA ends in *Art*$^{-/-}$ cells upon G1 arrest allows

repair by slow error-prone mechanisms, as is evidenced by the presence of low levels of coding joins in these cells. However, an increase in coding join formation after IR suggests a role for IR-induced DNA damage response in mediating end joining.

Elevated levels of genomic instability in *Art*$^{-/-}$ lymphocytes after low-dose IR

Increased interchromosomal trans-rearrangements in *Art*$^{-/-}$ lymphocytes after IR, particularly between TCRγ and TCRβ loci, suggests that the DNA-damage induced end joining is translocation-prone. Human TCRγ and TCRβ loci are both located on chromosome 7, and aberrant end-joining can lead to deletions or inversions [271]. Inversions between IgV_H and TCRJα segments, located on chromosome 14, have been observed in some B cell leukemia [276]. We also observed complex breakpoint junctions within these translocations. One such translocation junction from *Art*$^{-/-}$ c.4 cells contained a 59 bp long sequence from chromosome 3. This might have resulted from joining of IR-damaged DNA with the coding ends through unclear mechanisms, as there were no obvious microhomologies within that junction. Trans-rearrangements are frequently observed in cells with *ATM*, *NBS1* or *MRE11* mutations [170, 220, 221]. Loss of DNA ends indicated by hybrid join formation in these cells (Figure 1.6), has suggested that these proteins play roles in maintaining DNA end complex stability [128, 166]. We have also recently shown increased frequency of trans-rearrangements and deletional hybrid joins in lymphocytes harboring a hypomorphic *Artemis* mutation (Chapter 2) [82]. We, however, did not detect hybrid joins (data not shown) in *Art*$^{-/-}$ lymphocytes after irradiation despite the presence of robust hairpin opening and end-joining activities. This suggests that other processes involving complex and erroneous end processing and decreased bias towards intrachromosomal joining might be promoting aberrant repair after irradiation in the absence of Artemis.

IR-induced V(D)J rearrangements in *Art*$^{-/-}$ lymphocytes are dependent on ATM kinase activity.

ATM localizes to RAG-induced breaks and plays an important role in maintaining genomic stability during antigen receptor assembly [125, 129]. ATM deficiency alone does not markedly impair V(D)J recombination. During V(D)J recombination ATM has functional

redundancies with DNA-PKcs for efficient signal join formation [277, 278]. Combined XLF and ATM deficiency results in severe block in lymphocyte development [275]. ATM also regulates transcription in developing lymphocytes following RAG-induced breaks or genotoxic DSBs [279]. ATM-deficient cells exhibit increased coding end accumulation and loss of chromosomal integrity at the antigen receptor loci [125, 128]. This suggests that ATM is not essential for coding join formation but plays important role as a tumor suppressor during V(D)J recombination by preventing genomic instability.

In this study, we have delineated the role of ATM-dependent DNA damage response in inducing chromosomal transrearrangements in C-NHEJ-deficient developing lymphocytes. We observed marked reductions in normal and aberrant V(D)J rearrangements and in T lymphocyte development in *Art*$^{-/-}$*Atm*$^{-/-}$ mice after IR compared to that seen in *Art*$^{-/-}$ mice post-IR. Hence, ATM is required to mediate the IR-induced events observed with Artemis deficeincy. It is possible that *Art*$^{-/-}$*Atm* $^{-/-}$ lymphocytes undergo DNA-PKcs-mediated apoptosis due to accumulation of DNA breaks and IR hypersensitivity. DNA-PKcs phosphorylates p53 in ATM-deficient but not wild-type lymphocytes after IR which triggers apoptosis [280]. However, we demonstrated that ATM kinase inhibition in immortalized *Art*$^{-/-}$ pre-B cells does not affect survival of G1-arrested cells after IR and yet replicates our findings in irradiated *Art*$^{-/-}$*Atm*$^{-/-}$ mice. Using inducible pre-B cells also allowed us to examine the role of ATM kinase activity specifically in G1, independent of its role in cell cycle checkpoint activation. Lack of DNA end complex stability, in the absence of either ATM or ATM kinase activity, may at least partially account for the decreased intralocus V(D)J rearrangement in *Art*$^{-/-}$*Atm*$^{-/-}$ primary T lymphocytes and *Art*$^{-/-}$ pre-B cells treated with ATM kinase inhibitor. However, we reason that loss of this function should also predispose to more translocations due to aberrant repair of prematurely released ends in the absence of C-NHEJ upon irradiation. Because IR failed to induce translocations in *Art*$^{-/-}$*Atm*$^{-/-}$ lymphocytes, the ATM-dependent damage response must have additional roles beyond maintaining DNA end complex stability.

Mechanisms of ATM kinase-dependent end-joining induced by IR in the absence of Artemis.

Formation of coding joins in the absence of Artemis requires another nuclease to open the hairpins prior to end-joining. Low level alternative nuclease(s) activity is indicated by the presence of some coding joins in *Art*$^{-/-}$ lymphocytes. I have shown that alternative nuclease activity is highly inducible by low-dose IR, is associated with extensive resection and is linked to addition of long stretches of P-nucleotides at the junctions. The IR-induced response can rarely lead to aberrant end-joining in the wild-type cells involving longer resection of the coding ends. However, end-joining induced by IR in the absence of Artemis is associated with increased junctional complexity that is not observed in unirradiated *Art*$^{-/-}$ cells or in irradiated WT cells. This suggests that distinct factors might be involved in mediating aberrant end-joining after IR in the absence of Artemis.

MRE11 and CtIP are involved in DNA end resection during homologous recombination and have been implicated in error-prone alternative end-joining [121, 124, 126]. MRE11 has 3' to 5' exonuclease activity and can also open hairpin loops *in vitro* [123]. CtIP interacts with MRE11 for double-strand break resection during homologous recombination [121]. CtIP also promotes end resection of RAG-generated breaks via MMEJ in the absence of H2AX and this resection is dependent on ATM kinase [126]. This nucleolytic activity is associated with extensive resections, and probably does not play a prominent role during normal V(D)J recombination [121]. The MRN complex and CtIP are both phosphorylated by ATM during the DNA damage response [72]. Therefore, MRE11 and CtIP are strong candidates in mediating alternative end joining in Artemis-deficient lymphocytes and investigating the roles of MRE11-CtIP in IR-induced end-joining will further improve our understanding of alternative end-joining.

Qualitative analysis of breakpoint junctions including those from transrearrangements isolated from irradiated *Art*$^{-/-}$ cells revealed complex junctions. Templated nucleotide insertions from regions close to the breakpoints suggest a role for IR-induced, error-prone, template-dependent polymerases. Similar complex template nucleotide insertions have been observed at translocation junctions in follicular and mantle cell lymphomas [281]. DNA polymerase theta (PolQ), which is expressed in testicular and lymphoid tissue and overexpressed in colon, stomach and lung cancers, has been shown to lead to such complex partially-templated

insertions in *Drosophila* [281, 282]. Interestingly, combined ATM and PolQ deficiency in mice results in reduced viability and delayed thymic lymphoma onset suggesting a role for PolQ in DNA DSB repair [283, 284]. The function of mammalian PolQ needs to be further characterized, especially during aberrant V(D)J recombination. Gap-filling synthesis by DNA polymerases with established roles during V(D)J recombination, such as Polμ/λ, is also susceptible to template slippage resulting in direct repeats and frameshift synthesis [285, 286]. These polymerases are actively involved in DNA repair by NHEJ. We suggest that IR-induced endonuclease activity leads to extensive DNA end resection and that DNA polymerases perform error-prone gap-filling synthesis to prevent extreme resection and promote end-joining. These polymerases might also generate synthesis-dependent microhomologies. In this scenario, the junctional modifications are the result of combined processing of the ends by nucleases and polymerases. Further characterizing the roles of these factors in V(D)J recombination will improve our understanding of DNA end processing and the contributions of error-prone nucleases and polymerases to aberrant end-joining.

We did not observe markedly increased use of microhomologies at the joins from the irradiated *Art*$^{-/-}$ lymphocytes. This might be due to our small sample size. Alternatively, it might suggest that once the hairpins are opened, at least some of them are joined by DNA LigIV/XRCC4. Malu *et al*. recently identified Artemis C-terminal regions critical for direct interaction with LigIV and for coding join formation in plasmid substrates [76]. In the absence of this interaction, the coding joins were not qualitatively different from wild-type joins. This suggests that even in the absence of Artemis-LigIV interaction, the DNA ends can be joined by LigIV/XRCC4. This might be mediated through interactions of LigIV with factors upstream of Artemis such as RAG and/or DNA-PK. Irradiation of SCID$^{DNA\text{-}PKcs}$ mice induced rearrangements at TCRγ, β and δ loci. These joins contained smaller-sized and less frequent P-nucleotides than junctions from unirradiated cells [262, 266]. The differences we observed might be due to the presence of intact downstream C-NHEJ factors which may be recruited and activated by the Ku/truncated DNA-PKcs complex and perhaps other proteins including ATM after induction of DNA damage response [159]. Thus, the specific nature of C-NHEJ defect might play an important role in determining the factors involved in end-processing and joining.

Our studies show that ATM kinase-dependent DNA damage response induces pathways that are translocation-prone, particularly in cells with compromised C-NHEJ. This function is distinct from its role in preventing genomic instability in the absence of DNA damage response. Based on our findings, we propose that IR induces an increase in ATM activation at RAG-induced breaks by either increased phosphorylation of ATM already present at the DNA ends or increased ATM recruitment to the ends. In case of intact C-NHEJ, DNA damage response rarely leads to aberrant end-processing and interlocus end-joining of RAG-generated breaks. These rare events may result from erroneous resolution of a few DNA ends that persist and are accessible to error-prone pathways induced by IR. In case of Artemis deficiency, we propose two non-mutually-exclusive mechanisms by which the hairpin ends are processed and joined after IR (Figure 4.2). In the first model, in the absence of Artemis, alternative nuclease(s) are readily activated by ATM-dependent damage response to open the hairpin coding ends. The ends can then be joined by C-NHEJ ligation complex comprising of XRCC4 and Ligase IV. The alternative nuclease(s) activity is responsible for increased aberrant end-processing and chromosomal translocations. In the second model, the ATM-dependent IR-induced response triggers a distinct error-prone pathway consisting of a nuclease, polymerases and a ligation complex that will process and join ends in the absence of Artemis. MRE11/CtIP-mediated nuclease activity and ligation complex formed by Ligase III/XRCC1 or even Ligase I are potential candidates for this error-prone end-processing and joining. Studies examining combined deficiencies of Artemis with other factors would help dissect these pathways. MRE11 inhibition, CtIP knockdown in *Art*$^{-/-}$ pre-B cells will help us examine the role of this nuclease activity in mediating end-joining after IR. Using DNA LigIV inhibitor in this pre-B cell system will allow us to determine the differences in junctional structures and thus contribution of intact downstream C-NHEJ ligation complex to end-joining in *Art*$^{-/-}$ cells after IR.

ATM-independent end-joining:

The presence of low levels of coding joins in the context of combined Artemis- and ATM-deficiencies after IR indicates that IR-induced ATM-independent mechanisms also contribute to end-joining. This end-joining might proceed in an MRN-dependent manner or through DNA-

PKcs. The latter has redundant functions with ATM; it is capable of phosphorylating many DDR proteins, including H2AX [280]. Additionally, RAG-mediated endonuclease activity can catalyze hairpin opening *in vitro* [21]. Two out of four unique sequences isolated from $Art^{-/-}Atm^{-/-}$ irradiated mice contained 7-8 bp long P-nucleotides at both coding ends within each junction, a feature unique to these junctions. This is suggestive of RAG-mediated hairpin opening as RAG can nick the hairpin substrates as much as 10 bp away from the apex *in vitro* [21].

In summary, our study suggests a role for ATM-dependent DNA damage response in translocation formation in Artemis-deficient lymphocytes during V(D)J recombination. Radio- or chemotherapy, such as topoisomerase inhibitors, that induce DSBs can induce ATM-mediated responses. This may lead to oncogenic events that may manifest later in life as therapy-mediated tumors. Concurrent inhibition of ATM kinase or othefactors that constitute A-EJ pathway may help reduce the risk of such oncogenic events.

3.5 Materials and Methods

Mice. WT, $Art^{-/-}$, $Atm^{-/-}$ and $Art^{-/-}Atm^{-/-}$ were on mixed 129Svev/C57Bl6 background. Mice were housed in a specific pathogen-free facility for immunodeficient animals. All the protocols were approved by University Committee on Use and Care of Animals (UCUCA) at the University of Michigan.

Irradiation and flow analysis of lymphoid tissues. Mice were irradiated at 3 to 5-weeks of age with a single dose of 2.5 Gy using 137-Cs source. 3 weeks later, they were analyzed. Bone marrow, thymus, spleen and lymph nodes were collected. Single cell suspensions were prepared and analyzed by flow cytometry using CD4, CD8, TCRβ antibodies for T lymphocytes and B220, IgM and CD3 antibodies for B lymphocytes. Thymocytes were also permeabilized and fixed using 4% paraformaldehyde and 0.1% saponin and stained for TCRβ and CD4. Flow analysis was done on BD Accuri C6 flowcytometer. Data was analyzed in Flowjo.

PCR analysis for TCR rearrangements. PCRs for intralocus V(D)J rearrangements were performed as described previously [82]. Transrearrangement PCRs were performed as

described by Jacobs et al. [287]. PCR analyses were done on all the irradiated $Art^{-/-}$ and $Art^{-/-}$ $ATM^{-/-}$ mice.

Culture of v-abl pre-B lymphocytes. V-abl pre-B cells were cultured in DMEM supplemented with 10%FBS, HEPES, NEA, glutamine,penicillamine, β-ME. For G1 arrest, 10^7 cells were treated with 3μM STI571. Cells were irradiated 48 hours later at 1, 2.5 or 5 Gy. For cycling cells, 10^7 cells were plated just before irradiation. For ATM-kinase inhibition experiments, 15μM KU55933 was added to cells at the time of STI571 treatment or an hour before irradiation. Cells not receiving KU55933 were treated with 15μl of DMSO. Cells were irradiated using 137-Cs source. Cells were analyzed by BD Accuri C6 flow cytometer. To express full-length Artemis in pre-B cell lines, Artemis cDNA was cloned into an MSCV retroviral vector containing an IRES-dsRed sequence. Retrovirus was produced in HEK293T cells and viral supernatant was used to transduce an Artemis null pre-B cell line. dsRed positivity was used as a marker for transduced cells. Transduced cells were then sorted to generate single cell clones expressing wildtype Artemis.

PCR analysis for Igκ and pMX-INV rearrangements. Igκ and pMX-INV coding join PCRs were performed as described previously [128]. For PCR analysis of Igκ to pMX-INV trans-rearrangements, primers flanking Vκ6-23 and IRES sequences were used. We used primers (15pM per reaction) that were used for coding join analysis [128]. 0.1μg of DNA was amplified using the following PCR conditions: 25 cycles of 94°C, 60°C and 72°C for 30 seconds each using JMS 528 and JMS579. This was followed by 25 cycles of the same PCR conditions using pB and pκ6d primers. The PCR products were run on 1.5% agarose gel and transferred to Zetaprobe membranes to be analyzed by Southern blot. The membranes were probed with radiolabeled probes. PCR analyses were done on samples collected in at least three independent experiments. Samples from two independent experiments were repeated at least twice.

Sequencing analsysis. PCR products were subcloned using pCR Topo2.1 and sequenced. Sequences were analyzed using SeqMan Pro software, and online NCBI Blast and IMGT sequence alignment tools.

Acknowledgements

I thank Dr. Sekiguchi, Dr. Ferguson, members of my thesis committee and Sekiguchi lab members for helpful discussions regarding these experiments. I also thank William Giblin, Hilary Moale, Allen Washington Junior and James P. Kelly for performing experiments, William Lu for the Art-/- c.30 cell line with full-length Artemis, and Drs. Sleckman and Bassing for the Art-/- pre-B cell lines.

Figure S3.1: Low-dose IR does not induce changes in T lymphocyte differentiation in WT mice

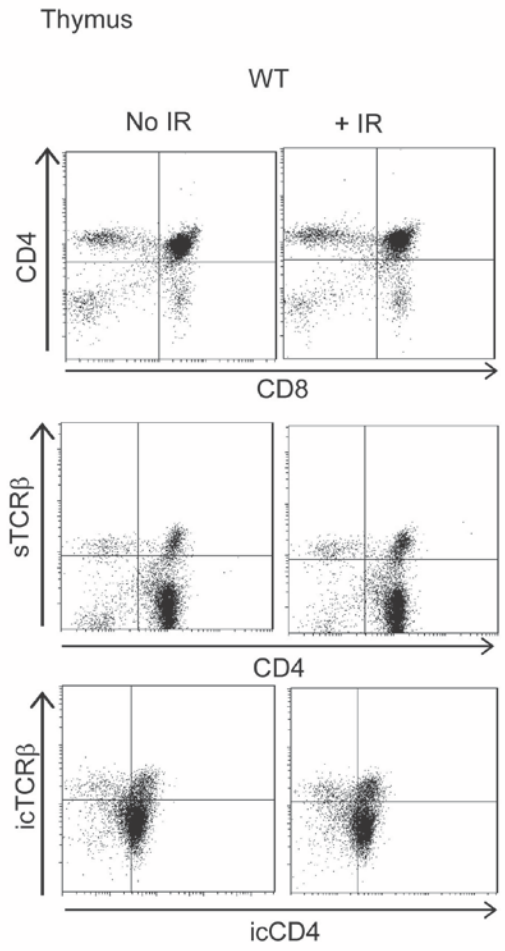

3 to 5-weeks-old WT mice were exposed to 2.5 Gy and analyzed 3 weeks later for lymphocyte development. **(A)** Flow cytometric analysis was done on thymocytes from the unirradiated and the irradiated mice for cell surface CD4, CD8, TCRβ and intracellular CD4 and TCRβ expression.

Figure S3.2: Sequence analysis of Dβ1-to-Jβ1 coding joins

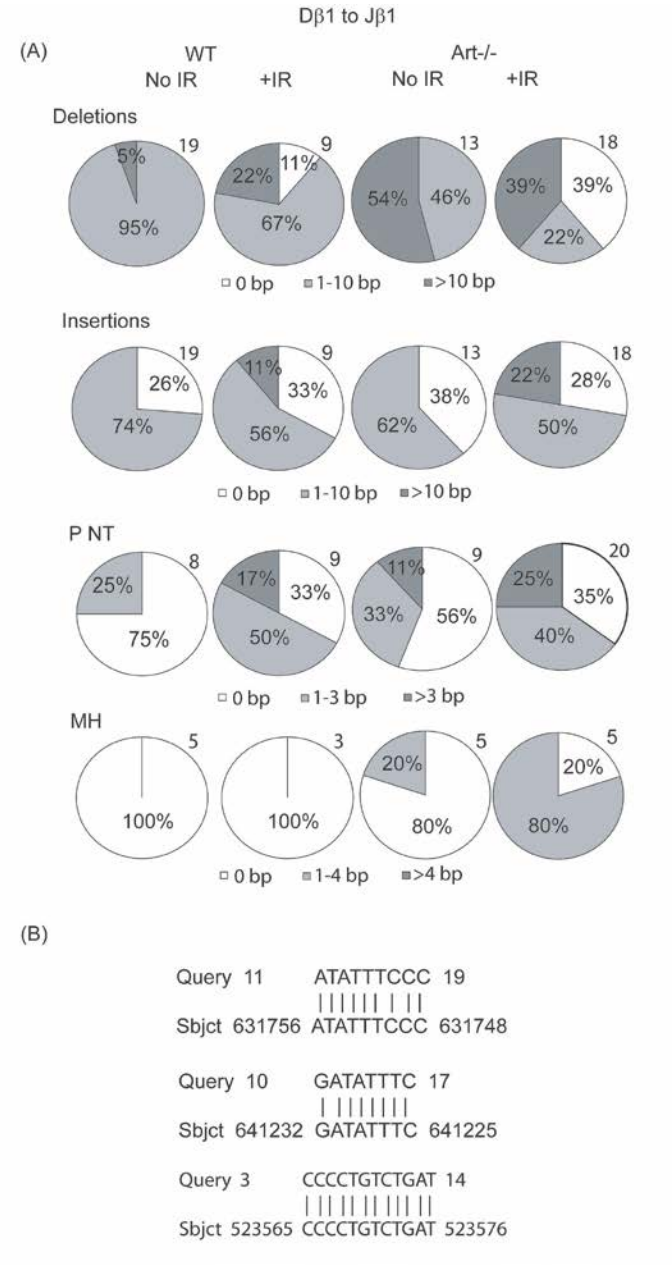

PCR products for Dβ1 to Jβ1 rearrangements were subcloned into the TOPO2.1 vector and sequenced. Analysis of sequences from two irradiated Artemis-null mice is shown. **(A)** Pie charts showing the percentages of sequences with deletions of 0 bp, 1-10 bp and >10 bp, insertions of 0 bp, 1-10 bp and >10 bp, P NT of 0 bp, 1-3 bp and >3 bp and MH of 0 bp, 1-4 bp and > 4bp. **(B)** Blast analysis was done to map the sequences inserted (query) at the breakpoint junction to the mouse TCRb locus (subject). The lines indicate the matched sequences.

Figure S3.3. Survival of pre-B cells after IR

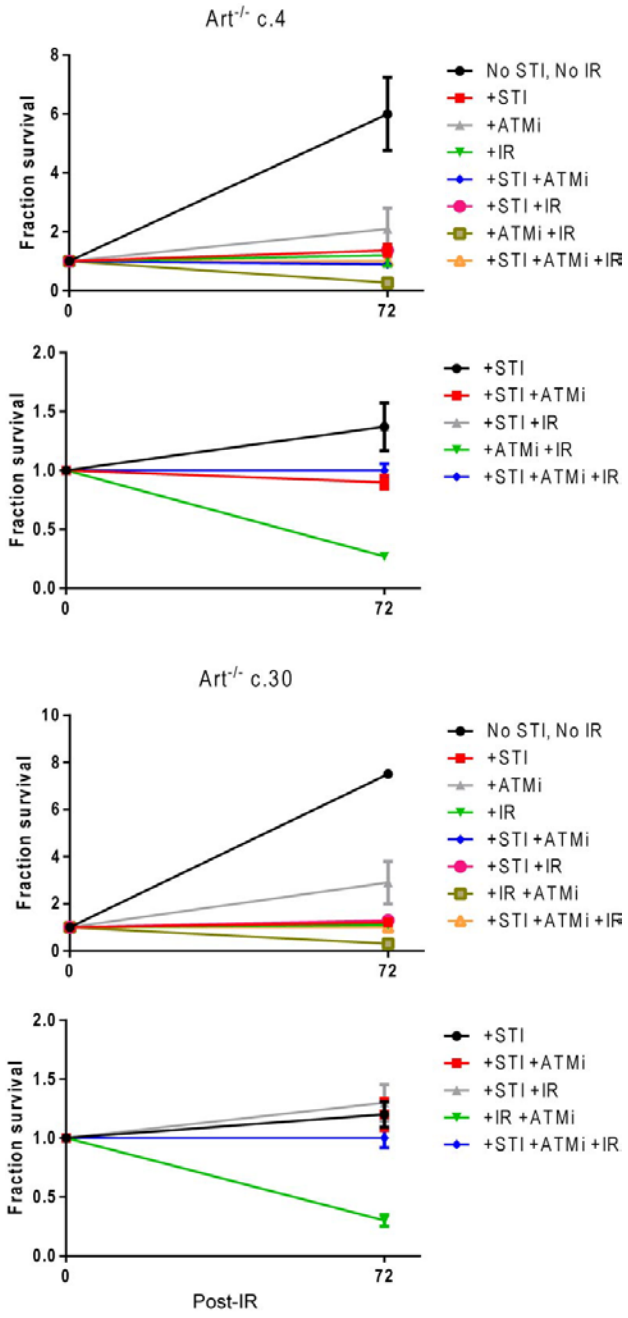

10^7 cells were plated per sample and cells were counted again at the time of harvest. The ratio of cell counts at the time of harvest to 10^7 was used to measure the fraction survival.

Figure S3.4: Dβ1-to-Jβ1 and Vγ-Jβ Sequences

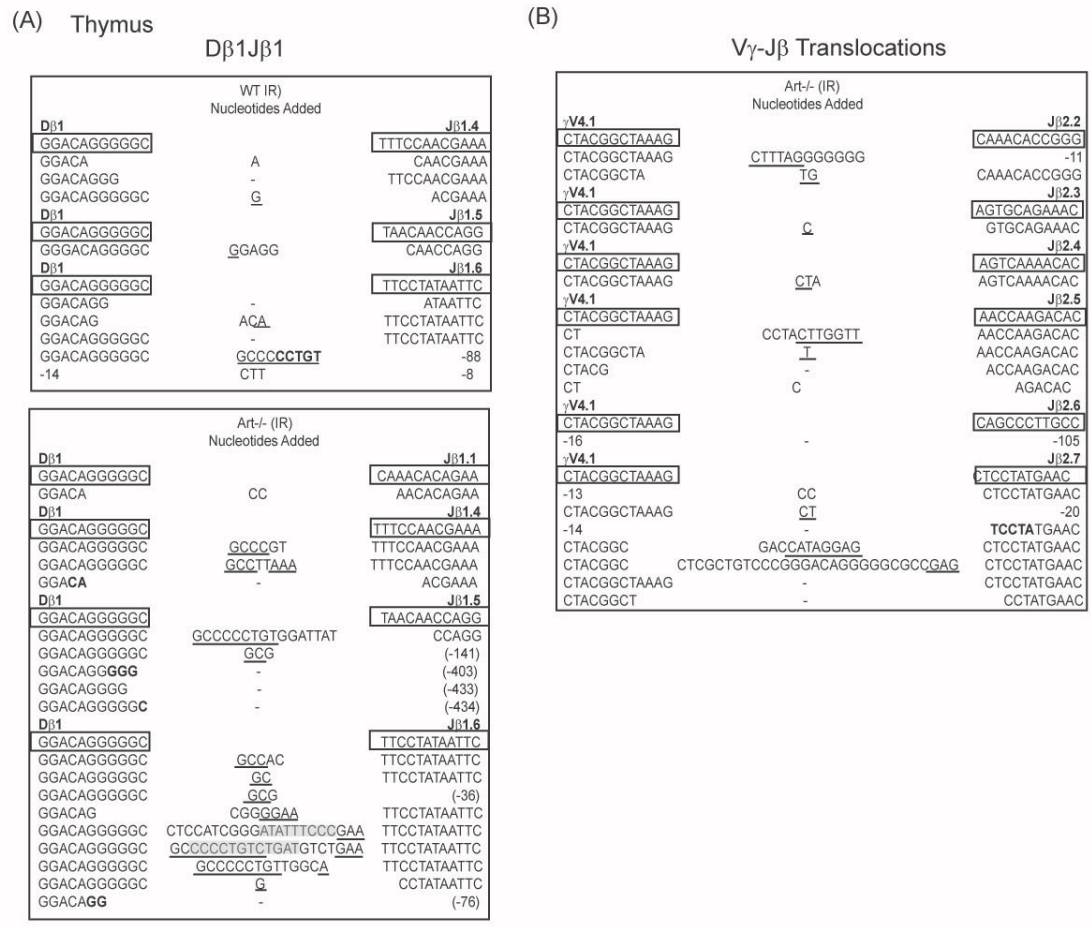

Coding end sequences are shown in boxes above the rearrangements. P NT are underlined. N NT are indicated between the coding segments. MH are represented in bold. Sequences derived from the adjacent sequences are highlighted. Sequences for the unirradiated mice were previously published by our lab [82].

Figure S3.5: Coding join sequences (WT INV5)

pMX-INV Coding Joins

No IR		
5' CE	P/N/P	3' CE
GGAACGTCTG		CAGCCTACAA
GGAACGTC	CTGTGC	GCCTACAA
GGAACG	G	CAGCCTACAA
GGAAC	CTTTG	-15
GGAACGTCTG	CCCCCACTG	CAGCCTACAA
GGAACG	AA	CAGCCTACAA
GGAACGTC	CG	CAGCCTACAA
GGAACGTCTG	G	ACAA
GGAACG	CCCCC	A
GGAACG	A	AA
-22	GGGGA	-51
+IR		
5' CE	P/N/P	3' CE
GGAACGTCTG		CAGCCTACAA
GGAACG	AG	AA
GGAACGTCT	AAGGCCGC	CCTACAA
GGAACGTC	CT	CAGCCTACAA
GGAACGTCT	G	CAGCCTACAA
GGTGTC -20	CGT	CAGCCTACAA
GGAACG	GTG	CAGCCTACAA
GGAACGTCT	C	CCTACAA
GGAACGTCTG	G	ACAA
GGAACGTCTG	-	CAGCCTACAA

WT-INV 5
Igκ Coding Joins

No IR		
Vκ6-23	P/N/P	Jκ1*01
GCTATCCTCT		GTGGACGTTC
GCTATCCT	T	TGGACGTTC
GCTATCCT	GA	GACGTTC
GCTATCCTC**T**	-	GGACGTTC
-10	CTCCTTCC	GTGGACGTTC
GCTA	CCCAC	GTGGACGTTC
GCTA	A	GTGGACGTTC
GCTATC	-	GTGGACGTTC
GCTATC	-	GGACGTTC
GCTATCCTC	A	GACGTTC
-10	TCC	GTGGACGTTC
+IR		
Vκ6-23	P/N/P	Jκ1*01
GCTATCCTCT		GTGGACGTTC
GCT	C	GTGGACGTTC
GCTATC	TC	TGGACGTTC
GCTATCCTCT	-	ACGTTC
GCTATCCTCN	-	TGGACGTTC
GCTATCCTC	C	GTGGACGTTC
-10	CTCC	TGGACGTTC
GCTATCC	-	GTGGACGTTC

Coding end sequences are shown in boxes above the rearrangements. P NT are underlined. N NT are indicated between the coding segments. MH are represented in bold.

Figure S3.6: Igκ coding join sequences (*Art*$^{-/-}$ c.30)

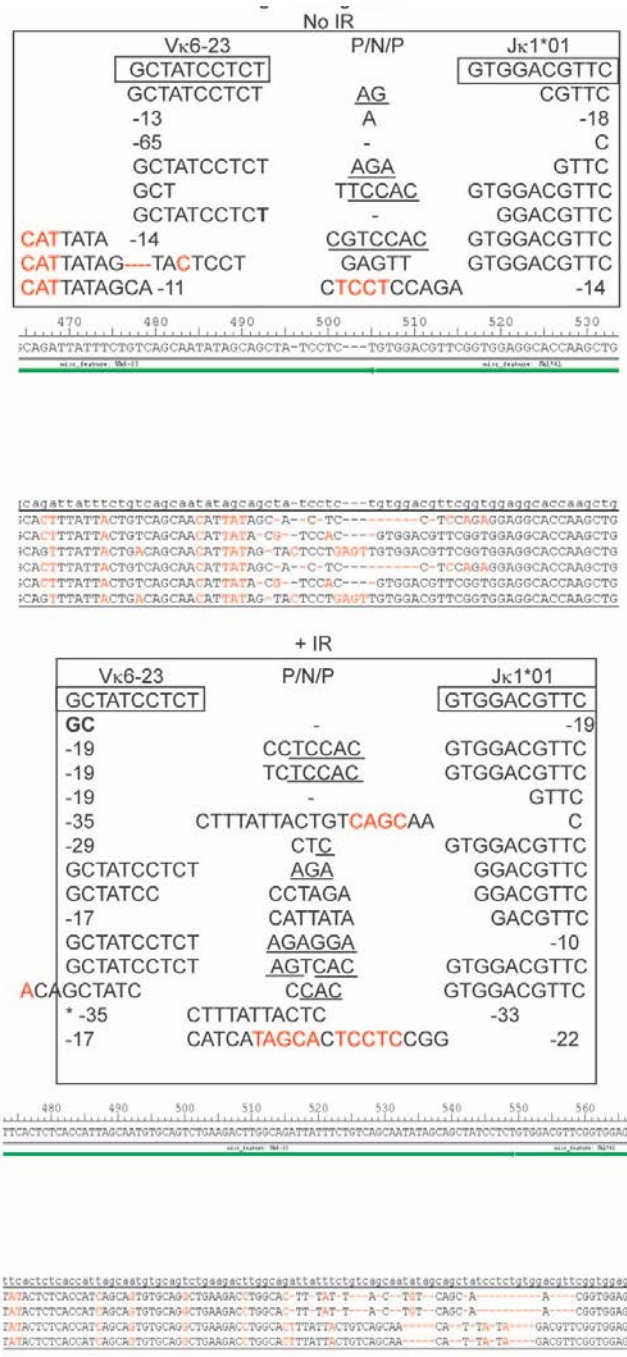

Coding end sequences are shown in boxes above the rearrangements. P NT are underlined. N NT are indicated between the coding segments. MH are represented in bold. The sequences were aligned in Seqman Pro. The mismatched sequences near the breakpoint junctions are shown in red.

Figure S3.7: pMX-INV coding join sequences (*Art*$^{-/-}$ c.30)

No IR

5' CE	P/N/P	3' CE
GGAACGTCTG		CAGCCTACAA
GG	G	-14
-24	A	-21
-19	CTCTG	CAGCCTACAA
-27	GGCTG	CAGCCTACAA
GGAACGTCTG	-	CAA
GGA**AC**	-	-34
GGAACGTCTG	ACGCTGCGT	-12
-46	TCC	-39
G -29	-	-17
-62	CACT	-40
A -11	-	-27
-18	-	CAA
GGAACG	G	-12
GGA	-	-22
GGAACGTCTG	-	CAGCCTACAA
GGAACGTCTG	CAA	CTACAA
G	AGA	-11

+ IR

5' CE	P/N/P	3' CE
GGAACGTCTG		CAGCCTACAATTCCGCCC
-70	CCG	-16
-35	C	CAGCCTACAATTCCGCCC
GGAACGTCTG	CCTG	CAATTCCGCCC
GGAACGTCTG	-	CAGCCTACAATTCCGCCC
-11	TGCGTTTGTCTATATGTT	-82
G -51	-	-42
-23	A	CCTACAATTCCGCCC
GG	CCCGCTG	CAGCCTACAATTCCGCCC
-22	-	-18
GGA	-	CTACAATTCCGCCC
GGAACG	-	CTACAATTCCGCCC
-52	TGGTCGCTACCG	-17
-14	GTAGGCCCT	CAGCCTACAATTCCGCCC
GGAACGTCT	-	ACAATTCCGCCC
GGAACGTCTG	CAGACT	CAATTCCGCCC
GGAACGTCTG	CAAG	CAATTCCGCCC
GGAACGTTTG	G	CTACAATTCCG- CC
GGAACG	-	AATTCCG- CC

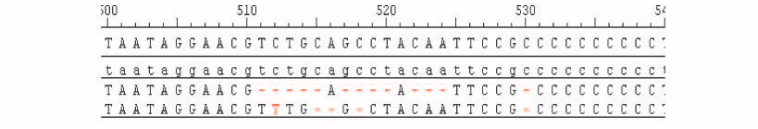

Coding end sequences are shown in boxes above the rearrangements. P NT are underlined. N NT are indicated between the coding segments. MH are represented in bold. The mismatched sequences near the breakpoint junctions are shown in red.

Figure S3.8: Igκ coding joins sequences (*Art*$^{-/-}$ c.4)

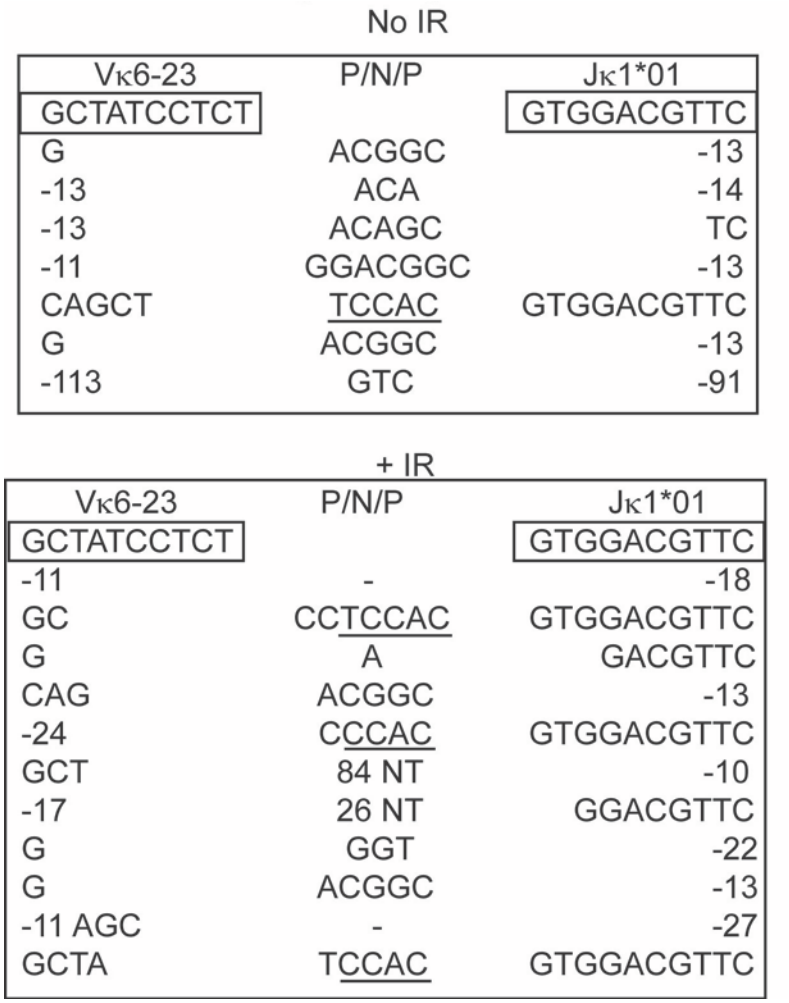

No IR

Vκ6-23	P/N/P	Jκ1*01
GCTATCCTCT		GTGGACGTTC
G	ACGGC	-13
-13	ACA	-14
-13	ACAGC	TC
-11	GGACGGC	-13
CAGCT	TCCAC	GTGGACGTTC
G	ACGGC	-13
-113	GTC	-91

+ IR

Vκ6-23	P/N/P	Jκ1*01
GCTATCCTCT		GTGGACGTTC
-11	-	-18
GC	CCTCCAC	GTGGACGTTC
G	A	GACGTTC
CAG	ACGGC	-13
-24	CCCAC	GTGGACGTTC
GCT	84 NT	-10
-17	26 NT	GGACGTTC
G	GGT	-22
G	ACGGC	-13
-11 AGC	-	-27
GCTA	TCCAC	GTGGACGTTC

Coding end sequences are shown in boxes above the rearrangements. P NT are underlined. N NT are indicated between the coding segments. MH are represented in bold.

Figure S3.9: pMX-INV coding join sequences (*Art*$^{-/-}$ c.4)

No IR

5' CE	P/N/P	3' CE
GGAACGTCTG		CAGCCTACAA
CC -32	-	-23
-80	-	-67
-14	-	**A**CAA
GGA	C	GCCTACAA
GGAACGTCTG	C	CAA
-19	CTCTG	CAGCCTACAA
GGA	TT	CCTACAA
GGAACGT**C**	-	AGCCTACAA
GGAAC	CG	CAGCCTACAA
-34	T	-82
T -24	-	-11
GGA	CGTCC	CAGCCTACAA
-21	CAG	-21
GGAACGTCTG	CAGGG	A
GGAACGT	ATC	-19
GGAACGTCTG	-	CAGCCTACAA
-118	-	-100
GGAACG	-	CCTACAA
GGAACGTCTG	-	CAA

+ IR

5' CE	P/N/P	3' CE
GGAACGTCTG		CAGCCTACAA
-20	T	-88
GGAACG	-	ACAA
G	-	-19
-30	TACTG	CAGCCTACAA
GGCCG -77	-	-56
-44	GCCATTACCAA	AA
GGAACGTCTG	-	CAGCCTACAA
G -79	-	-101
C -42	-	-109
GGAACGTCTG	CAGACGAG	AA
GGAACG**T**	-	-12
GGAACGTCTG	CGGA	-11
GGAACGTCTG	_AGG	-12
-254	-	-40
GGAACGTCTG	-	CAA
GGAA	ATTCCGC	-15

Coding end sequences are shown in boxes above the rearrangements. P NT are underlined. N NT are indicated between the coding segments. MH are represented in bold. The sequences derived from the adjacent sequences are shown in red.

Chapter 4

Conclusions and Future Directions

4.1 Overview

The process of V(D)J recombination, although essential for adaptive immunity and antigen receptor diversity, poses a risk to chromosomal integrity. Integration of processes, such as germline transcription, chromatin modification, RAG-mediated cleavage, DNA end-complex stability, end-processing and joining, DNA damage response and cell death activation in case ends are not repaired, is vital to preventing genomic instability. Over the last two decades, pathways and factors that have tumor suppressor function or oncogenic potential during V(D)J recombination have been identified. However, interactions between these factors and contributions of different end-joining mechanisms are still not fully characterized due to functional redundancies. I investigated the mechanisms that underlie spontaneously arising or ionizing-radiation induced structural chromosomal aberrations during V(D)J recombination. In the following chapter, I will first summarize my conclusions about the potential mechanisms of aberrant end-joining of RAG-induced breaks in different mutant backgrounds. I will also discuss potential future studies that will help further understand these processes. The second part of this chapter addresses the implications of these findings for tumor development in patients and potential interventions.

4.2 Mechanisms of Genomic Instability Associated with Defective V(D)J Recombination

My studies have offered useful insight into the mechanisms that lead to spontaneous genomic instability in non-malignant cells from mice with hypomorphic *RAG1* and *Artemis* gene mutations [82, 200]. These mutations are associated with increased frequency of mis-repair of the coding ends resulting in aberrant interchromosomal transrearrangement. Indeed, these mice develop lymphoid tumors on a p53-null background. These studies provide the first *in vivo* evidence for potential functions of RAG1 and Artemis proteins in maintaining post-cleavage complex (PCC) stability during V(D)J recombination. Additionally, I have also demonstrated that ATM kinase-mediated DNA damage response can facilitate robust error-prone alternative end-joining in Artemis-deficient lymphocytes.

Does Artemis have a role in maintenance of postcleavage complex (PCC) stability?

What constitutes a postcleavage complex?

Biochemical studies examining pre- and post-cleavage complex assembly during V(D)J recombination have mainly examined the interaction of RAG proteins with DNA ends. After cleavage, the newly generated DNA ends are maintained in a complex comprising of RAG proteins. The association of hairpins in the PCC is labile *in vitro* with majority of the hairpins dissociating from the complex [181]. How C-NHEJ factor access the cleaved ends remains elusive. Contribution of C-NHEJ factors to PCC stability has also not been directly examined. Two models can be used to explain how C-NHEJ factors gain access to DNA ends. In one model, Ku70/80 heterdimer, DNA-PKcs and subsequently Artemis, access DNA ends held by RAG proteins within the PCC complex. Thus, DNA ends will be associated with proteins throughout the process of recombination. Alternatively, coding ends are released from the complex and then readily recognized by Ku proteins. In this model coding ends will be transiently free between release from the PCC and binding by C-NHEJ factors and potentially accessible to error prone end joining pathways. Both Ku and DNA-Pkcs have been suggested to bridge DNA ends *in vitro* [288]. Ku70/80 also directly interacts with RAG1. Therefore, it is highly likely that Ku70/80 are recruited to the DNA ends by RAG and then RAG, DNA-PK and other factors localizing to the DNA ends form a scaffolding complex that retains DNA ends at cleavage-joining interphase.

How may Artemis contribute to PCC stability?

The contribution of Artemis to PCC stability has not been explored before our studies in Art-P70 mice. The increased frequency of trans-rearrangements and deletional hybrid joins in Art-P70 but not *Art*$^{-/-}$ murine lymphocytes indicates the significance of Artemis C terminus in preventing genomic instability. Based on our findings, it is reasonable to infer that Artemis plays important role in DNA end complex stability via its C-terminus. This function is distinct from its role in hairpin opening during normal V(D)J recombination. ATM, MRE11 and NBS1 have been previously suggested to have a role in stabilizing the DNA ends after cleavage [128, 166]. These proteins do not appear to play essential roles in normal V(D)J recombination. However, their deficiency is associated with an increase in aberrant rearrangements of the RAG-induced breaks suggesting that they are important in preventing aberrant V(D)J recombination and genomic instability. Based on these findings, I propose a model in which ATM, MRN complex (MRE11, RAD50, NBS1) and Artemis, via its C-terminus, may act in the same pathway of DNA end-tethering during antigen receptor assembly (Figure 4.1). ATM most likely mediates this effect by phosphorylating the MRN complex, Artemis C-terminus and H2AX. Phosphorylated H2AX (γH2AX), in turn, protects the RAG-induced ends from excessive resection by regulating the access of certain DNA damage response factors [126]. The MRN complex may have direct roles in retention of the ends within the complex. Artemis C-terminus may induce conformational changes within the PCC either directly or through interaction with other factors such as MRN complex that are important to retain DNA ends. Loss of Artemis C-terminus would interfere with these changes thus resulting in premature release of DNA ends.

Figure 4.1: Model of Postcleavage Complex Instability in Art-P70 Mutant Lymphocytes

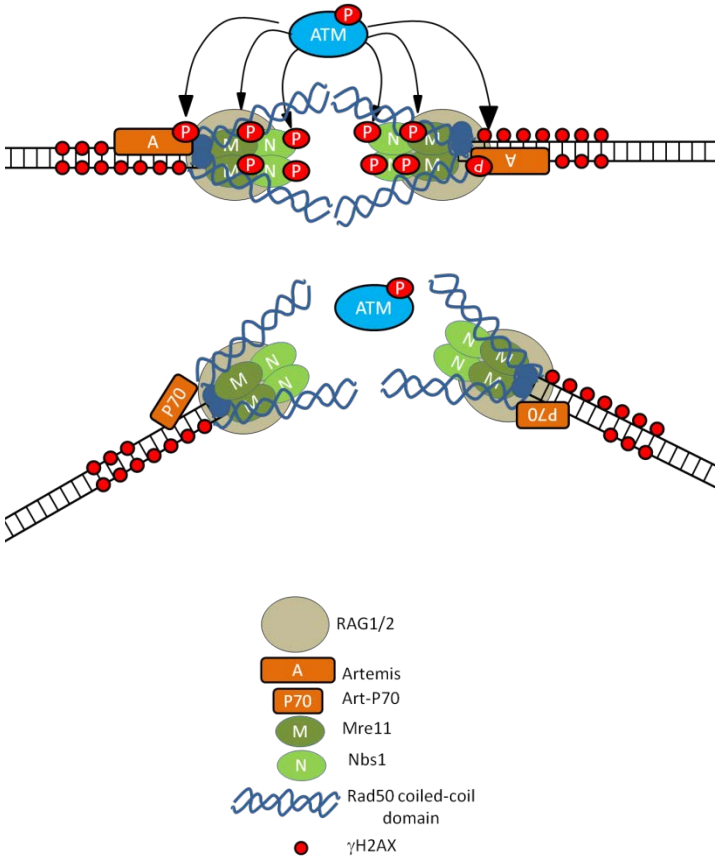

Figure 4.1. At the RAG-induced breaks, ATM phosphorylates Artemis C-terminus, H2AX and the MRN complex. Artemis and MRN play key roles in tethering the DNA ends together in the postcleavage complexes. Loss of Artemis C-terminus results in loss of ATM phosphorylation sites which may induces conformational changes within the complex resulting in premature release of ends and aberrant rearrangements.

Future studies.

The precise spatiotemporal mechanisms that govern DNA end stabilization within the PCC by various proteins are still undefined. Determining the composition of the PCC and protein-DNA contacts within this complex is necessary to understand how DNA ends are transferred from RAG complex to C-NHEJ factors. Characterization of discrete PCC in the presence of not only RAG but other proteins of interest *in vitro* using physiologically relevant substrates,

electrophoretic mobility shift assays (EMSA) and in-gel DNA footprinting assays will provide important information about the contribution of C-NHEJ factors to DNA end retention. These biochemical assays can also be used to examine the interactions of Art-P70 and other mutant proteins with RAG-generated ends.

Technical difficulties in examining the direct interaction of these proteins with each other and with the DNA ends within an end-complex have posed challenges to understanding these processes. Recently, Wang *et al*. used fluorescence resonance energy transfer (FRET) to examine RAG-mediated cleavage reaction and PCC stability with core RAG proteins and a RAG2 mutant that had been suggested to destabilize the complex [289]. This sensitive system could also be used for continuous and real-time monitoring of the kinetics of PCC formation and retention or release of coding ends from complexes in the presence of RAG, C-NHEJ factors and defective proteins such as Artemis-P70 and RAG1-S723C.

To understand the role of the Artemis-C terminus in stabilizing DNA ends, it is critical to define regions that might be involved in this process. Expressing deletion constructs in Artemis-deficient lymphocytes followed by site-directed mutagenesis can be useful in identifying these critical regions.

Malu *et al.* recently identified three critical regions in the Artemis C-terminus for direct interaction with DNA Ligase IV (LigIV) that are important for coding join formation in plasmid substrates and are missing in Art-P70 [76]. Though the levels of coding joins were low after ablation of this interaction through site-directed mutagenesis, the coding junctions formed were not qualitatively different from those recovered from wild-type cells. We also did not observe an increase in frequency of joins with aberrant sequences in Art-P70 mutant lymphocytes [82]. These two studies suggest that even in the absence of Artemis-LigIV interaction, the DNA ends can be joined by LigIV/XRCC4 complex. This might be mediated through interactions of LigIV with factors upstream of Artemis such as RAG and/or DNA-PK complexes. It would be interesting to determine the *in vivo* effect of loss of Artemis-LigIV interaction on aberrant V(D)J recombination and define the significance of this interaction in terms of PCC stability and DNA repair pathway choice. Expression of mutant proteins defective

in this interaction in v-abl pre-B cell system or a knock-in mouse model will help understand the significance of these interactions.

How does RAG1-S723C contribute to genomic instability?

RAG proteins have been shown to function directly in complex assembly and stability through their interactions with the DNA ends and/or with chromatin. For RAG1-S723C mutation, we have proposed two mechanisms which are not mutually exclusive: pre-cleavage substrate recognition errors and postcleavage end complex instability. Characterizing their individual contribution will help us understand the precise mechanism of genomic instability in RAG1-S723C mice. Chromatin immunoprecipitation (ChIP) assays could be used to determine localization of RAG1-S723C/RAG2 to genomic regions that are not within antigen receptor loci.

We also examined the effect of general DNA damage induction on V(D)J recombination in these mice. Although irradiation failed to induce development or intralocus V(D)J rearrangements in RAG-S723C lymphocytes (Figure S4.1), whether irradiation induced interchromosomal trans-rearrangements was not examined. It would be interesting to determine if coding ends are processed differently after DNA damage response induction in RAG1-S723C lymphocytes.

How is DNA repair pathway choice determined?

The presence of truncated Artemis protein that retains endonucleolytic activity may block the access of other nucleases to DNA ends. Thus, the composition of proteins in the PCC may be an important determinant of DNA repair pathway choice. Consistent with this idea, abrogation of RAG1 or RAG2 protein-protein interactions results in premature release of coding ends from PCC with joins suggestive of alternative end-joining (A-EJ) [65, 181, 185]. Mutations that make the complexes extremely unstable during early V(D)J recombination may be associated with end-joining by alternative pathways. Alternatively, this may result from loss of regions critical for interaction with C-NHEJ factors thus making the ends available for A-EJ. A frameshift RAG2 mutant that predisposes to error-prone end-joining was once thought to be dysfunctional in post-cleavage complex-coding end stabilization [185]. Recently, it was shown

that an unstable coding end complex might not be responsible for this end-joining defect [289]. Thus, other factors that link RAG1/2-mediated cleavage and repair by NHEJ may contribute to defective end-joining and need to be investigated. Interestingly, we observed that RAG1-S723C mutation, also associated with premature release of DNA ends, was associated with coding joins that are qualitatively similar to WT joins [200]. The difference in repair pathway selection might result from retention of the regions in the RAG1-S723C/RAG2 complex important for interactions with C-NHEJ factors. Structure-function and biochemical studies to identify specific functions within certain regions and defining critical residues within these proteins are thus critical to our understanding of the full functional spectrum of these proteins.

Is IR-induced end-joining observed in the absence of Artemis mediated by a distinct pathway or merely by nuclease substitution?

Currently, there is no consensus on the molecular components of alternative end-joining pathway (A-EJ). It is also not clear if A-EJ is one distinct pathway or several different pathways which may or may not have functional redundancies with C-NHEJ factors. A distinct pathway would require at least one nuclease, a polymerase and a ligase. Alternatively, a certain non-C-NHEJ factor may substitute for a missing C-NHEJ factor. Based on my findings, I propose that in the absence of Artemis, another nuclease opens the hairpin coding ends with slow kinetics. This nucleolytic activity may be enhanced after IR. Alternatively, a distinct nucleolytic activity might be induced by IR. The ends could then be joined by LigIV/XRCC4 and/or other ligation complexes. On the other hand, a completely distinct end-joining pathway comprising of completely different nucleases, polymerases and ligation complex may be induced after IR. These two models are not mutually exclusive and are discussed in detail in section 3.4 (Figure 4.2).

Figure 4.2: Potential Mechanisms of IR-Induced V(D)Recombination in the Absence of Artemis

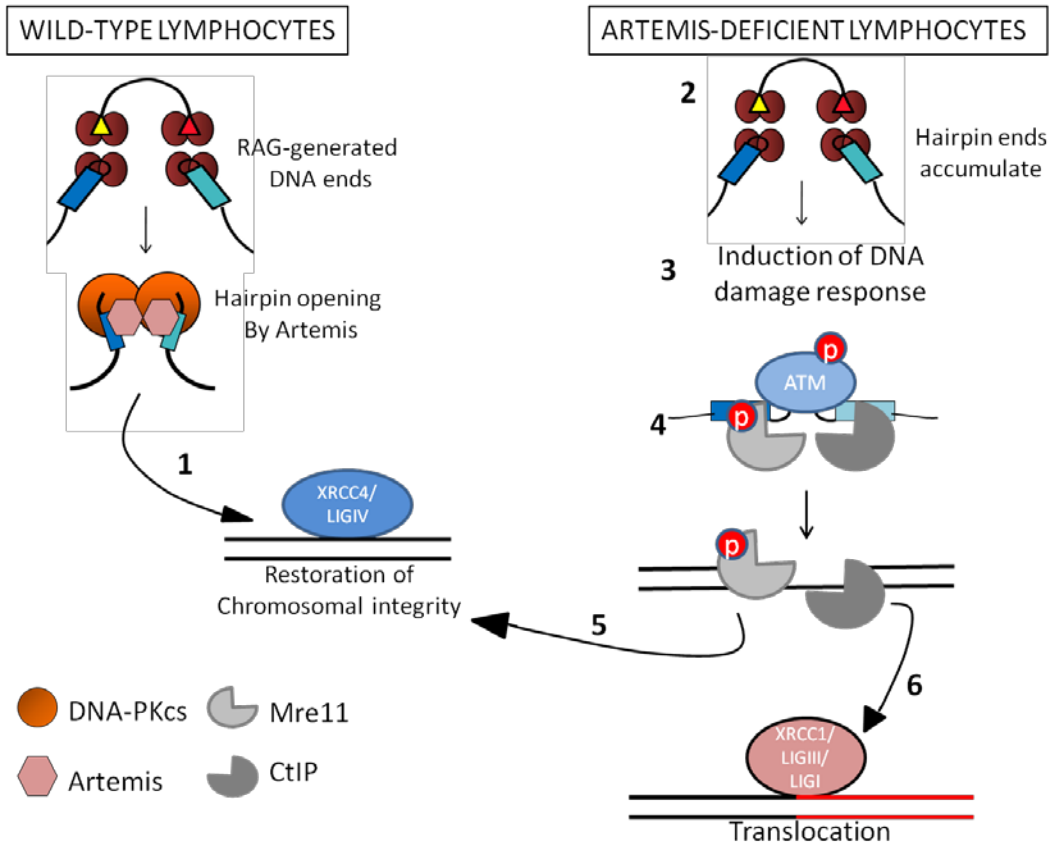

Figure 4.2. In the wild-type lymphocytes, V(D)J recombination proceeds normally in the presence of Artemis (1). In the Artemis-deficient lymphocytes, hairpin coding ends accumulate (2). After general DNA damage response (DDR) induction, ATM is activated and mediates end-joining through some as-yet undetermined mechanisms (3). This may involve MRE11- and CtIP-promoted hairpin opening (4). Extensive resection occurs at the ends (5). The ends could then be ligated by either XRCC4/LigIV complex (5), or by XRCC1/LigIII/LigI - the activities of which are associated with increased translocation frequency (6).

How is IR-induced end-joining different in DNA-PKcs and Artemis-mutant mice?

Irradiation of DNA-PKcs defective mice and pre-B cells also induces V(D)J recombination [262, 266]. However, IR-induced joins were qualitatively different from those we observed in irradiated *Art*$^{-/-}$ murine lymphocytes. Binnie *et al*. observed fewer P-nucleotide insertions after IR in DNA-PKcs-mutant mice [266]. In contrast, we observed an increase in the frequency and

length of P-nucleotide insertions at the breakpoint junctions from the irradiated *Art*$^{-/-}$ lymphocytes. The difference in our findings might be due to the use of extrachromosomal plasmid substrates by Binnie *et al*., whereas we examined V(D)J recombination at the endogenous and chromosomally integrated loci. Alternatively, the temporal sequence of events may also determine how the ends are processed. After IR, ATM might phosphorylate Artemis in DNA-PKcs-deficient cells, and the intact downstream C-NHEJ factors might still be able to process and join the ends in a wild-type manner. In contrast, in the absence of Artemis, another nuclease would have to be recruited in order to open coding ends after irradiation. This nuclease may be prone to adding long stretches of P-nucleotides by nicking several nucleotides away from the apex of the hairpins. In addition, ends processed with slow kinetics may also be available to a completely distinct A-EJ pathway.

What factors are involved in IR-induced end joining? Several factors have been implicated but none have been established as definitive A-EJ factors. MRE11- and CtIP-mediated resection has been suggested to be involved in microhomology-mediated end joining (MMEJ) as discussed in sections 1.8 and 3.4. The role of error-prone polymerases in this process also needs to be delineated. Polymerase recruitment is locus-specific, and polymerase expression often varies by lymphocyte developmental stage [19, 20]. TdT and DNA polymerase μ have been shown to be recruited by Ku and DNA-PKcs *in vitro* [290-292]. Thus, it is not surprising that, in Ku- or DNA-PKcs-deficient cells, there is a paucity of N-nucleotides [161, 293, 294]. However, N-NT are not absent in *Art*$^{-/-}$ cells, and after IR, nucleotide insertions are increased. This might result from IR-induced polymerase activity at breakpoint junctions lacking Artemis. Gap-filling synthesis by DNA polymerases (Polμ/λ) prevents extensive deletions, but these polymerases are error prone and susceptible to template slippage and frameshift synthesis [285]. Template slippage would result in direct repeats. The character of joins in Artemis-deficient mice after IR is suggestive of error-prone gap filling. A detailed analysis of the complex roles of these polymerases in IR-induced V(D)J recombination would improve our understanding of breakpoint processing. A potential role of different ligase/XRCC complexes has been discussed earlier.

Future Studies

To identify the molecular components of the poorly characterized A-EJ pathway during V(D)J recombination, combined deficiencies can be utilized. Inhibiting or knocking down potential candidates such as MRE11/CtIP in our *Art*$^{-/-}$ pre-B cells would allow us to examine the roles of these factors in A-EJ.

Ochi *et al.* recently used structural analysis to describe Artemis-LigIV interaction and predicted that a similar interaction between Artemis and DNA Ligase I is possible. DNA Ligase I is a potential A-EJ factor. Similar protein interactions may exist to recruit other proteins when a C-NHEJ factor is missing. Using a LigIV inhibitor in v-abl *Art*$^{-/-}$ pre-B cells to determine join qualitative and quantitative differences would thus be interesting [295]. Combined Artemis and LigIII deficiencies can also provide useful information about the role of ligases during IR-induced end-joining.

4.3 Implications for Tumor Development in Patients

These studies have important prognostic implications for patients. Undiagnosed hypomorphic mutations that lead to mild immunodeficiency symptoms may increase predisposition to tumorigenesis later in life. Also, patients receiving bone marrow transplants might still be at risk of developing tumors.

My studies that examine IR-induced activation of translocation-promoting alternative end-joining suggest a mechanism by which systemic DSB-inducing radio- and chemo-therapy might cause aberrant chromosomal rearrangements. This may result in drug resistance, relapse of tumors which are genetically distinct from the primary tumor or development of therapy-induced tumors in other tissues. Type II topoisomerase poisons that stabilize DNA DSBs are frequently used to treat cancers [296]. Their use is associated with high incidence of therapy-related secondary leukemia harboring 11q23 translocations involving the MLL gene. Combined chemo- and radiotherapy for solid tumors is also rarely associated with acute leukemia with chromosomal aberrations that may involve duplications and translocations including BCR/ABL1 rearrangement [297].

Understanding these mechanisms will help us define the etiology of therapy-related tumors as well as develop novel therapeutic interventions. Concomitant inhibition of DNA damage response has been suggested to sensitize tumors. I suggest that this will have the added benefit of preventing future oncogenic events. Developing ATM-inhibitors for clinical use could be useful in this regard.

Figure S4.1: Low dose ionizing radiation induces apoptosis in RAG1-S723C lymphocytes and fails to rescue arrest in T lymphocyte development and V(D)J rearrangements

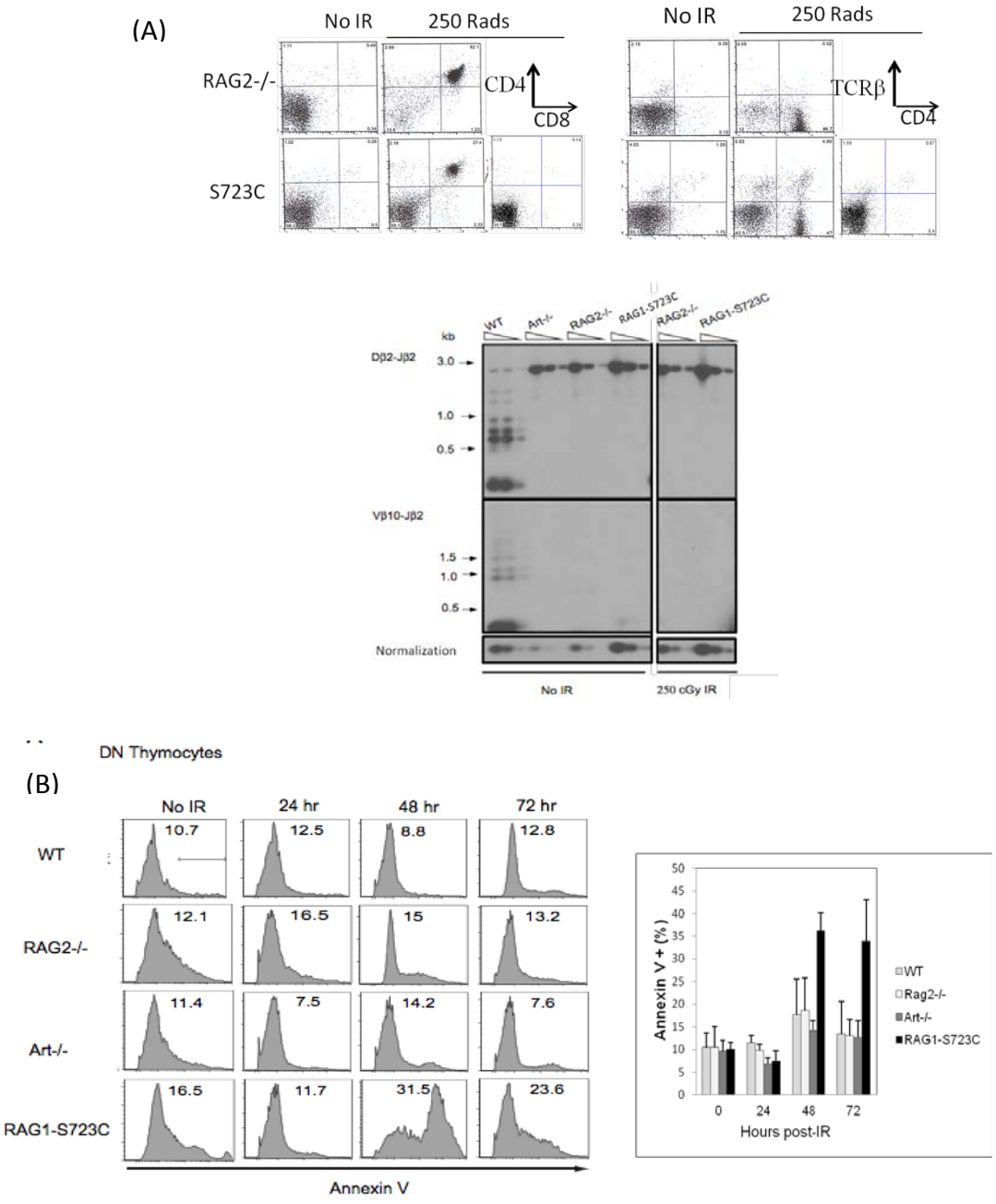

(A)RAG1-null and RAG1-S723C mice were irradiated at 3-5 weeks of age at 250 cGy. Three weeks later they were analyzed for lymphocyte development (top panel) and V(D)J rearrangements (bottom panel). (B) Mice were irradiated at 250 cGy and analyzed 24, 48 and 72 hours later for apoptosis. Apoptosis was determined by Annexin V positive population in double negative (DN) T lymphocytes that were negative for 7-AAD (left panel). Graphs representing Annexin V+ cells with bars indicating means and standard error of means are shown (right panel).

REFERENCES

1. Hsu, E., *V(D)J recombination: of mice and sharks.* Adv Exp Med Biol, 2009. **650**: p. 166-79.
2. Tonegawa, S., *Somatic generation of antibody diversity.* Nature, 1983. **302**(5909): p. 575-81.
3. Ramsden, D.A., T.T. Paull, and M. Gellert, *Cell-free V(D)J recombination.* Nature, 1997. **388**(6641): p. 488-91.
4. Schatz, D.G., M.A. Oettinger, and D. Baltimore, *The V(D)J recombination activating gene, RAG-1.* Cell, 1989. **59**(6): p. 1035-48.
5. Oettinger, M.A., et al., *RAG-1 and RAG-2, adjacent genes that synergistically activate V(D)J recombination.* Science, 1990. **248**(4962): p. 1517-23.
6. Ramsden, D.A., K. Baetz, and G.E. Wu, *Conservation of sequence in recombination signal sequence spacers.* Nucleic Acids Res, 1994. **22**(10): p. 1785-96.
7. Schatz, D.G. and Y. Ji, *Recombination centres and the orchestration of V(D)J recombination.* Nat Rev Immunol, 2011. **11**(4): p. 251-63.
8. McBlane, J.F., et al., *Cleavage at a V(D)J recombination signal requires only RAG1 and RAG2 proteins and occurs in two steps.* Cell, 1995. **83**(3): p. 387-95.
9. Schlissel, M., et al., *Double-strand signal sequence breaks in V(D)J recombination are blunt, 5'-phosphorylated, RAG-dependent, and cell cycle regulated.* Genes Dev, 1993. **7**(12B): p. 2520-32.
10. Roth, D.B., et al., *V(D)J recombination: broken DNA molecules with covalently sealed (hairpin) coding ends in scid mouse thymocytes.* Cell, 1992. **70**(6): p. 983-91.
11. Puebla-Osorio, N. and C. Zhu, *DNA damage and repair during lymphoid development: antigen receptor diversity, genomic integrity and lymphomagenesis.* Immunologic Research, 2008. **41**(2): p. 103-122.
12. Lieber, M.R., et al., *The mechanism of vertebrate nonhomologous DNA end joining and its role in V(D)J recombination.* DNA Repair (Amst), 2004. **3**(8-9): p. 817-26.
13. Buck, D., et al., *Cernunnos, a novel nonhomologous end-joining factor, is mutated in human immunodeficiency with microcephaly.* Cell, 2006. **124**(2): p. 287-99.
14. Ahnesorg, P., P. Smith, and S.P. Jackson, *XLF interacts with the XRCC4-DNA ligase IV complex to promote DNA nonhomologous end-joining.* Cell, 2006. **124**(2): p. 301-13.
15. Ma, Y., et al., *Hairpin opening and overhang processing by an Artemis/DNA-dependent protein kinase complex in nonhomologous end joining and V(D)J recombination.* Cell, 2002. **108**(6): p. 781-94.
16. Hammel, M., et al., *Ku and DNA-dependent protein kinase dynamic conformations and assembly regulate DNA binding and the initial non-homologous end joining complex.* J Biol Chem, 2010. **285**(2): p. 1414-23.
17. Goodarzi, A.A., et al., *DNA-PK autophosphorylation facilitates Artemis endonuclease activity.* EMBO J, 2006. **25**(16): p. 3880-9.
18. Pannicke, U., et al., *Functional and biochemical dissection of the structure-specific nuclease ARTEMIS.* EMBO J, 2004. **23**(9): p. 1987-97.

19. Bertocci, B., et al., *Nonoverlapping functions of DNA polymerases mu, lambda, and terminal deoxynucleotidyltransferase during immunoglobulin V(D)J recombination in vivo.* Immunity, 2006. **25**(1): p. 31-41.
20. Bertocci, B., et al., *Immunoglobulin kappa light chain gene rearrangement is impaired in mice deficient for DNA polymerase mu.* Immunity, 2003. **19**(2): p. 203-11.
21. Gellert, M., *V(D)J recombination: RAG proteins, repair factors, and regulation.* Annu Rev Biochem, 2002. **71**: p. 101-32.
22. Bogue, M.A., C. Jhappan, and D.B. Roth, *Analysis of variable (diversity) joining recombination in DNAdependent protein kinase (DNA-PK)-deficient mice reveals DNA-PK-independent pathways for both signal and coding joint formation.* Proc Natl Acad Sci U S A, 1998. **95**(26): p. 15559-64.
23. Gao, Y., et al., *A targeted DNA-PKcs-null mutation reveals DNA-PK-independent functions for KU in V(D)J recombination.* Immunity, 1998. **9**(3): p. 367-76.
24. Beetz, S., D. Diekhoff, and L.A. Steiner, *Characterization of terminal deoxynucleotidyl transferase and polymerase mu in zebrafish.* Immunogenetics, 2007. **59**(9): p. 735-44.
25. Flajnik, M.F. and L. Du Pasquier, *Evolution of innate and adaptive immunity: can we draw a line?* Trends Immunol, 2004. **25**(12): p. 640-4.
26. Rast, J.P. and G.W. Litman, *Towards understanding the evolutionary origins and early diversification of rearranging antigen receptors.* Immunol Rev, 1998. **166**: p. 79-86.
27. Sakano, H., et al., *Sequences at the somatic recombination sites of immunoglobulin light-chain genes.* Nature, 1979. **280**(5720): p. 288-94.
28. van Gent, D.C., K. Mizuuchi, and M. Gellert, *Similarities between initiation of V(D)J recombination and retroviral integration.* Science, 1996. **271**(5255): p. 1592-4.
29. Kapitonov, V.V. and J. Jurka, *RAG1 core and V(D)J recombination signal sequences were derived from Transib transposons.* PLoS Biol, 2005. **3**(6): p. e181.
30. Fugmann, S.D., et al., *An ancient evolutionary origin of the Rag1/2 gene locus.* Proc Natl Acad Sci U S A, 2006. **103**(10): p. 3728-33.
31. Haren, L., B. Ton-Hoang, and M. Chandler, *Integrating DNA: transposases and retroviral integrases.* Annu Rev Microbiol, 1999. **53**: p. 245-81.
32. Hencken, C.G., X. Li, and N.L. Craig, *Functional characterization of an active Rag-like transposase.* Nat Struct Mol Biol, 2012. **19**(8): p. 834-6.
33. Agrawal, A., Q.M. Eastman, and D.G. Schatz, *Transposition mediated by RAG1 and RAG2 and its implications for the evolution of the immune system.* Nature, 1998. **394**(6695): p. 744-51.
34. Hiom, K., M. Melek, and M. Gellert, *DNA transposition by the RAG1 and RAG2 proteins: a possible source of oncogenic translocations.* Cell, 1998. **94**(4): p. 463-70.
35. Fugmann, S.D., et al., *The RAG proteins and V(D)J recombination: complexes, ends, and transposition.* Annu Rev Immunol, 2000. **18**: p. 495-527.
36. Matthews, A.G. and M.A. Oettinger, *Regulation of RAG transposition.* Adv Exp Med Biol, 2009. **650**: p. 16-31.
37. Ramsden, D.A., B.D. Weed, and Y.V.R. Reddy, *V(D)J recombination: Born to be wild.* Seminars in Cancer Biology, 2010. **20**(4): p. 254-260.

38. Jones, J.M. and C. Simkus, *The roles of the RAG1 and RAG2 "non-core" regions in V(D)J recombination and lymphocyte development.* Arch Immunol Ther Exp (Warsz), 2009. **57**(2): p. 105-16.
39. Difilippantonio, M.J., et al., *RAG1 mediates signal sequence recognition and recruitment of RAG2 in V(D)J recombination.* Cell, 1996. **87**(2): p. 253-62.
40. Spanopoulou, E., et al., *The homeodomain region of Rag-1 reveals the parallel mechanisms of bacterial and V(D)J recombination.* Cell, 1996. **87**(2): p. 263-76.
41. Swanson, P.C., S. Kumar, and P. Raval, *Early steps of V(D)J rearrangement: insights from biochemical studies of RAG-RSS complexes.* Adv Exp Med Biol, 2009. **650**: p. 1-15.
42. Yin, F.F., et al., *Structure of the RAG1 nonamer binding domain with DNA reveals a dimer that mediates DNA synapsis.* Nat Struct Mol Biol, 2009. **16**(5): p. 499-508.
43. Schatz, D.G. and P.C. Swanson, *V(D)J recombination: mechanisms of initiation.* Annu Rev Genet, 2011. **45**: p. 167-202.
44. Swanson, P.C., *The DDE motif in RAG-1 is contributed in trans to a single active site that catalyzes the nicking and transesterification steps of V(D)J recombination.* Mol Cell Biol, 2001. **21**(2): p. 449-58.
45. Gomez, C.A., et al., *Mutations in conserved regions of the predicted RAG2 kelch repeats block initiation of V(D)J recombination and result in primary immunodeficiencies.* Mol Cell Biol, 2000. **20**(15): p. 5653-64.
46. Shimazaki, N., et al., *Mechanistic basis for RAG discrimination between recombination sites and the off-target sites of human lymphomas.* Mol Cell Biol, 2012. **32**(2): p. 365-75.
47. Brady, B.L., N.C. Steinel, and C.H. Bassing, *Antigen receptor allelic exclusion: an update and reappraisal.* J Immunol, 2010. **185**(7): p. 3801-8.
48. Balasubramanian, D., et al., *H3K4me3 inversely correlates with DNA methylation at a large class of non-CpG-island-containing start sites.* Genome Med, 2012. **4**(5): p. 47.
49. Matthews, A.G. and M.A. Oettinger, *RAG: a recombinase diversified.* Nat Immunol, 2009. **10**(8): p. 817-21.
50. van Gent, D.C., et al., *Stimulation of V(D)J cleavage by high mobility group proteins.* EMBO J, 1997. **16**(10): p. 2665-70.
51. Thomas, J.O. and A.A. Travers, *HMG1 and 2, and related 'architectural' DNA-binding proteins.* Trends Biochem Sci, 2001. **26**(3): p. 167-74.
52. Little, A.J., et al., *Cooperative recruitment of HMGB1 during V(D)J recombination through interactions with RAG1 and DNA.* Nucleic Acids Res, 2013. **41**(5): p. 3289-301.
53. Liu, Y., L. Zhang, and S. Desiderio, *Temporal and spatial regulation of V(D)J recombination: interactions of extrinsic factors with the RAG complex.* Adv Exp Med Biol, 2009. **650**: p. 157-65.
54. Yancopoulos, G.D. and F.W. Alt, *Developmentally controlled and tissue-specific expression of unrearranged VH gene segments.* Cell, 1985. **40**(2): p. 271-81.
55. Ji, Y., et al., *Promoters, enhancers, and transcription target RAG1 binding during V(D)J recombination.* J Exp Med, 2010. **207**(13): p. 2809-16.
56. Del Blanco, B., et al., *Control of V(D)J Recombination through Transcriptional Elongation and Changes in Locus Chromatin Structure and Nuclear Organization.* Genet Res Int, 2011. **2011**: p. 970968.

57. Hiom, K. and M. Gellert, *A stable RAG1-RAG2-DNA complex that is active in V(D)J cleavage.* Cell, 1997. **88**(1): p. 65-72.
58. Swanson, P.C. and S. Desiderio, *V(D)J recombination signal recognition: distinct, overlapping DNA-protein contacts in complexes containing RAG1 with and without RAG2.* Immunity, 1998. **9**(1): p. 115-25.
59. Swanson, P.C., *A RAG-1/RAG-2 tetramer supports 12/23-regulated synapsis, cleavage, and transposition of V(D)J recombination signals.* Mol Cell Biol, 2002. **22**(22): p. 7790-801.
60. De, P., et al., *Thermal dependency of RAG1 self-association properties.* BMC Biochem, 2008. **9**: p. 5.
61. Bailin, T., X. Mo, and M.J. Sadofsky, *A RAG1 and RAG2 tetramer complex is active in cleavage in V(D)J recombination.* Mol Cell Biol, 1999. **19**(7): p. 4664-71.
62. Mundy, C.L., et al., *Assembly of the RAG1/RAG2 synaptic complex.* Mol Cell Biol, 2002. **22**(1): p. 69-77.
63. Landree, M.A., S.B. Kale, and D.B. Roth, *Functional organization of single and paired V(D)J cleavage complexes.* Mol Cell Biol, 2001. **21**(13): p. 4256-64.
64. Dudley, D.D., et al., *Mechanism and control of V(D)J recombination versus class switch recombination: similarities and differences.* Adv Immunol, 2005. **86**: p. 43-112.
65. Deriano, L., et al., *The RAG2 C terminus suppresses genomic instability and lymphomagenesis.* Nature, 2011. **471**(7336): p. 119-23.
66. Zhang, L., et al., *Coupling of V(D)J recombination to the cell cycle suppresses genomic instability and lymphoid tumorigenesis.* Immunity, 2011. **34**(2): p. 163-74.
67. Callebaut, I., et al., *Metallo-beta-lactamase fold within nucleic acids processing enzymes: the beta-CASP family.* Nucleic Acids Res, 2002. **30**(16): p. 3592-601.
68. Poinsignon, C., et al., *The metallo-beta-lactamase/beta-CASP domain of Artemis constitutes the catalytic core for V(D)J recombination.* J Exp Med, 2004. **199**(3): p. 315-21.
69. de Villartay, J.P., et al., *A histidine in the beta-CASP domain of Artemis is critical for its full in vitro and in vivo functions.* DNA Repair (Amst), 2009. **8**(2): p. 202-8.
70. Kurosawa, A. and N. Adachi, *Functions and regulation of Artemis: a goddess in the maintenance of genome integrity.* J Radiat Res, 2010. **51**(5): p. 503-9.
71. Ma, Y., et al., *The DNA-dependent protein kinase catalytic subunit phosphorylation sites in human Artemis.* J Biol Chem, 2005. **280**(40): p. 33839-46.
72. Malu, S., et al., *Role of non-homologous end joining in V(D)J recombination.* Immunol Res, 2012. **54**(1-3): p. 233-46.
73. Poinsignon, C., et al., *Phosphorylation of Artemis following irradiation-induced DNA damage.* Eur J Immunol, 2004. **34**(11): p. 3146-55.
74. Soubeyrand, S., et al., *Artemis phosphorylated by DNA-dependent protein kinase associates preferentially with discrete regions of chromatin.* J Mol Biol, 2006. **358**(5): p. 1200-11.
75. Niewolik, D., et al., *DNA-PKcs dependence of Artemis endonucleolytic activity, differences between hairpins and 5' or 3' overhangs.* J Biol Chem, 2006. **281**(45): p. 33900-9.

76. Malu, S., et al., *Artemis C-terminal region facilitates V(D)J recombination through its interactions with DNA Ligase IV and DNA-PKcs.* J Exp Med, 2012. **209**(5): p. 955-63.
77. De Ioannes, P., et al., *Structural basis of DNA ligase IV-Artemis interaction in nonhomologous end-joining.* Cell Rep, 2012. **2**(6): p. 1505-12.
78. Ochi, T., Gu, X., Blundell, T.L., *Structure of the Catalytic Region of DNA Ligase IV in Complex with an Artemis Fragment Sheds Light on Double-Strand Break Repair.* Structure, 2013. **21**(4): p. 672-679.
79. Ma, Y., K. Schwarz, and M.R. Lieber, *The Artemis:DNA-PKcs endonuclease cleaves DNA loops, flaps, and gaps.* DNA Repair (Amst), 2005. **4**(7): p. 845-51.
80. Dahm, K., *Functions and regulation of human artemis in double strand break repair.* Journal of Cellular Biochemistry, 2007. **100**(6): p. 1346-1351.
81. Riballo, E., et al., *A pathway of double-strand break rejoining dependent upon ATM, Artemis, and proteins locating to gamma-H2AX foci.* Mol Cell, 2004. **16**(5): p. 715-24.
82. Huang, Y., et al., *Impact of a hypomorphic Artemis disease allele on lymphocyte development, DNA end processing, and genome stability.* J Exp Med, 2009. **206**(4): p. 893-908.
83. Lieber, M.R., *The mechanism of double-strand DNA break repair by the nonhomologous DNA end-joining pathway.* Annu Rev Biochem, 2010. **79**: p. 181-211.
84. Schatz, D.G. and E. Spanopoulou, *Biochemistry of V(D)J Recombination*. 2005, Springer Berlin Heidelberg: Berlin, Heidelberg. p. 49.
85. Lewis, S.M., et al., *Novel strand exchanges in V(D)J recombination.* Cell, 1988. **55**(6): p. 1099-107.
86. Morzycka-Wroblewska, E., F.E. Lee, and S.V. Desiderio, *Unusual immunoglobulin gene rearrangement leads to replacement of recombinational signal sequences.* Science, 1988. **242**(4876): p. 261-3.
87. Glusman, G., et al., *Comparative genomics of the human and mouse T cell receptor loci.* Immunity, 2001. **15**(3): p. 337-49.
88. Stanhope-Baker, P., et al., *Cell type-specific chromatin structure determines the targeting of V(D)J recombinase activity in vitro.* Cell, 1996. **85**(6): p. 887-97.
89. Romano, R., et al., *From murine to human nude/SCID: the thymus, T-cell development and the missing link.* Clin Dev Immunol, 2012. **2012**: p. 467101.
90. Isoda, T., et al., *Process for immune defect and chromosomal translocation during early thymocyte development lacking ATM.* Blood, 2012. **120**(4): p. 789-99.
91. Li, Y.S., K. Hayakawa, and R.R. Hardy, *The regulated expression of B lineage associated genes during B cell differentiation in bone marrow and fetal liver.* J Exp Med, 1993. **178**(3): p. 951-60.
92. Bassing, C.H., W. Swat, and F.W. Alt, *The mechanism and regulation of chromosomal V(D)J recombination.* Cell, 2002. **109 Suppl**: p. S45-55.
93. Johnson, K., K.L. Reddy, and H. Singh, *Molecular pathways and mechanisms regulating the recombination of immunoglobulin genes during B-lymphocyte development.* Adv Exp Med Biol, 2009. **650**: p. 133-47.
94. Hopfner, K.P., et al., *The Rad50 zinc-hook is a structure joining Mre11 complexes in DNA recombination and repair.* Nature, 2002. **418**(6897): p. 562-6.

95. Williams, R.S., et al., *Mre11 dimers coordinate DNA end bridging and nuclease processing in double-strand-break repair.* Cell, 2008. **135**(1): p. 97-109.
96. Uziel, T., et al., *Requirement of the MRN complex for ATM activation by DNA damage.* EMBO J, 2003. **22**(20): p. 5612-21.
97. Strathern, J.N., B.K. Shafer, and C.B. McGill, *DNA synthesis errors associated with double-strand-break repair.* Genetics, 1995. **140**(3): p. 965-72.
98. You, Z., et al., *ATM activation and its recruitment to damaged DNA require binding to the C terminus of Nbs1.* Mol Cell Biol, 2005. **25**(13): p. 5363-79.
99. Bakkenist, C.J. and M.B. Kastan, *DNA damage activates ATM through intermolecular autophosphorylation and dimer dissociation.* Nature, 2003. **421**(6922): p. 499-506.
100. Blundred, R.M. and G.S. Stewart, *DNA double-strand break repair, immunodeficiency and the RIDDLE syndrome.* Expert Rev Clin Immunol, 2011. **7**(2): p. 169-85.
101. Shiloh, Y., *ATM: ready, set, go.* Cell Cycle, 2003. **2**(2): p. 116-7.
102. Bednarski, J.J. and B.P. Sleckman, *Lymphocyte development: integration of DNA damage response signaling.* Adv Immunol, 2012. **116**: p. 175-204.
103. Morales, M., et al., *The Rad50S allele promotes ATM-dependent DNA damage responses and suppresses ATM deficiency: implications for the Mre11 complex as a DNA damage sensor.* Genes Dev, 2005. **19**(24): p. 3043-54.
104. Burma, S., et al., *ATM phosphorylates histone H2AX in response to DNA double-strand breaks.* J Biol Chem, 2001. **276**(45): p. 42462-7.
105. Kuhne, M., et al., *A double-strand break repair defect in ATM-deficient cells contributes to radiosensitivity.* Cancer Res, 2004. **64**(2): p. 500-8.
106. Zhang, Y., et al., *The Role of Mechanistic Factors in Promoting Chromosomal Translocations Found in Lymphoid and Other Cancers.* 2010. **106**: p. 93-133.
107. McElhinny, S.A.N., Ramsden, D.A., *Sibling rivalry: competition between Pol X family members in V(D)J recombination and general double strand break repair.* Immunological Reviews, 2004. **200**(156-164).
108. Akopiants, K., et al., *Requirement for XLF/Cernunnos in alignment-based gap filling by DNA polymerases lambda and mu for nonhomologous end joining in human whole-cell extracts.* Nucleic Acids Res, 2009. **37**(12): p. 4055-62.
109. Gostissa, M., F.W. Alt, and R. Chiarle, *Mechanisms that Promote and Suppress Chromosomal Translocations in Lymphocytes.* Annual Review of Immunology, 2011. **29**(1): p. 319-350.
110. Nussenzweig, A. and M.C. Nussenzweig, *Origin of Chromosomal Translocations in Lymphoid Cancer.* Cell, 2010. **141**(1): p. 27-38.
111. Boboila, C., F.W. Alt, and B. Schwer, *Classical and Alternative End-Joining Pathways for Repair of Lymphocyte-Specific and General DNA Double-Strand Breaks.* 2012. **116**: p. 1-49.
112. Boboila, C., et al., *Robust chromosomal DNA repair via alternative end-joining in the absence of X-ray repair cross-complementing protein 1 (XRCC1).* Proceedings of the National Academy of Sciences, 2012. **109**(7): p. 2473-2478.
113. Xie, A., A. Kwok, and R. Scully, *Role of mammalian Mre11 in classical and alternative nonhomologous end joining.* Nat Struct Mol Biol, 2009. **16**(8): p. 814-8.

114. Roth, D.B. and J.H. Wilson, *Nonhomologous recombination in mammalian cells: role for short sequence homologies in the joining reaction.* Mol Cell Biol, 1986. **6**(12): p. 4295-304.
115. Audebert, M., B. Salles, and P. Calsou, *Involvement of poly(ADP-ribose) polymerase-1 and XRCC1/DNA ligase III in an alternative route for DNA double-strand breaks rejoining.* J Biol Chem, 2004. **279**(53): p. 55117-26.
116. Simsek, D., et al., *DNA ligase III promotes alternative nonhomologous end-joining during chromosomal translocation formation.* PLoS Genet, 2011. **7**(6): p. e1002080.
117. Lee-Theilen, M., et al., *CtIP promotes microhomology-mediated alternative end joining during class-switch recombination.* Nat Struct Mol Biol, 2011. **18**(1): p. 75-9.
118. Deriano, L., et al., *Roles for NBS1 in alternative nonhomologous end-joining of V(D)J recombination intermediates.* Mol Cell, 2009. **34**(1): p. 13-25.
119. Bennardo, N., et al., *Alternative-NHEJ is a mechanistically distinct pathway of mammalian chromosome break repair.* PLoS Genet, 2008. **4**(6): p. e1000110.
120. Rass, E., et al., *Role of Mre11 in chromosomal nonhomologous end joining in mammalian cells.* Nature Structural & Molecular Biology, 2009. **16**(8): p. 819-824.
121. Sartori, A.A., et al., *Human CtIP promotes DNA end resection.* Nature, 2007. **450**(7169): p. 509-14.
122. Yun, M.H. and K. Hiom, *CtIP-BRCA1 modulates the choice of DNA double-strand-break repair pathway throughout the cell cycle.* Nature, 2009. **459**(7245): p. 460-3.
123. Paull, T.T. and M. Gellert, *The 3' to 5' exonuclease activity of Mre 11 facilitates repair of DNA double-strand breaks.* Mol Cell, 1998. **1**(7): p. 969-79.
124. Della-Maria, J., et al., *Human Mre11/Human Rad50/Nbs1 and DNA Ligase III /XRCC1 Protein Complexes Act Together in an Alternative Nonhomologous End Joining Pathway.* Journal of Biological Chemistry, 2011. **286**(39): p. 33845-33853.
125. Perkins, E.J., *Sensing of intermediates in V(D)J recombination by ATM.* Genes & Development, 2002. **16**(2): p. 159-164.
126. Helmink, B.A., et al., *H2AX prevents CtIP-mediated DNA end resection and aberrant repair in G1-phase lymphocytes.* Nature, 2010. **469**(7329): p. 245-249.
127. Helmink, B.A., et al., *MRN complex function in the repair of chromosomal Rag-mediated DNA double-strand breaks.* Journal of Experimental Medicine, 2009. **206**(3): p. 669-679.
128. Bredemeyer, A.L., et al., *ATM stabilizes DNA double-strand-break complexes during V(D)J recombination.* Nature, 2006. **442**(7101): p. 466-70.
129. Bredemeyer, A.L., et al., *ATM stabilizes DNA double-strand-break complexes during V(D)J recombination.* Nature, 2006. **442**(7101): p. 466-470.
130. Sobacchi, C., et al., *RAG-dependent primary immunodeficiencies.* Hum Mutat, 2006. **27**(12): p. 1174-84.
131. Villa, A., et al., *V(D)J recombination defects in lymphocytes due to RAG mutations: severe immunodeficiency with a spectrum of clinical presentations.* Blood, 2001. **97**(1): p. 81-8.
132. Fischer, A., et al., *Severe combined immunodeficiency. A model disease for molecular immunology and therapy.* Immunol Rev, 2005. **203**: p. 98-109.
133. Kutukculer, N., et al., *Novel mutations and diverse clinical phenotypes in recombinase-activating gene 1 deficiency.* Ital J Pediatr, 2012. **38**: p. 8.

134. Fischer, A., *Human primary immunodeficiency diseases: a perspective.* Nat Immunol, 2004. **5**(1): p. 23-30.
135. Moshous, D., et al., *Artemis, a novel DNA double-strand break repair/V(D)J recombination protein, is mutated in human severe combined immune deficiency.* Cell, 2001. **105**(2): p. 177-86.
136. Le Deist, F., et al., *Artemis sheds new light on V(D)J recombination.* Immunol Rev, 2004. **200**: p. 142-55.
137. Pannicke, U., et al., *The most frequent DCLRE1C (ARTEMIS) mutations are based on homologous recombination events.* Hum Mutat, 2010. **31**(2): p. 197-207.
138. van der Burg, M., et al., *A DNA-PKcs mutation in a radiosensitive T-B- SCID patient inhibits Artemis activation and nonhomologous end-joining.* J Clin Invest, 2009. **119**(1): p. 91-8.
139. Ben-Omran, T.I., et al., *A patient with mutations in DNA Ligase IV: clinical features and overlap with Nijmegen breakage syndrome.* Am J Med Genet A, 2005. **137A**(3): p. 283-7.
140. Chistiakov, D.A., N.V. Voronova, and A.P. Chistiakov, *Ligase IV syndrome.* Eur J Med Genet, 2009. **52**(6): p. 373-8.
141. Nakada, S., *Abnormalities in DNA double-strand break response beyond primary immunodeficiency.* Int J Hematol, 2011. **93**(4): p. 425-33.
142. de Villartay, J.P., *V(D)J recombination deficiencies.* Adv Exp Med Biol, 2009. **650**: p. 46-58.
143. Omenn, G.S., *Familial Reticuloendotheliosis with Eosinophilia.* N Engl J Med, 1965. **273**: p. 427-32.
144. Corneo, B., et al., *Identical mutations in RAG1 or RAG2 genes leading to defective V(D)J recombinase activity can cause either T-B-severe combined immune deficiency or Omenn syndrome.* Blood, 2001. **97**(9): p. 2772-6.
145. Ege, M., et al., *Omenn syndrome due to ARTEMIS mutations.* Blood, 2005. **105**(11): p. 4179-86.
146. Villa, A., et al., *Partial V(D)J recombination activity leads to Omenn syndrome.* Cell, 1998. **93**(5): p. 885-96.
147. Moshous, D., et al., *Partial T and B lymphocyte immunodeficiency and predisposition to lymphoma in patients with hypomorphic mutations in Artemis.* J Clin Invest, 2003. **111**(3): p. 381-7.
148. Riballo, E., et al., *Identification of a defect in DNA ligase IV in a radiosensitive leukaemia patient.* Curr Biol, 1999. **9**(13): p. 699-702.
149. Toita, N., et al., *Epstein-Barr virus-associated B-cell lymphoma in a patient with DNA ligase IV (LIG4) syndrome.* Am J Med Genet A, 2007. **143**(7): p. 742-5.
150. Yue, J., et al., *Identification of the DNA repair defects in a case of dubowitz syndrome.* PLoS ONE, 2013. **8**(1): p. e54389.
151. Staples, E.R., et al., *Immunodeficiency in ataxia telangiectasia is correlated strongly with the presence of two null mutations in the ataxia telangiectasia mutated gene.* Clin Exp Immunol, 2008. **153**(2): p. 214-20.
152. Giovannetti, A., et al., *Skewed T-cell receptor repertoire, decreased thymic output, and predominance of terminally differentiated T cells in ataxia telangiectasia.* Blood, 2002. **100**(12): p. 4082-9.

153. Aurias, A., et al., *High frequencies of inversions and translocations of chromosomes 7 and 14 in ataxia telangiectasia.* Mutat Res, 1980. **69**(2): p. 369-74.
154. Varon, R., et al., *Nibrin, a novel DNA double-strand break repair protein, is mutated in Nijmegen breakage syndrome.* Cell, 1998. **93**(3): p. 467-76.
155. Digweed, M. and K. Sperling, *Nijmegen breakage syndrome: clinical manifestation of defective response to DNA double-strand breaks.* DNA Repair (Amst), 2004. **3**(8-9): p. 1207-17.
156. Stewart, G.S., et al., *The DNA double-strand break repair gene hMRE11 is mutated in individuals with an ataxia-telangiectasia-like disorder.* Cell, 1999. **99**(6): p. 577-87.
157. Rooney, S., et al., *Defective DNA Repair and Increased Genomic Instability in Artemis-deficient Murine Cells.* Journal of Experimental Medicine, 2003. **197**(5): p. 553-565.
158. Rooney, S., et al., *Leaky Scid phenotype associated with defective V(D)J coding end processing in Artemis-deficient mice.* Mol Cell, 2002. **10**(6): p. 1379-90.
159. Blunt, T., et al., *Identification of a nonsense mutation in the carboxyl-terminal region of DNA-dependent protein kinase catalytic subunit in the scid mouse.* Proc Natl Acad Sci U S A, 1996. **93**(19): p. 10285-90.
160. Zhu, C., et al., *Ku86-deficient mice exhibit severe combined immunodeficiency and defective processing of V(D)J recombination intermediates.* Cell, 1996. **86**(3): p. 379-89.
161. Bogue, M.A., et al., *V(D)J recombination in Ku86-deficient mice: distinct effects on coding, signal, and hybrid joint formation.* Immunity, 1997. **7**(1): p. 37-47.
162. Gu, Y., et al., *Growth retardation and leaky SCID phenotype of Ku70-deficient mice.* Immunity, 1997. **7**(5): p. 653-65.
163. Frank, K.M., et al., *Late embryonic lethality and impaired V(D)J recombination in mice lacking DNA ligase IV.* Nature, 1998. **396**(6707): p. 173-7.
164. Marrella, V., et al., *A hypomorphic R229Q Rag2 mouse mutant recapitulates human Omenn syndrome.* J Clin Invest, 2007. **117**(5): p. 1260-9.
165. Khiong, K., et al., *Homeostatically proliferating CD4 T cells are involved in the pathogenesis of an Omenn syndrome murine model.* J Clin Invest, 2007. **117**(5): p. 1270-81.
166. Helmink, B.A., et al., *MRN complex function in the repair of chromosomal Rag-mediated DNA double-strand breaks.* J Exp Med, 2009. **206**(3): p. 669-79.
167. Liyanage, M., et al., *Abnormal rearrangement within the alpha/delta T-cell receptor locus in lymphomas from Atm-deficient mice.* Blood, 2000. **96**(5): p. 1940-6.
168. Xu, Y., et al., *Targeted disruption of ATM leads to growth retardation, chromosomal fragmentation during meiosis, immune defects, and thymic lymphoma.* Genes Dev, 1996. **10**(19): p. 2411-22.
169. Elson, A., et al., *Pleiotropic defects in ataxia-telangiectasia protein-deficient mice.* Proc Natl Acad Sci U S A, 1996. **93**(23): p. 13084-9.
170. Kang, J., R.T. Bronson, and Y. Xu, *Targeted disruption of NBS1 reveals its roles in mouse development and DNA repair.* EMBO J, 2002. **21**(6): p. 1447-55.
171. Bassing, C.H., et al., *Histone H2AX: a dosage-dependent suppressor of oncogenic translocations and tumors.* Cell, 2003. **114**(3): p. 359-70.
172. Celeste, A., et al., *H2AX haploinsufficiency modifies genomic stability and tumor susceptibility.* Cell, 2003. **114**(3): p. 371-83.

173. Lewis, S.M., et al., *Cryptic signals and the fidelity of V(D)J joining.* Mol Cell Biol, 1997. **17**(6): p. 3125-36.
174. Zhang, M. and P.C. Swanson, *V(D)J recombinase binding and cleavage of cryptic recombination signal sequences identified from lymphoid malignancies.* J Biol Chem, 2008. **283**(11): p. 6717-27.
175. Cayuela, J.M., B. Gardie, and F. Sigaux, *Disruption of the multiple tumor suppressor gene MTS1/p16(INK4a)/CDKN2 by illegitimate V(D)J recombinase activity in T-cell acute lymphoblastic leukemias.* Blood, 1997. **90**(9): p. 3720-6.
176. Lieber, M.R., et al., *Nonhomologous DNA End Joining (NHEJ) and Chromosomal Translocations in Humans.* 2010. **50**: p. 279-296.
177. Raghavan, S.C., I.R. Kirsch, and M.R. Lieber, *Analysis of the V(D)J recombination efficiency at lymphoid chromosomal translocation breakpoints.* J Biol Chem, 2001. **276**(31): p. 29126-33.
178. Raghavan, S.C., et al., *The structure-specific nicking of small heteroduplexes by the RAG complex: implications for lymphoid chromosomal translocations.* DNA Repair (Amst), 2007. **6**(6): p. 751-9.
179. Raghavan, S.C. and M.R. Lieber, *DNA structures at chromosomal translocation sites.* Bioessays, 2006. **28**(5): p. 480-94.
180. Tsai, C.L., A.H. Drejer, and D.G. Schatz, *Evidence of a critical architectural function for the RAG proteins in end processing, protection, and joining in V(D)J recombination.* Genes Dev, 2002. **16**(15): p. 1934-49.
181. Kumar, S. and P.C. Swanson, *Full-length RAG1 promotes contact with coding and intersignal sequences in RAG protein complexes bound to recombination signals paired in cis.* Nucleic Acids Res, 2009. **37**(7): p. 2211-26.
182. Yin, B., et al., *Histone H2AX stabilizes broken DNA strands to suppress chromosome breaks and translocations during V(D)J recombination.* Journal of Experimental Medicine, 2009. **206**(12): p. 2625-2639.
183. Weinstock, D.M., et al., *Modeling oncogenic translocations: distinct roles for double-strand break repair pathways in translocation formation in mammalian cells.* DNA Repair (Amst), 2006. **5**(9-10): p. 1065-74.
184. Robbiani, D.F. and M.C. Nussenzweig, *Chromosome translocation, B cell lymphoma, and activation-induced cytidine deaminase.* Annu Rev Pathol, 2013. **8**: p. 79-103.
185. Corneo, B., et al., *Rag mutations reveal robust alternative end joining.* Nature, 2007. **449**(7161): p. 483-6.
186. Rooney, S., J. Chaudhuri, and F.W. Alt, *The role of the non-homologous end-joining pathway in lymphocyte development.* Immunol Rev, 2004. **200**: p. 115-31.
187. Feeney, A.J., P. Goebel, and C.R. Espinoza, *Many levels of control of V gene rearrangement frequency.* Immunol Rev, 2004. **200**: p. 44-56.
188. Cuomo, C.A., C.L. Mundy, and M.A. Oettinger, *DNA sequence and structure requirements for cleavage of V(D)J recombination signal sequences.* Mol Cell Biol, 1996. **16**(10): p. 5683-90.
189. Gerstein, R.M. and M.R. Lieber, *Coding end sequence can markedly affect the initiation of V(D)J recombination.* Genes Dev, 1993. **7**(7B): p. 1459-69.

190. Jung, D., et al., *Extrachromosomal recombination substrates recapitulate beyond 12/23 restricted VDJ recombination in nonlymphoid cells.* Immunity, 2003. **18**(1): p. 65-74.
191. Yu, K. and M.R. Lieber, *Mechanistic basis for coding end sequence effects in the initiation of V(D)J recombination.* Mol Cell Biol, 1999. **19**(12): p. 8094-102.
192. Leu, T.M., Q.M. Eastman, and D.G. Schatz, *Coding joint formation in a cell-free V(D)J recombination system.* Immunity, 1997. **7**(2): p. 303-14.
193. Agrawal, A. and D.G. Schatz, *RAG1 and RAG2 form a stable postcleavage synaptic complex with DNA containing signal ends in V(D)J recombination.* Cell, 1997. **89**(1): p. 43-53.
194. Jones, J.M. and M. Gellert, *Intermediates in V(D)J recombination: a stable RAG1/2 complex sequesters cleaved RSS ends.* Proc Natl Acad Sci U S A, 2001. **98**(23): p. 12926-31.
195. Qiu, J.X., et al., *Separation-of-function mutants reveal critical roles for RAG2 in both the cleavage and joining steps of V(D)J recombination.* Mol Cell, 2001. **7**(1): p. 77-87.
196. Huye, L.E., et al., *Mutational analysis of all conserved basic amino acids in RAG-1 reveals catalytic, step arrest, and joining-deficient mutants in the V(D)J recombinase.* Mol Cell Biol, 2002. **22**(10): p. 3460-73.
197. Yarnell Schultz, H., et al., *Joining-deficient RAG1 mutants block V(D)J recombination in vivo and hairpin opening in vitro.* Mol Cell, 2001. **7**(1): p. 65-75.
198. Lee, G.S., et al., *RAG proteins shepherd double-strand breaks to a specific pathway, suppressing error-prone repair, but RAG nicking initiates homologous recombination.* Cell, 2004. **117**(2): p. 171-84.
199. Nagawa, F., et al., *Joining mutants of RAG1 and RAG2 that demonstrate impaired interactions with the coding-end DNA.* J Biol Chem, 2004. **279**(37): p. 38360-8.
200. Giblin, W., et al., *Leaky severe combined immunodeficiency and aberrant DNA rearrangements due to a hypomorphic RAG1 mutation.* Blood, 2009. **113**(13): p. 2965-75.
201. Gao, Y., et al., *A critical role for DNA end-joining proteins in both lymphogenesis and neurogenesis.* Cell, 1998. **95**(7): p. 891-902.
202. Taccioli, G.E., et al., *Targeted disruption of the catalytic subunit of the DNA-PK gene in mice confers severe combined immunodeficiency and radiosensitivity.* Immunity, 1998. **9**(3): p. 355-66.
203. Dudley, D.D., et al., *Impaired V(D)J recombination and lymphocyte development in core RAG1-expressing mice.* J Exp Med, 2003. **198**(9): p. 1439-50.
204. Liang, H.E., et al., *The "dispensable" portion of RAG2 is necessary for efficient V-to-DJ rearrangement during B and T cell development.* Immunity, 2002. **17**(5): p. 639-51.
205. Walter, J.E., et al., *Expansion of immunoglobulin-secreting cells and defects in B cell tolerance in Rag-dependent immunodeficiency.* J Exp Med, 2010. **207**(7): p. 1541-54.
206. Darroudi, F., et al., *Role of Artemis in DSB repair and guarding chromosomal stability following exposure to ionizing radiation at different stages of cell cycle.* Mutat Res, 2007. **615**(1-2): p. 111-24.
207. Evans, P.M., et al., *Radiation-induced delayed cell death in a hypomorphic Artemis cell line.* Hum Mol Genet, 2006. **15**(8): p. 1303-11.

208. Kobayashi, N., et al., *Novel Artemis gene mutations of radiosensitive severe combined immunodeficiency in Japanese families.* Hum Genet, 2003. **112**(4): p. 348-52.
209. Lagresle-Peyrou, C., et al., *Restoration of human B-cell differentiation into NOD-SCID mice engrafted with gene-corrected CD34+ cells isolated from Artemis or RAG1-deficient patients.* Mol Ther, 2008. **16**(2): p. 396-403.
210. Li, L., et al., *A founder mutation in Artemis, an SNM1-like protein, causes SCID in Athabascan-speaking Native Americans.* J Immunol, 2002. **168**(12): p. 6323-9.
211. Musio, A., et al., *Damaging-agent sensitivity of Artemis-deficient cell lines.* Eur J Immunol, 2005. **35**(4): p. 1250-6.
212. Noordzij, J.G., et al., *Radiosensitive SCID patients with Artemis gene mutations show a complete B-cell differentiation arrest at the pre-B-cell receptor checkpoint in bone marrow.* Blood, 2003. **101**(4): p. 1446-52.
213. Rohr, J., et al., *Chronic inflammatory bowel disease as key manifestation of atypical ARTEMIS deficiency.* J Clin Immunol, 2010. **30**(2): p. 314-20.
214. van der Burg, M., et al., *Defective Artemis nuclease is characterized by coding joints with microhomology in long palindromic-nucleotide stretches.* Eur J Immunol, 2007. **37**(12): p. 3522-8.
215. van Zelm, M.C., et al., *Gross deletions involving IGHM, BTK, or Artemis: a model for genomic lesions mediated by transposable elements.* Am J Hum Genet, 2008. **82**(2): p. 320-32.
216. Brandt, V.L. and D.B. Roth, *Recent insights into the formation of RAG-induced chromosomal translocations.* Adv Exp Med Biol, 2009. **650**: p. 32-45.
217. Yannone, S.M., et al., *Coordinate 5' and 3' endonucleolytic trimming of terminally blocked blunt DNA double-strand break ends by Artemis nuclease and DNA-dependent protein kinase.* Nucleic Acids Res, 2008. **36**(10): p. 3354-65.
218. Gu, J., et al., *DNA-PKcs regulates a single-stranded DNA endonuclease activity of Artemis.* DNA Repair (Amst), 2010. **9**(4): p. 429-37.
219. Livak, F., et al., *Characterization of TCR gene rearrangements during adult murine T cell development.* J Immunol, 1999. **162**(5): p. 2575-80.
220. Kobayashi, Y., et al., *Transrearrangements between antigen receptor genes in normal human lymphoid tissues and in ataxia telangiectasia.* J Immunol, 1991. **147**(9): p. 3201-9.
221. Stern, M.H., et al., *Inversion of chromosome 7 in ataxia telangiectasia is generated by a rearrangement between T-cell receptor beta and T-cell receptor gamma genes.* Blood, 1989. **74**(6): p. 2076-80.
222. Lista, F., et al., *The absolute number of trans-rearrangements between the TCRG and TCRB loci is predictive of lymphoma risk: a severe combined immune deficiency (SCID) murine model.* Cancer Res, 1997. **57**(19): p. 4408-13.
223. Ward, I.M., et al., *53BP1 cooperates with p53 and functions as a haploinsufficient tumor suppressor in mice.* Mol Cell Biol, 2005. **25**(22): p. 10079-86.
224. Kang, J., et al., *Functional interaction of H2AX, NBS1, and p53 in ATM-dependent DNA damage responses and tumor suppression.* Mol Cell Biol, 2005. **25**(2): p. 661-70.

225. Lipkowitz, S., M.H. Stern, and I.R. Kirsch, *Hybrid T cell receptor genes formed by interlocus recombination in normal and ataxia-telangiectasis lymphocytes.* J Exp Med, 1990. **172**(2): p. 409-18.
226. Carroll, A.M. and M.J. Bosma, *T-lymphocyte development in scid mice is arrested shortly after the initiation of T-cell receptor delta gene recombination.* Genes Dev, 1991. **5**(8): p. 1357-66.
227. Donehower, L.A., et al., *Mice deficient for p53 are developmentally normal but susceptible to spontaneous tumours.* Nature, 1992. **356**(6366): p. 215-21.
228. Jacks, T., et al., *Tumor spectrum analysis in p53-mutant mice.* Curr Biol, 1994. **4**(1): p. 1-7.
229. Dujka, M.E., et al., *ATM and p53 are essential in the cell-cycle containment of DNA breaks during V(D)J recombination in vivo.* Oncogene, 2010. **29**(7): p. 957-65.
230. Guidos, C.J., et al., *V(D)J recombination activates a p53-dependent DNA damage checkpoint in scid lymphocyte precursors.* Genes Dev, 1996. **10**(16): p. 2038-54.
231. Negrini, S., V.G. Gorgoulis, and T.D. Halazonetis, *Genomic instability--an evolving hallmark of cancer.* Nat Rev Mol Cell Biol, 2010. **11**(3): p. 220-8.
232. Zhu, C., et al., *Unrepaired DNA breaks in p53-deficient cells lead to oncogenic gene amplification subsequent to translocations.* Cell, 2002. **109**(7): p. 811-21.
233. Mills, K.D., D.O. Ferguson, and F.W. Alt, *The role of DNA breaks in genomic instability and tumorigenesis.* Immunol Rev, 2003. **194**: p. 77-95.
234. Rooney, S., et al., *Artemis and p53 cooperate to suppress oncogenic N-myc amplification in progenitor B cells.* Proc Natl Acad Sci U S A, 2004. **101**(8): p. 2410-5.
235. Difilippantonio, M.J., et al., *Evidence for replicative repair of DNA double-strand breaks leading to oncogenic translocation and gene amplification.* J Exp Med, 2002. **196**(4): p. 469-80.
236. Liao, M.J., et al., *No requirement for V(D)J recombination in p53-deficient thymic lymphoma.* Mol Cell Biol, 1998. **18**(6): p. 3495-501.
237. Haines, B.B., et al., *Block of T cell development in P53-deficient mice accelerates development of lymphomas with characteristic RAG-dependent cytogenetic alterations.* Cancer Cell, 2006. **9**(2): p. 109-20.
238. Vanasse, G.J., et al., *Genetic pathway to recurrent chromosome translocations in murine lymphoma involves V(D)J recombinase.* J Clin Invest, 1999. **103**(12): p. 1669-75.
239. Nacht, M. and T. Jacks, *V(D)J recombination is not required for the development of lymphoma in p53-deficient mice.* Cell Growth Differ, 1998. **9**(2): p. 131-8.
240. Gladdy, R.A., et al., *The RAG-1/2 endonuclease causes genomic instability and controls CNS complications of lymphoblastic leukemia in p53/Prkdc-deficient mice.* Cancer Cell, 2003. **3**(1): p. 37-50.
241. De, P. and K.K. Rodgers, *Putting the pieces together: identification and characterization of structural domains in the V(D)J recombination protein RAG1.* Immunol Rev, 2004. **200**: p. 70-82.
242. Cowell, L.G., et al., *Prospective estimation of recombination signal efficiency and identification of functional cryptic signals in the genome by statistical modeling.* J Exp Med, 2003. **197**(2): p. 207-20.

243. Marculescu, R., et al., *Recombinase, chromosomal translocations and lymphoid neoplasia: targeting mistakes and repair failures.* DNA Repair (Amst), 2006. **5**(9-10): p. 1246-58.
244. Bredemeyer, A.L., et al., *Aberrant V(D)J recombination in ataxia telangiectasia mutated-deficient lymphocytes is dependent on nonhomologous DNA end joining.* J Immunol, 2008. **181**(4): p. 2620-5.
245. Hsieh, C.L., C.F. Arlett, and M.R. Lieber, *V(D)J recombination in ataxia telangiectasia, Bloom's syndrome, and a DNA ligase I-associated immunodeficiency disorder.* J Biol Chem, 1993. **268**(27): p. 20105-9.
246. Barlow, C., et al., *Atm-deficient mice: a paradigm of ataxia telangiectasia.* Cell, 1996. **86**(1): p. 159-71.
247. Borghesani, P.R., et al., *Abnormal development of Purkinje cells and lymphocytes in Atm mutant mice.* Proc Natl Acad Sci U S A, 2000. **97**(7): p. 3336-41.
248. Xu, Y. and D. Baltimore, *Dual roles of ATM in the cellular response to radiation and in cell growth control.* Genes Dev, 1996. **10**(19): p. 2401-10.
249. Mahaney, B.L., K. Meek, and S.P. Lees-Miller, *Repair of ionizing radiation-induced DNA double-strand breaks by non-homologous end-joining.* Biochem J, 2009. **417**(3): p. 639-50.
250. Zha, S., et al., *ATM-deficient thymic lymphoma is associated with aberrant tcrd rearrangement and gene amplification.* J Exp Med, 2010. **207**(7): p. 1369-80.
251. Osborne, C.S., et al., *Myc dynamically and preferentially relocates to a transcription factory occupied by Igh.* PLoS Biol, 2007. **5**(8): p. e192.
252. Wang, J.H., et al., *Mechanisms promoting translocations in editing and switching peripheral B cells.* Nature, 2009. **460**(7252): p. 231-6.
253. Zha, S., et al., *Complementary functions of ATM and H2AX in development and suppression of genomic instability.* Proc Natl Acad Sci U S A, 2008. **105**(27): p. 9302-6.
254. Rooney, S., et al., *Artemis-independent functions of DNA-dependent protein kinase in Ig heavy chain class switch recombination and development.* Proc Natl Acad Sci U S A, 2005. **102**(7): p. 2471-5.
255. Petiniot, L.K., et al., *Recombinase-activating gene (RAG) 2-mediated V(D)J recombination is not essential for tumorigenesis in Atm-deficient mice.* Proc Natl Acad Sci U S A, 2000. **97**(12): p. 6664-9.
256. Gao, Y., et al., *Interplay of p53 and DNA-repair protein XRCC4 in tumorigenesis, genomic stability and development.* Nature, 2000. **404**(6780): p. 897-900.
257. Desiderio, S., W.C. Lin, and Z. Li, *The cell cycle and V(D)J recombination.* Curr Top Microbiol Immunol, 1996. **217**: p. 45-59.
258. Oettinger, M.A., *V(D)J recombination: on the cutting edge.* Curr Opin Cell Biol, 1999. **11**(3): p. 325-9.
259. Lieber, M.R., et al., *The mechanism of vertebrate nonhomologous DNA end joining and its role in V(D)J recombination.* DNA Repair, 2004. **3**(8-9): p. 817-826.
260. Martin-Subero, J.I., et al., *Amplification of IGH/MYC fusion in clinically aggressive IGH/BCL2-positive germinal center B-cell lymphomas.* Genes Chromosomes Cancer, 2005. **43**(4): p. 414-23.

261. Rooney, S., *Artemis and p53 cooperate to suppress oncogenic N-myc amplification in progenitor B cells.* Proceedings of the National Academy of Sciences, 2004. **101**(8): p. 2410-2415.
262. Danska, J.S., et al., *Rescue of T cell-specific V(D)J recombination in SCID mice by DNA-damaging agents.* Science, 1994. **266**(5184): p. 450-5.
263. Wang, C., et al., *Irradiation-induced rescue of thymocyte differentiation and V(D)J recombination in mice lacking the catalytic subunit of DNA-dependent protein kinase.* J Immunol, 1999. **163**(11): p. 6065-71.
264. Zúñiga-Pflücker, J., et al., *Sublethal gamma-radiation induces differentiation of CD4-/CD8- into CD4+/CD8+ thymocytes without T cell receptor beta rearrangement in recombinase activation gene 2-/- mice.* J Exp Med, 1994. **180**(4): p. 1517-21.
265. Guidos, C.J., et al., *Development of CD4+CD8+ thymocytes in RAG-deficient mice through a T cell receptor beta chain-independent pathway.* J Exp Med, 1995. **181**(3): p. 1187-95.
266. Binnie, A., et al., *Gamma-irradiation directly affects the formation of coding joints in SCID cell lines.* J Immunol, 1999. **163**(10): p. 5418-26.
267. D'Amours, D. and S.P. Jackson, *The Mre11 complex: at the crossroads of dna repair and checkpoint signalling.* Nat Rev Mol Cell Biol, 2002. **3**(5): p. 317-27.
268. Zhou, B.B. and S.J. Elledge, *The DNA damage response: putting checkpoints in perspective.* Nature, 2000. **408**(6811): p. 433-9.
269. Taylor, A.M., et al., *Leukemia and lymphoma in ataxia telangiectasia.* Blood, 1996. **87**(2): p. 423-38.
270. Chen, H.T., et al., *Response to RAG-mediated VDJ cleavage by NBS1 and gamma-H2AX.* Science, 2000. **290**(5498): p. 1962-5.
271. Helmink, B.A. and B.P. Sleckman, *The response to and repair of RAG-mediated DNA double-strand breaks.* Annu Rev Immunol, 2012. **30**: p. 175-202.
272. Murphy, W., et al., *Induction of T cell differentiation and lymphomagenesis in the thymus of mice with severe combined immune deficiency (SCID).* J Immunol, 1994. **153**(3): p. 1004-14.
273. Hickson, I., et al., *Identification and characterization of a novel and specific inhibitor of the ataxia-telangiectasia mutated kinase ATM.* Cancer Res, 2004. **64**(24): p. 9152-9.
274. Nacht, M., et al., *Mutations in the p53 and SCID genes cooperate in tumorigenesis.* Genes Dev, 1996. **10**(16): p. 2055-66.
275. Strasser, A., et al., *Bcl-2 expression promotes B- but not T-lymphoid development in scid mice.* Nature, 1994. **368**(6470): p. 457-60.
276. Baer, R., et al., *Fusion of an immunoglobulin variable gene and a T cell receptor constant gene in the chromosome 14 inversion associated with T cell tumors.* Cell, 1985. **43**(3 Pt 2): p. 705-13.
277. Gapud, E.J. and B.P. Sleckman, *Unique and redundant functions of ATM and DNA-PKcs during V(D)J recombination.* Cell Cycle, 2011. **10**(12): p. 1928-1935.
278. Zha, S., et al., *ATM damage response and XLF repair factor are functionally redundant in joining DNA breaks.* Nature, 2010. **469**(7329): p. 250-254.
279. Bredemeyer, A.L., et al., *DNA double-strand breaks activate a multi-functional genetic program in developing lymphocytes.* Nature, 2008. **456**(7223): p. 819-823.

280. Callen, E., et al., *Essential role for DNA-PKcs in DNA double-strand break repair and apoptosis in ATM-deficient lymphocytes.* Mol Cell, 2009. **34**(3): p. 285-97.
281. Chan, S.H., A.M. Yu, and M. McVey, *Dual roles for DNA polymerase theta in alternative end-joining repair of double-strand breaks in Drosophila.* PLoS Genet, 2010. **6**(7): p. e1001005.
282. Yousefzadeh, M.J. and R.D. Wood, *DNA polymerase POLQ and cellular defense against DNA damage.* DNA Repair (Amst), 2013. **12**(1): p. 1-9.
283. Shima, N., R.J. Munroe, and J.C. Schimenti, *The mouse genomic instability mutation chaos1 is an allele of Polq that exhibits genetic interaction with Atm.* Mol Cell Biol, 2004. **24**(23): p. 10381-9.
284. Zhu, C. and E. Hsu, *Error-prone DNA repair activity during somatic hypermutation in shark B lymphocytes.* J Immunol, 2010. **185**(9): p. 5336-47.
285. Bebenek, K., et al., *The frameshift infidelity of human DNA polymerase lambda. Implications for function.* J Biol Chem, 2003. **278**(36): p. 34685-90.
286. Zhang, Y., et al., *Highly frequent frameshift DNA synthesis by human DNA polymerase mu.* Mol Cell Biol, 2001. **21**(23): p. 7995-8006.
287. Jacobs, C., et al., *A hypomorphic Artemis human disease allele causes aberrant chromosomal rearrangements and tumorigenesis.* Hum Mol Genet, 2011. **20**(4): p. 806-19.
288. Weterings, E., et al., *The role of DNA dependent protein kinase in synapsis of DNA ends.* Nucleic Acids Res, 2003. **31**(24): p. 7238-46.
289. Wang, G., et al., *Real-time monitoring of RAG-catalyzed DNA cleavage unveils dynamic changes in coding end association with the coding end complex.* Nucleic Acids Res, 2012. **40**(13): p. 6082-96.
290. Mahajan, K.N., et al., *Association of terminal deoxynucleotidyl transferase with Ku.* Proc Natl Acad Sci U S A, 1999. **96**(24): p. 13926-31.
291. Mickelsen, S., et al., *Modulation of terminal deoxynucleotidyltransferase activity by the DNA-dependent protein kinase.* J Immunol, 1999. **163**(2): p. 834-43.
292. Gu, J., et al., *XRCC4:DNA ligase IV can ligate incompatible DNA ends and can ligate across gaps.* EMBO J, 2007. **26**(4): p. 1010-23.
293. Purugganan, M.M., et al., *Ku80 is required for addition of N nucleotides to V(D)J recombination junctions by terminal deoxynucleotidyl transferase.* Nucleic Acids Res, 2001. **29**(7): p. 1638-46.
294. Fish, S.M. and M.J. Bosma, *Abnormal deletions in the T-cell receptor delta locus of mouse thymocytes.* Mol Cell Biol, 1994. **14**(7): p. 4455-64.
295. Srivastava, M., et al., *An Inhibitor of Nonhomologous End-Joining Abrogates Double-Strand Break Repair and Impedes Cancer Progression.* Cell, 2012. **151**(7): p. 1474-1487.
296. Cowell, I.G. and C.A. Austin, *Mechanism of generation of therapy related leukemia in response to anti-topoisomerase II agents.* Int J Environ Res Public Health, 2012. **9**(6): p. 2075-91.
297. Cho, J.H., et al., *Therapy-related acute leukemia with mixed phenotype and t(9;22)(q32;q11.2): a case report and review of the literature.* Hum Pathol, 2012. **43**(4): p. 605-9.